April 11, 1994

Ronald D. Powell, MR 3D-C

KINGSTON FOSSIL PLANT - LEACHATE CONTAINMENT ANALYSIS FOR DRY ASH STACK

We understand that Gilbert/Commonwealth has submitted a proposal to you to prepare the solid waste disposal permit package associated with a dry ash disposal area at Kingston Fossil Plant (KIF). One component of the permit package involves a leachate containment analysis using the HELP code. Since we have recently performed a leachate analysis for a proposed FGD waste area at KIF for Technology Advancements (Attachment 1), we may be able to provide a similar analysis for the dry ash area at a competitive price.

The analysis will follow that described in Attachment 1, and will include a complete water budget analysis for alternative surface cap and bottom-liner/collection-system designs. Daily meteorological data for the HELP simulations will be obtained from historical records for a first-order weather station in Oak Ridge. The physical and hydraulic properties of the ash will be based on previous data for KIF fly ash reported in Attachment 2 unless there is reason to expect there might be significant differences between the two ashes (i.e, different coal sources or burn processes). Our analysis will also account for the changes in dry stack area and thickness that will occur over the operational life of the stack.

The leachate containment analysis and a report describing the methods and results will be completed within one month of our receiving complete design specifications for the dry ash stack. The direct cost for analysis will be $5,000. If you have questions regarding the proposed workscope or budget, please contact Steve Young (632-1893).

J. Mark Boggs

J. Mark Boggs
Hydraulic Engineering
Engineering Laboratory
LAB 1A-N

JMB:CP
Attachments
cc: Vahid Alavian, LAB 1A-N
Steve Young, LAB 1A-N
Files, LAB 1A-N

Attachment 1

WR28-1-36-119

FGD BY-PRODUCT LEACHATE CONTAINMENT STUDIES FOR THE KINGSTON FOSSIL PLANT

TENNESSEE VALLEY AUTHORITY
ENGINEERING LABORATORY
NORRIS, TENNESSEE

TENNESSEE VALLEY AUTHORITY
RESOURCE GROUP, ENGINEERING SERVICES
HYDRAULIC ENGINEERING

FGD BY-PRODUCT LEACHATE CONTAINMENT STUDIES FOR THE KINGSTON FOSSIL PLANT

Report No. WR28-1-36-119

Prepared by
Steven C. Young

Engineering Laboratory
Norris, Tennessee
September 1993

EXECUTIVE SUMMARY

The HELP2 model was used to compare the alternatives for dry stacking Flue-Gas Desulfurization (FGD) by-product at the Kingston Fossil Plant over a 20-year period. Annual water budget components were predicted for the following FGD dry stack designs: (a) no bottom liner and no closure cap; (b) no bottom liner with a closure cap; (c) a bottom liner and no closure cap; and, (d) a bottom liner with a closure cap. The 20-year meteorological data set was created based on 20 years of temperature and rainfall data from a National Oceanographic and Atmospheric Administration station located approximately 15 miles from the Kingston Fossil Plant. A maximum stack height of 70 feet and a stacking rate of 14 feet/year for the dry stack were used in the simulations. Hydraulic properties of the FGD by-product were determined from laboratory tests on FGD samples from the Shawnee Fossil Plant. The FGD by-product had a hydraulic conductivity of 1.7×10^{-5} cm/s. The hydraulic conductivity for the closure cap and the bottom liner was 1×10^{-7} and 1×10^{-6} cm/s, respectively. Simulation of the closure cap began in the sixth year.

For the four dry stack designs, the average leachate rate varied between 4.9 and 9.8 inches/year. With no closure cap, the average annual leachate was 9.8 and 8.9 inches/year for no soil liner and with a soil liner, respectively. With a closure cap, the leachate was 5.6 and 4.9 inches/year for no soil liner and with a soil liner, respectively. The stack design feature most effective in minimizing leachate was the clay cap, which acts to reduce leachate generation by approximately 50 percent whether or not a clay liner was present. Since the analysis shows that the bottom liner provides little additional leachate reduction when a surface cap is present, it may be feasible to obtain a variance on the bottom liner requirement from the state. For example, bottom liner variances have recently been granted for new dry ash and gypsum disposal facilities at Shawnee and Cumberland based on similar leachate containment engineering analyses. The cost savings associated with such a variance can be expected to be substantial, considering that bottom liner costs generally range from \$1.7 million to \$2.0 million for a 3-ft liner covering a 50-acre area.

CONTENTS

LIST OF FIGURES

LIST OF TABLES

FGD BY-PRODUCT LEACHATE CONTAINMENT STUDIES FOR THE KINGSTON FOSSIL PLANT

1.0 INTRODUCTION

1.1 Background

Based on successful pilot plant studies of Flue-Gas Desulfurization (FGD) at the Shawnee Fossil Plant, a full-scale FGD system is being considered for the Kingston Fossil Plant. An FGD system includes spraying the flue gas from coal combustion with a fine mist of calcium hydroxide solution to remove sulfur dioxide. The FGD system proposed for the Kingston Fossil Plant includes adding chlorine to the calcium hydroxide mist to enhance the removal of atmospheric sulfur. A by-product of the FGD process is a mixture of calcium/sulfur precipitate and coal ash that requires land disposal.

During the last several years, TVA has been dry-stacking coal-combustion wastes at several of its fossil plants. One advantage of dry-stacking compared to sluicing by-products into ponds is less leachate production. The generation and management of leachate are important environmental concerns to both TVA and regulatory agencies. With regard to permit applications for solid waste disposal facilities, the state of Tennessee recommends using the HELP2 code (Schroeder et al., 1988) to predict leachate amounts.

1.2 Objective and Scope of Work

This report describes the application of the HELP2 model to quantify the effect of a clay bottom liner and a surface closure cap on the water budget of a proposed Kingston FGD dry stack. Major tasks include: (1) assembling meteorological data for the vicinity of Kingston, TN; (2) measuring the hydraulic and physical properties of FGD by-product from the Shawnee Fossil Plant; and, (3) performing the HELP2 simulations. Simulations were conducted for the following stack design cases: (a) no bottom liner and no closure cap; (b) no bottom liner with a closure cap; (c) a bottom liner with no closure cap; and, (d) a bottom liner with a closure cap.

2.0 KINGSTON FOSSIL PLANT

2.1 Site Description

The Kingston Fossil Plant began operations in 1955 and has a generating capacity of 1,700 megawatts. The plant is located on a peninsula formed by the Clinch and Emory Rivers at Clinch River Mile 2.6. Topography ranges from approximately 920 ft MSL to approximately 740 ft MSL at the shores of the peninsula. The plant is in the Valley and Ridge physiographic province of the Appalachian Highlands. This region is characterized by parallel ridges and valleys striking northeast-southwest. Bensiger and Kellberg (1951), Milligan and Ruane (1980), Harris and Foxx (1982) describe the site geology. Carpenter and Bohac (undated) and Velasco and Bohac (1991) provide useful soil, bedrock and geophysical logs.

Overburden at the plant site ranges from 10 to 50 feet. Most of the overburden consists of clays ranging from fat to silty with colors of dark brown, red, and light yellow. Soil cores from drilling reveals occasional layers of silty clay chert and of sandy clay. An average saturated hydraulic conductivity for the overburden is estimated at 2×10^{-5} cm/s (Velasco and Bohac, 1991). The overburden primarily overlays limestone bedrock.

Bedrock at the site is primarily deformed, but unmetamorphosed, sedimentary rock consisting mostly of limestones, dolomites, and shales. A large thrust fault in the vicinity of the plant has placed older bedrock from the southeast on top of younger rocks. Dips vary from vertical to 10 but averages 45 to 40 degrees toward the southeast. The most prevalent bedrocks are from the Conasauga and Knox Group of Ordovician and Cambrian age. The Knox Group primarily includes the Cooper Ridge Formation. The Conasauga Group includes the Nolichucky, Maryville, Rogersville, Rutledge, and Pumpkin Valley Formations. Across the plant sites, lenses of pure limestone range from one inch to several feet (TVA, 1965). Over time, some of the pure limestone zones have dissolved creating solution conduits and sinkholes.

2.2 FGD By-Product and FGD Dry Stack

The proposed FGD dry stacking area is located southeast of the Kingston Fossil Plant. Representative FGD by-products were taken from the Shawnee Pilot Plant and sent to Daniel B. Stephens & Associates for analysis. Analysis included: dry bulk density, porosity, saturated hydraulic conductivity, moisture retention curves, particle size analysis, Q and R shear strength, particle density, and proctor compaction (see Daniel B. Stephens & Associates, 1993).

Results from the Proctor compaction tests indicate an optimum gravimetric moisture content of 39.5 percent and a maximum dry bulk density of 1.17 g/cm^3. Most of the existing TVA dry stacks have been designed with the criterion of compacting coal combustion by-products to 90 percent of their maximum density. The density of the FGD samples used for the hydraulic testing were 1.04 g/cm^3. Test results needed for the HELP2 model are presented in Section 4.1.

Because of the large areal extent (> 10 acres) of the proposed Kingston dry-stack, the infiltration of precipitation will be essentially vertical. As a result, the quasi-two-dimensional HELP2 model is appropriate for predicting the dry stack water budget. The maximum height of the dry stack is estimated at 70 feet and a stacking rate of 14 feet/year is assumed.

3.0 HELP2 WATER BUDGET MODEL

3.1 Model Description and Requirements

The Hydrogeologic Evaluation of Landfill Performance (HELP) Model-Version 2 is a quasi-two-dimensional, deterministic water budget model (Schroeder et al., 1988). The model was developed and adapted from the U.S. Environmental Protection Agency's (EPA) Hydrologic Simulation Model for Estimating Percolation at Solid Waste Disposal Sites (HSSWDS) and from the U.S. Department of Agriculture's Chemical Runoff and Erosion from Agricultural Management Systems (CREAMS) Model.

HELP2 routes infiltration through three layer types: vertical percolation, lateral percolation, and barrier soil. In a vertical percolation layer, flow can be downward due to gravity or upward due to evapotranspiration. Capillary forces are neglected and a downward hydraulic gradient of unity is assumed. In a lateral percolation layer, both lateral drainage and vertical percolation can occur. Lateral drainage can occur only if a drain plane is specified by the user. In a barrier soil layer, which is assigned a permeability low enough to restrict vertical flow in the layers above it, only vertical percolation can occur but the downward hydraulic gradient can exceed unity when a saturated mound forms (see Section 3.2.5).

HELP2 does not account for lateral inflow or surface run-on. Requirements of the model include meteorological data, soil characteristics, landfill design specifications, a leaf area index value, an evaporative depth, and a Soil Conservation Service (SCS) curve number for runoff estimates. The soil requirements include porosity, field capacity, wilting point, saturated hydraulic conductivity, and initial moisture content. The landfill design specifications include number, type and thickness of layers, and slope of the landfill.

3.2 Major Subroutines in the HELP2 Model

The primary subroutines in HELP2 can be divided into five categories: (1) unsaturated hydraulic conductivity, (2) potential evaporation, (3) runoff, (4) evaporation, and (5) groundwater flow.

3.2.1 Unsaturated Hydraulic Conductivity--Porosity, field capacity, wilting point, and saturated hydraulic conductivity are soil properties required by HELP2. Porosity is the volumetric water content at saturation. Field capacity is the volumetric water content at 1/3 bar. Wilting point is the volumetric water content at 15 bars. HELP2 estimates the unsaturated hydraulic conductivity with a two-step process. In the first step, the pore-size distribution index for the Brooks-Corey equation (Brooks and Corey, 1964) is calculated. In the second step, the distribution index and the power function of Campbell (1974) is used to calculate the unsaturated hydraulic conductivity. Equations 3.2.1 through 3.2.4 are used to calculate unsaturated hydraulic conductivity. Equation 3.2.1 estimates the residual moisture from the wilting point. Equation 3.2.2 is a form of the Brooks-Corey equation. Equation 3.2.3 is a form of the Campbell power function.

$$\theta_r = 0.014 + 0.253\ (WP) \qquad 3.2.1$$

$$\left[\frac{Y_b}{Y}\right]^{\lambda} = \frac{(\theta - \theta_r)}{(\theta_s - \theta_r)} \qquad 3.2.2$$

$$\lambda = (-0.262) ln \left[\frac{WP-\theta_r}{FC-\theta_r}\right] \qquad 3.2.3$$

$$K(\theta) = K_s \left[\frac{\theta-\theta_r}{\theta_s-\theta_r}\right]^{[3 + (2/\lambda)]} \qquad 3.2.4$$

where: Y_b = Bubbling pressure
Y = Capillary pressure for a given moisture content
λ = Pore-size distribution index
θ = Volumetric moisture content, vol/vol
θ_r = Residual moisture content, vol/vol
θ_s = Saturated moisture content (porosity), vol/vol
WP = Wilting point
FC = Field capacity
$K(\theta)$ = Unsaturated hydraulic conductivity
K_s = Saturated hydraulic conductivity

3.2.2 Potential Evaporation--Meteorological requirements include daily precipitation, mean daily temperature, and total daily solar radiation. The meteorological data may be inputted by the user or generated by HELP2 algorithms. The potential evaporation is calculated using Equations 3.2.5 through 3.2.7, which are based on the Penman method used in CREAMS (Knisel, 1980).

$$PET = \frac{1.28 \times A_i \times H_i}{(A_i + G) \times 25.4} \qquad 3.2.5$$

$$A_i = \frac{5304\ e^{(21.255-5304/TK_i)}}{TK_i^2} \qquad 3.2.6$$

$$H_i = \frac{(1 - L)\, R_i}{58.3} \qquad 3.2.7$$

where: PET = Potential evapotranspiration
A_i = Slope of the saturation vapor pressure curve
H_i = Net solar radiation
G = Psychometric constant, assumed to equal 0.68
TK_i = Mean temperature in degrees Kelvin on day i
L = Albedo for solar radiation (assumed to remain constant at 0.23)
R_i = Solar radiation on day i, Langleys

3.2.3 Runoff--HELP2 uses the Soil Conservation Service (SCS) curve number method (USDA, 1972) to calculate runoff. The method permits runoff to occur only when the rainfall rate is greater than the infiltration rate and only when the initial demands of interception, infiltration, and surface storage have been satisfied. The empirical SCS relationships are given in Equations 3.2.8 and 3.2.9. The user is required to supply the value for the SCS curve number.

$$R = \frac{(P - 0.2 \times S)^2}{P + 0.8 \times S} \qquad 3.2.8$$

$$S = \frac{1000}{CN} - 10 \qquad 3.2.9$$

where: R = Runoff (inches)
P = Rainfall (inches)
S = Potential Maximum Retention (inches)
CN = SCS curve number (-)

3.2.4 Evaporation--In the HELP2 model, the rate of evaporation depends on the potential evaporation, surface wetness, vegetative growth, soil moisture conditions, and the soil's hydraulic properties. Ponded or stored precipitation on the landfill are the first sources used to satisfy the potential evaporation. Once the surface wetness is depleted, HELP2 evaporates water from an evaporative depth selected by the user. Evaporation from the landfill occurs in two stages. In Stage I, evaporation occurs at a rate equal to the potential evaporation. In Stage II, evaporation is less than the potential evaporation and controlled by the soil's hydraulic properties.

HELP2 uses Equation 3.2.10 to determine the upper limit of the Stage I evaporation, which is designated by U. Stage I evaporation occurs when the cumulative evaporation minus the cumulative infiltration is less than U. When the difference between the cumulative evaporation and infiltration is greater than U, Stage II evaporation occurs. Stage II evaporation is calculated with Equation 3.2.11.

$$U = \frac{9\ (\alpha - 3) \times 0.42}{25.4} \qquad 3.2.10$$

$$ES2_i = \frac{\alpha\ [t_i \times 0.5 - (t_i - 1) \times 0.5]}{25.4} \qquad 3.2.11$$

where: U = Upper limit of Stage I evaporation (inches)
$ES2_i$ = Stage II evaporation for day i (inches)
t_i = Time since Stage I evaporation ended (days)
α = Evaporation coefficient ($mm/day^{0.5}$)

HELP2 calculates α based on the empirical relations given in Table 3.2.1, which Schroeder et al. (1988) developed from the results of Ritchie (1972).

TABLE 3.2.1

Calculation of the Evaporation Coefficient α as a Function of $K_{.1\ bar}$

For $K_{.1\ bar}$*	α
$K_{.1\ bar} < .05$	3.3
$.05 < K_{.1\ bar} < .15$	$2.44 + 17.19 \times K_{.1\ bar}$
$K_{.1\ bar} > .15$	5.1

*$K_{.1\ bar}$ = hydraulic conductivity (cm/s) at a suction of 0.1 bar

3.2.5 Groundwater Flow--HELP2 ignores hydraulic gradients caused by capillary forces and assumes the vertical hydraulic gradient in the water layers is unity. This assumption sets the vertical groundwater flow to the unsaturated hydraulic conductivity value in each waste layer. Vertical hydraulic greater than one can only occur in a layer designated as a barrier soil. HELP2 assumes that the barrier layer is saturated at all times and permits the thickness of the saturated zone on top of the barrier soil to increase the vertical hydraulic gradient across the barrier layer beyond unity according to Equation 3.2.12. In the barrier layer, vertical groundwater flow equals the product of the saturated hydraulic conductivity, K_{sat}, and the vertical hydraulic gradient, dh/dl.

$$\frac{dh}{dl} = \frac{(TH + TS)}{TS} \qquad 3.2.12$$

where: dh/dl = Vertical hydraulic gradient
TH = Thickness of saturated material above the barrier soil
TS = Thickness of the barrier soil

4.0 HELP2 WATER BUDGET SIMULATIONS FOR THE FGD DRY STACK

4.1 Model Scenarios

4.1.1 Dry Stack Design--In order to investigate the impact of a clay liner and a closure cap on the water budget for the proposed FGD dry stack, HELP2 was run for the four cases in Figure 4.1.1. The thicknesses of the clay liner, clay cap, and overlying soil are 3 feet, 1 foot, and 1 foot, respectively, as specified by the Tennessee Division of Solid Waste Management. Implicit in the design is a 1 to 2 percent slope on the clay cap toward the sides of the dry stack to promote runoff. Table 4.1.1 lists the hydraulic properties required by HELP2 for each soil type shown in Figure 4.1.1. The properties for the FGD by-product are based on Daniel B. Stephens & Associates (1993). The properties for the Kingston soils and depth to groundwater were obtained from Velasco and Bohac (1991). The field capacity, wilting point, and porosity for the clay cap and clay liner are those given by Schroeder et al. (1988) for a soil liner. The values for the top soils are those given by Schroeder et al., for a soil loam. For the HELP2 simulations, the top soil and the FGD material are designated as vertical percolation layers, and the clay cap and clay liner are designated as barrier soil layers (see Section 3.2.5).

TABLE 4.1.1

Material Properties Used in the HELP2 Simulations

Soil Type	Porosity	Field Capacity	Wilting Point	Initial Moisture Content (%)	Hydraulic Conductivity (cm/s)
Top Soil*	.463	.232	.116	.232	3.7×10^{-4}
Clay Cap	.430	.366	.280	.430	1.0×10^{-7}
FGD By-Product*	.582	.571	.582	.420	1.68×10^{-5}
Clay Liner	.430	.366	.280	.430	1.0×10^{-6}
Kingston Soil	.471	.340	.210	.270	2.0×10^{-5}

*Evaporation coefficient α is 5.1 mm/day $^{0.5}$

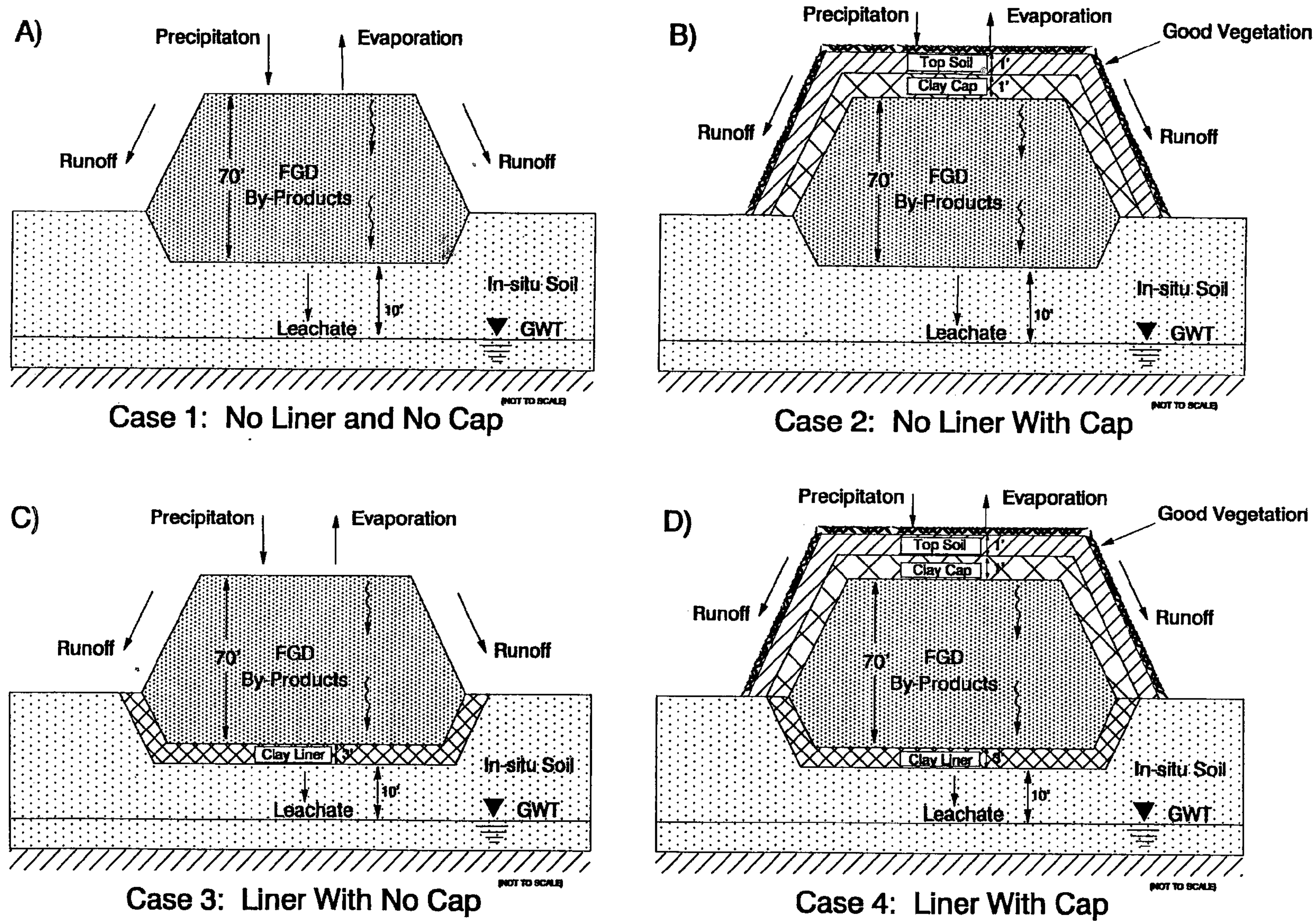

Figure 4.1.1. Four Kingston FGD Dry Stack Designs Evaluated With the HELP2 Model. Closure With a Clay Cap Occurs After 5 Years. Table 4.1.1 Lists the Hydraulic Properties for Each Material Type.

In addition to the properties in Table 4.1.1, HELP2 requires an SCS curve number and an evaporation depth. Both laboratory and numerical simulations with fly ash from Kingston and Colbert Fossil Plants demonstrate that the evaporation depth can approach several feet (Foust and Young, 1993). For the simulation, a conservative value of 24 inches is used for the FGD by-product. For the top soil, the evaporation depth equals the soil thickness of 12 inches. Using information given by Schroeder et al. (1988), the curve number for the top soil is calculated as 70. The curve number for the FGD by-product is set to 75 -- the value calculated from measured runoff from the Bull Run Fossil Plant fly ash dry stack (Young, 1989).

4.1.2 Meteorological Conditions--Meteorological data was compiled from a National Oceanographic and Atmospheric Administration (NOAA) station located in Oak Ridge, Tennessee. The NOAA station is approximately 15 miles from the Kingston Fossil Plant and was selected because of high quality data for a continuous 20-year period. The NOAA data includes daily rainfalls and mean daily temperatures from 1967 to 1987. Daily solar radiation was not available and was generated using a HELP2 subroutine that incorporates several factors including latitude and daily rainfall. Figure 4.1.2 summarizes the variability among the yearly averages for rainfall, temperature, and solar radiation.

4.2 Model Application

The construction of the FGD dry stack consists of a 5-year build-up and a 15-year closure interval. In any HELP2 application, there is uncertainty in how best to apply the model during the early years of a landfill. Because it assumes a constant landfill height, the HELP2 model has no provisions for modeling a build-up period during the construction of the landfill. Rationale for this approach is that over a landfill's life, leachate generated during the first several years of construction are minor. However, this assumption may not be valid for all modeling scenarios. As part of a sensitivity analysis of HELP2 simulations for a fly ash dry stack at Bull Run Fossil Plant, Young and Velasco (1991) showed that using a constant landfill height has no effect on runoff or evaporation amounts, but leads to lower leachate and higher storage amounts than if some type of build-up is considered. This result appears reasonable because if the dry stack's thickness is relatively thin during the first several years then rainfall has less distance to travel to become leachate and there is less storage capacity in the landfill.

Field data from Velasco and Bohac (1991) indicate that the bottom of the FGD dry stack will be approximately 10 feet above the average water table. Hence, any leachate must travel through a zone of unsaturated overburden before mixing with the groundwater. Water budget predictions with the unsaturated Kingston overburden indicate that this zone does not reduce leachate production. Because inclusion of this overburden zone prevents an assessment of the changes in the storage in the FGD dry stack, this overburden was excluded in the final HELP2 simulations.

In order to simulate the 5-year build-up period of the FGD dry stack, a procedure similar to that of Young and Velasco (1991) was followed. For the first year, the initial conditions included a 14-foot FGD layer with a possible clay liner. The initial moisture content for the different layers are listed in Table 4.1.1. For the second year, the initial conditions included

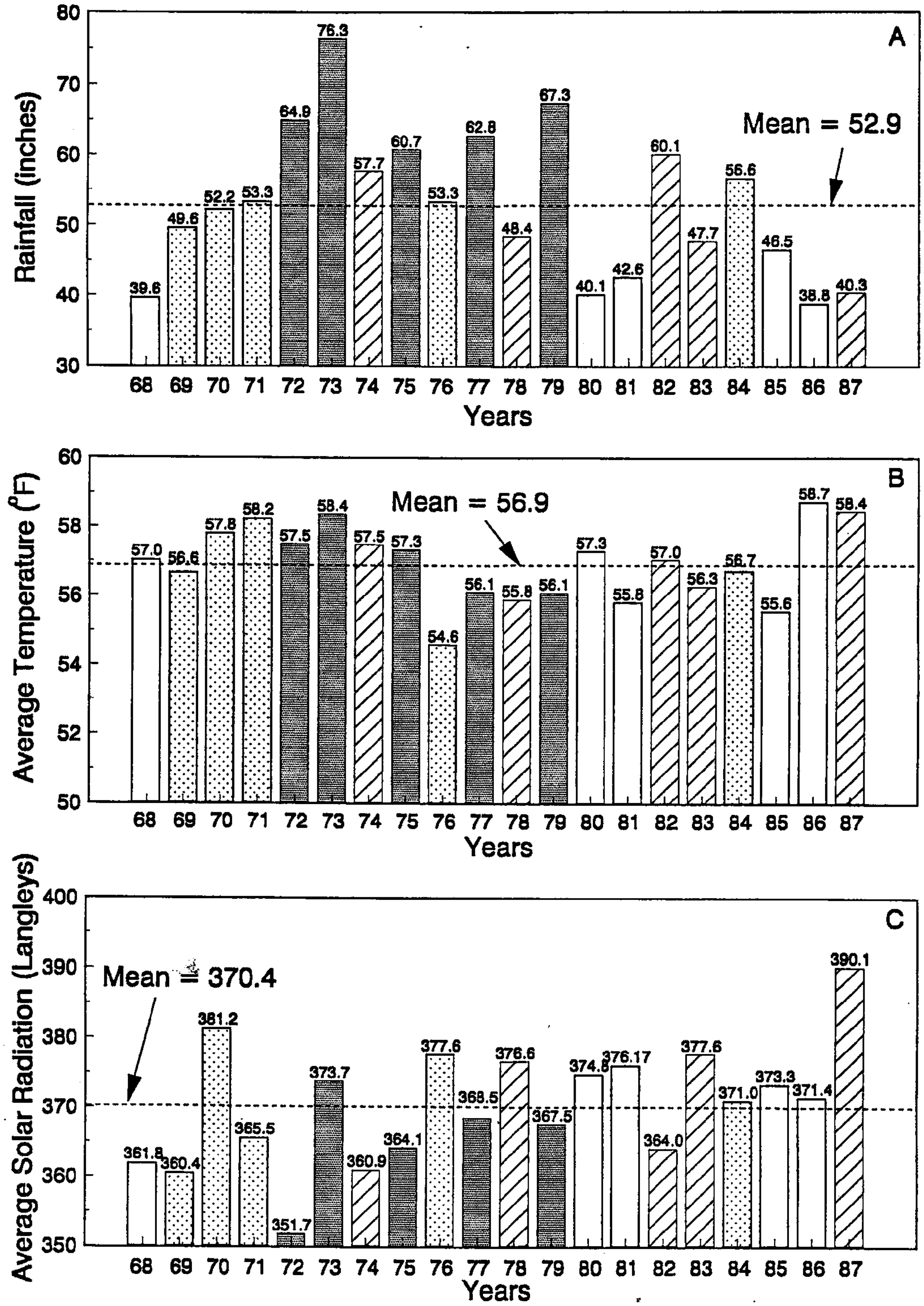

Figure 4.1.2. Annual Means for Rainfall, Daily Mean Temperature, and Daily Total Solar Radiation for the 20-Year Meteorological Data Used With the HELP2 Model

the final water contents from the year 1 simulation for each layer and a new 14-foot FGD layer with a 42 percent moisture content. The method used to create the initial conditions for the third, fourth, fifth, and sixth years were similar to those for the second year.

4.3 Model Results

Figure 4.3.1 shows the HELP2 predictions based on a 5-year averaging interval. Figures 4.3.2 and 4.3.3 show the effect of the dry stack design on the annual water budget components. As shown in Figure 4.3.2, runoff and evapotranspiration were unaffected by the presence of the clay liner. The closure cap had a significant effect on runoff but little effect on evaporation. For the four dry stack designs, the average leachate rate varied between 4.9 and 9.8 inches/year (Figure 4.3.3). With no closure cap, the average annual leachate was 9.8 and 8.9 inches/year for no soil liner and with a soil liner, respectively. With a closure cap, the leachate was 5.6 and 4.9 inches/year for no soil liner and with a soil liner, respectively. The stack design feature most effective in minimizing leachate was the clay cap, which acted to reduce leachate generation by approximately 50 percent relative to the uncapped scenarios for conditions of both a soil liner and no soil liner (Figure 4.3.3).

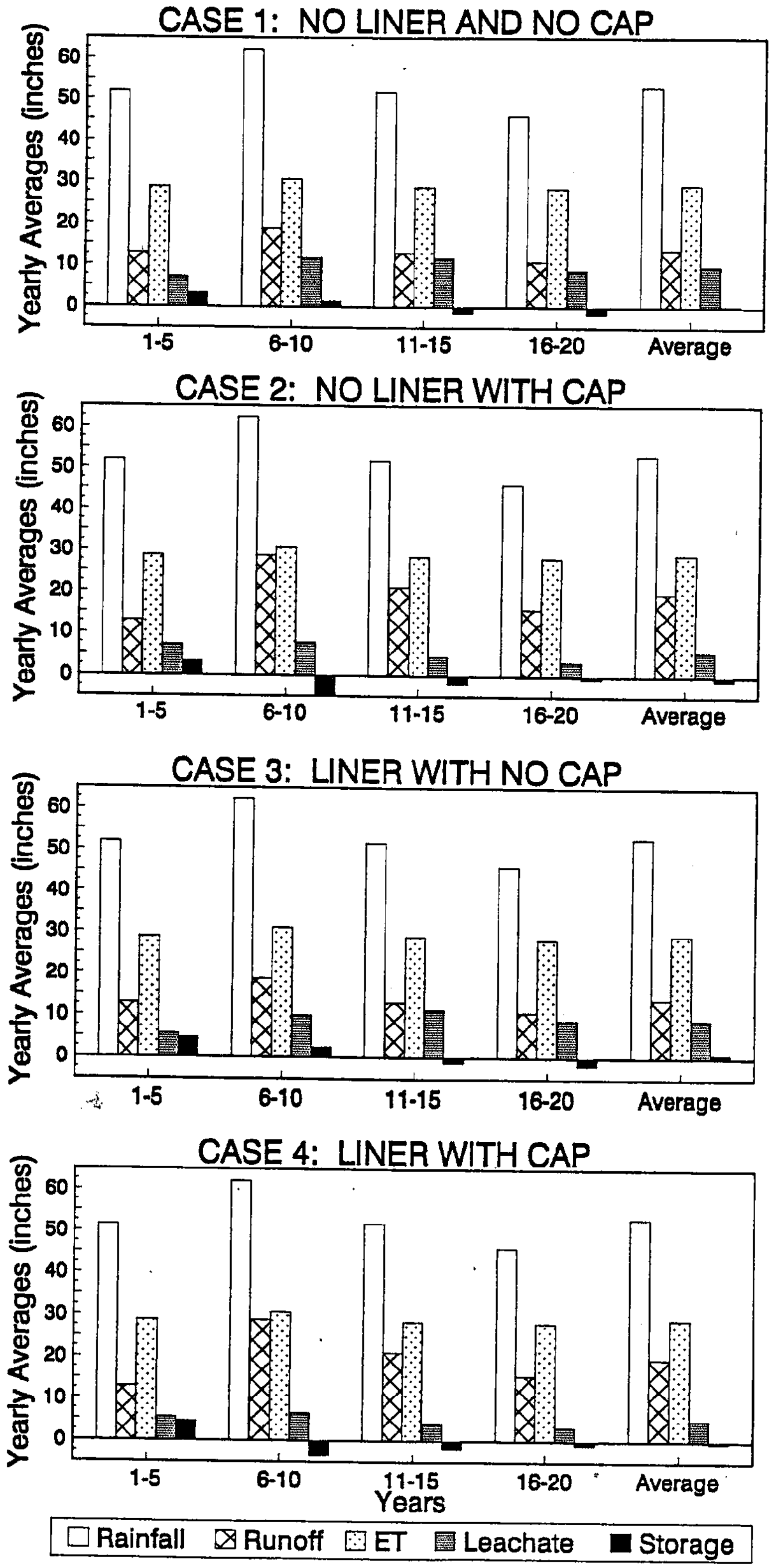

Figure 4.3.1. Five-Year Water Budget Averages Predicted by HELP2 for Four FGD Dry Stack Designs

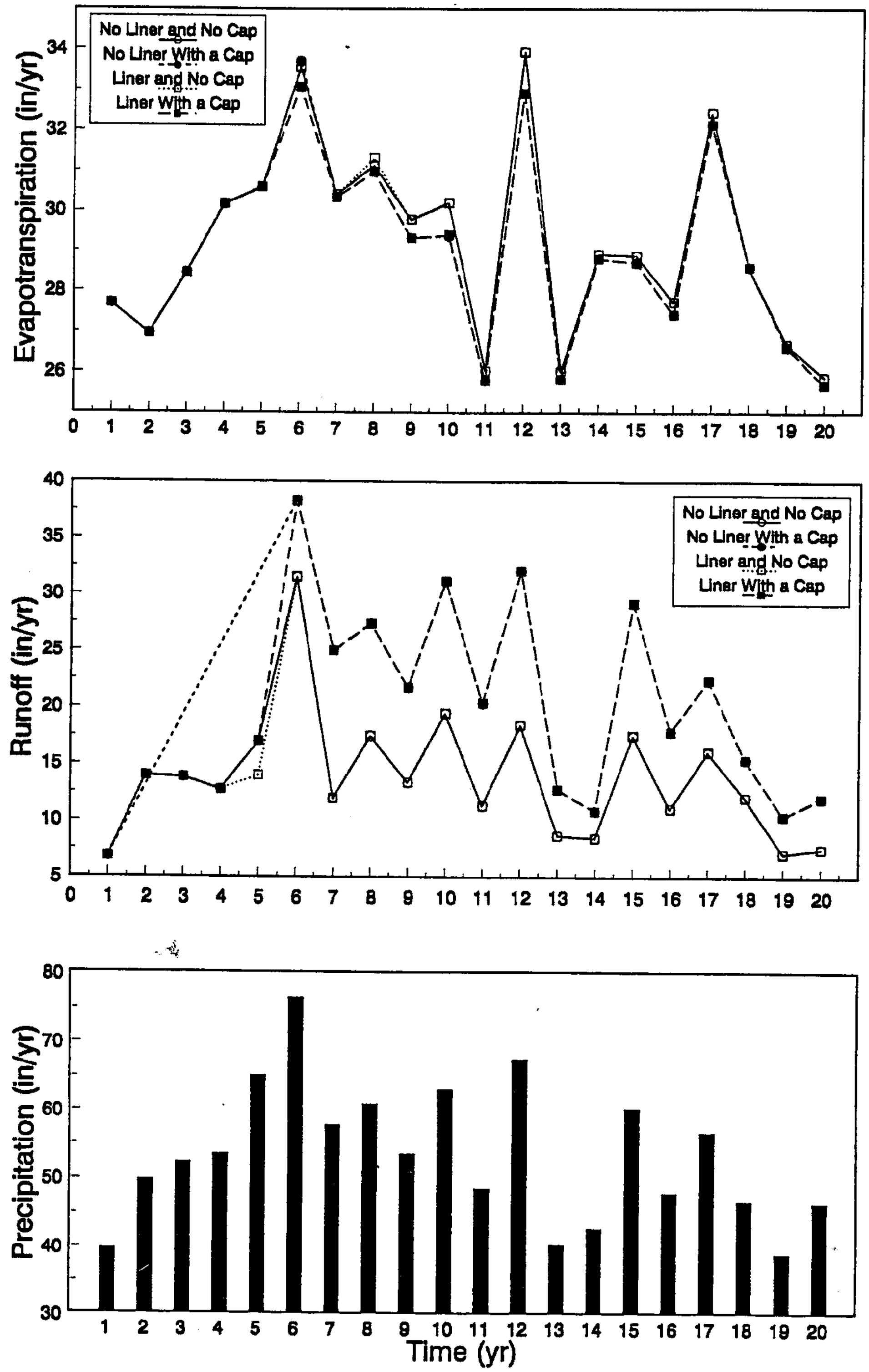

Figure 4.3.2. Annual Water Budgets Predicted by HELP2 for Runoff and Evapotranspiration for the Four FGD Dry Stack Designs

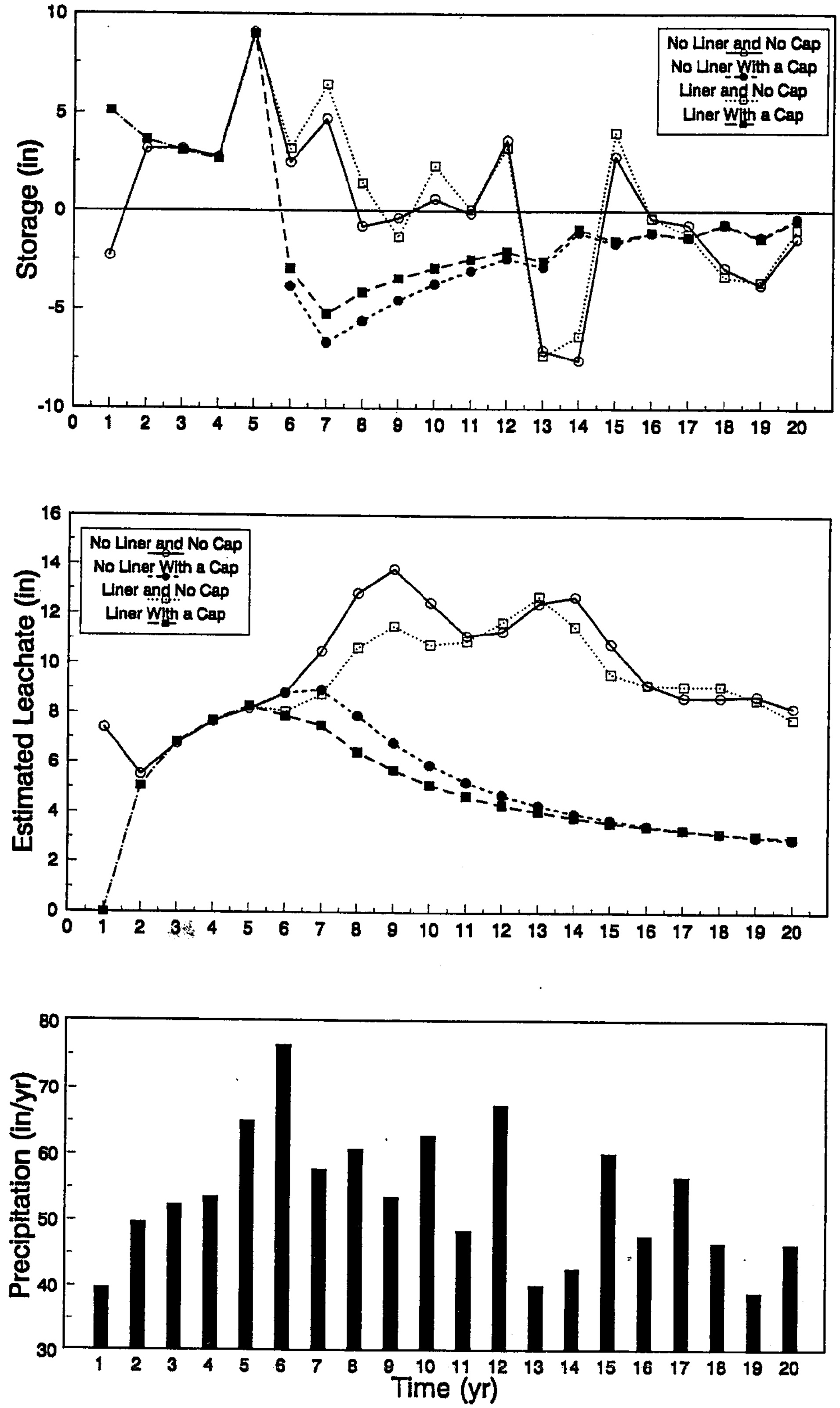

Figure 4.3.3. Annual Water Budgets Predicted by HELP2 for Storage and Estimated Leachate for the Four FGD Dry Stack Designs

5.0 REFERENCES

Bensiger, C. P., and J. M. Kellberg, 1951, "Preliminary Geological Investigations for Eastern Area Steam Plant," Division of Water Control Planning, Geologic Branch, Tennessee Valley Authority, Knoxville, Tennessee.

Brooks, R. H., and A. T. Corey, 1964, "Hydraulic Properties of Porous Media," Hydrology Paper 3, Colorado State University, Fort Collins, Colorado.

Campbell, S. G., 1974, "A Simple Method for Determining Unsaturated Hydraulic Conductivity From Moisture Retention Data," Soil Science, 117(6):311-314.

Carpenter, W. G., and C. E. Bohac, undated, "Kingston Environmental Assessment for Fly Ash Disposal," Tennessee Valley Authority, Chattanooga, Tennessee, TVA/WR/WQ-90/8.

Daniel B. Stephens & Associates, Inc., 1993, Laboratory Analysis of Soil Hydraulic Properties of Chloride-Rich FGD Waste, Report 793, Prepared for Tennessee Valley Authority, Albuquerque, New Mexico.

Foust, D. D., and S. C. Young, 1992, "Column Evaporation Studies With Fly Ash for the Evaluation of Numerical Water Budget Models," TVA Report WR28-1-520-181, Tennessee Valley Authority, Norris, Tennessee.

Harris, W. F., and S. Foxx, 1982, "Potential Ground-Water Quality Impacts at TVA Steam Plants," Report No. WR28-2-520-119, Tennessee Valley Authority, Norris, Tennessee.

Knisel, W. G., Editor, 1980, CREAMS, A Field Scale Model for Chemical Runoff and Erosion from Agricultural Management Systems, Volumes I, II, and III, Draft Copy, USDA-SEA, AR, Cons. Res. Report 24, 643 pp.

Milligan, J. D., and R. J. Ruane, 1980, "Effects of Coal Ash Leachate on Groundwater Quality," Report EPA-600-7-80-066, U.S. Environmental Protection Agency, Ada, Oklahoma.

Ritchie, J. T., 1972, "Model for Predicting Evaporation From a Fow Crop With Incomplete Cover," Water Resources Research, 8(5):1204-1212.

Schroeder, P. R., B. M. McEnroe, and J. Sjostrum, 1988, "Hydrologic Evaluation of Landfill Performance Model (Version 2)," Draft Report, U.S. Army Engineers Waterways Experiment Station, Vicksburg, Mississippi.

Tennessee Valley Authority, 1965, "The Kingston Steam Plant, a Report on the Planning, Design, Construction, Costs, and First Power Operations," Technical Report No. 54, Knoxville, Tennessee.

USDA, 1972, Conservation Service, National Engineering Handbook, Section 4, Hydrology, U.S. Government Printing Office, Washington, D.C.

Velasco, M. L., and C. E. Bohac, 1991, "Kingston Groundwater Assessment," Report No. WR28-1-36-115, Tennessee Valley Authority, Norris, Tennessee.

Young, S. C., 1989, "Leachate Generation From Dry Stacked Fly Ash at the Bull Run Fossil Plant, Part 1, Field Experiments," Report No. WR28-1-49-102, Tennessee Valley Authority, Norris, Tennessee.

Young, S. C., and M. L. Velasco, 1991, "Water Budget Predictions for an Active Fly Ash Dry Stack Using the HELP2 Model," Report No. WR28-1-49-106, Tennessee Valley Authority, Norris, Tennessee.

EPRI—*Leadership in Science and Technology*

ABOUT EPRI

The mission of the Electric Power Research Institute is to discover, develop, and deliver advances in science and technology for the benefit of member utilities, their customers, and society.

Funded through annual membership dues from some 700 member utilities, EPRI's work covers a wide range of technologies related to the generation, delivery, and use of electricity, with special attention paid to cost-effectiveness and environmental concerns.

At EPRI's headquarters in Palo Alto, California, more than 350 scientists and engineers manage some 1600 ongoing projects throughout the world. Benefits accrue in the form of products, services, and information for direct application by the electric utility industry and its customers.

Printed on Recycled Paper
Printed in USA

EPRI TR-101999 Hydraulic Properties of Coal Combustion Wastes Feb 19

EPRI
Electric Power
Research Institute

Keywords:
Solid waste disposal
Groundwater
Hydrodynamics
Leachate migration
Transport
Models

Attachment 2

01999
35-05
rt
393

Physical and Hydraulic Properties of Fly Ash and Other By-Products From Coal Combustion

Prepared by
Tennessee Valley Authority
Norris, Tennessee
and
Daniel B. Stephens & Associates, Inc.
Albuquerque, New Mexico

REPORT SUMMARY

Physical and Hydraulic Properties of Fly Ash and Other By-Products From Coal Combustion

Physical and hydraulic properties of six fly ashes and of wastes from flue gas desulfurization (FGD) and atmospheric fluidized-bed combustion (AFBC) have been compiled. Utilities can use this information to estimate leachate quantities.

INTEREST CATEGORIES

Land and water quality—hydrogeochemical modeling
Waste disposal and use
Land and water quality—chemistry and physics
Risk analysis, management, and assessment

KEYWORDS

Solid waste disposal
Groundwater
Hydrodynamics
Leachate migration
Transport
Models

BACKGROUND Approximately 80% of the electric utility industry's 80 million tons of coal combustion wastes—coal ash, coal bottom ash, oil ash, FGD sludge, and AFBC wastes—is disposed of in landfills or ponds. The movement of water through these disposal facilities dissolves chemicals and could potentially affect groundwater quality. To minimize environmental impact, utilities are reverting to dry stacking and are designing facilities with liners and leachate collection systems. The EPRI Solid Waste Environmental Studies Project has developed models—MYGRT™, FOWL™, and FASTCHEM™—for assessing the generation, transport, and fate of leachates from coal combustion waste disposal facilities. Affecting the ability of these models to accurately predict leachate volume and migration are the hydraulic and physical characteristics of the waste.

OBJECTIVES To compile the physical and hydraulic properties of fly ash, FGD sludge, and AFBC waste; and to review the laboratory methods used to measure these properties.

APPROACH The researchers gathered fly ash from six Tennessee Valley Authority (TVA) power plants as well as FGD and AFBC wastes from TVA's pilot plants. Laboratory tests were conducted with these materials to determine particle-size distribution, particle density, dry-bulk density, saturated hydraulic conductivity, moisture retention characteristic curves, and diffusivity. The laboratory-derived properties were compared with field measurements to provide some degree of validation for the data. Further, as another form of validation, the laboratory-measured hydraulic properties were used with two numerical models (one being EPRI FASTCHEM) to simulate a 20-day evaporation test on two fly ashes.

RESULTS The laboratory measurements were compiled and tabulated for easy use. From the standpoint of texture, the six fly ashes exhibited qualities of a silty loam. However, an examination of hydraulic properties revealed a range of saturated hydraulic conductivities from 1.33×10^{-5} to 1.51×10^{-4} cm/s, behavior more typical of finely textured soil. The researchers speculated that the occurrence of hydration reactions may have affected the retention of water in the FGD and AFBC wastes, rendering invalid conventional theories based on capillarity for estimating hydraulic diffusivity. A favorable validation of laboratory- and field-derived values of dry-bulk density and porosity was achieved. However, the comparison of saturated hydraulic conductivity produced variations of approximately a factor of two. In addition, the numerical models accurately simulated the 20-day evaporation experiment using laboratory-determined fly ash properties.

EPRI PERSPECTIVE For the first time, physical and hydraulic properties of several electric utility wastes have been compiled for use in the design and operation of waste disposal facilities. The information provided in this report will prove useful to environmental engineers involved in the estimation of leachate generation and in the design of collection and treatment systems. The FOWL code, version 2.0, provides the capability for simulating the geochemical reactions and hence the quality of the leachate generated from the leaching of coal combustion wastes. The FOWL code model as well as the EFLOW module of the FASTCHEM code package (EPRI report EA-5870-CCM, Vol. 2) can use the data developed by this study to predict the quantity of leachate to be handled by the collection and treatment systems.

PROJECT
RP2485-05
Project Manager: Dave A. McIntosh
Environment Division
Contractor: Tennessee Valley Authority

For further information on EPRI research programs, call EPRI Technical Information Specialists (415) 855-2411.

Physical and Hydraulic Properties of Fly Ash and Other By-Products From Coal Combustion

TR-101999
Research Project 2485-05

Final Report, February 1993

Prepared by
TENNESSEE VALLEY AUTHORITY
Engineering Laboratory
Norris, Tennessee 37828

Author
S. C. Young

DANIEL B. STEPHENS & ASSOCIATES, INC.
Albuquerque, New Mexico

Authors
R. Schmidt-Petersen
M. Ankeny
D. B. Stephens

Prepared for
Electric Power Research Institute
3412 Hillview Avenue
Palo Alto, California 94304

EPRI Project Manager
D. A. McIntosh

Land and Water Quality Studies Program
Environment Division

ORGANIZATION(S) THAT PREPARED THIS REPORT:
TENNESSEE VALLEY AUTHORITY
DANIEL B. STEPHENS & ASSOCIATES, INC.

ORDERING INFORMATION

Requests for copies of this report should be directed to the EPRI Distribution Center, 207 Coggins Drive, P.O. Box 23205, Pleasant Hill, CA 94523, (510) 934-4212. There is no charge for reports requested by EPRI member utilities and affiliates.

ABSTRACT

This report summarizes physical (e.g., specific gravity, bulk density) and hydraulic properties (e.g., moisture retention curves, saturated hydraulic conductivity) of six fly ashes, and wastes from Flue-Gas Desulfurization (FGD) and Atmospheric Fluidized Bed Combustion (AFBC) pilot plants. A review of the methods used to measure these properties is provided. The information can be used to estimate the properties of fly ash, AFBC by-products, or FGD by-products.

The physical and hydraulic properties are discussed in relation to natural soil properties and to several semi-empirical formulas to predict hydraulic properties. With regard to the soil textural triangle, all of the fly ash plot as silty loam. Because fly ash tends to be both well-sorted and have small-sized particles, they tend to have relatively high air entry values (e.g., a range between 100 to 400 cm potential) and relatively sharp breaks in the moisture retention characteristic curves. For similar reasons some of the AFBC and FGD by-products also have high air entry values >100 cm.

The Mualem coefficients α and N derived by fitting an analytical equation to moisture retention curves are useful for comparing fly ash properties to those of natural soils. The values α and N can be considered measures of the air entry value and of sorting, respectively. Tabulated values for α show that they vary from 0.0042 for silt loam to 0.12 for sand. The α for fly ash ranges from approximately 0.001 to 0.004. Compared to the α values for silty loam, the fly ash values are approximately an order of magnitude lower and therefore more typical of a finer textured soil. The tabulated N values for the six fly ash samples range from 1.18 for a silt loam to 5.8 for sand. The calculated N values range from 1.5 to 3.1 and thus fall within the broad range of N values calculated for natural soils.

Laboratory values of hydraulic diffusivity were compared to theoretical values calculated from values of α and N. A favorable comparison exists for two fly ash types--the remaining four have order-of-magnitude differences between the two curves. The greatest differences were observed for the AFBC and FGD wastes. In the FGD and AFBC wastes, chemical reactions are likely to occur and affect the retention of water. Reactions such as hydration of water could render useless equations for predicting hydraulic diffusivity curves that assume capillarity is the primary mechanism affecting water retention. In situations where chemical reactions occur that significantly affect the movement of water (such as the AFBC by-

products), the hydraulic diffusivity curve should not be calculated by conventional theories based on capillarity.

A concern with laboratory methods for characterizing hydraulic properties of porous media is whether the laboratory-determined properties are representative of field conditions. TVA has conducted field and laboratory studies to check the representativeness of the laboratory measured parameters. In one study, three different methods were used to estimate the saturated hydraulic conductivity in dry stacked fly ash. The methods were (1) laboratory permeameter measurements on undisturbed cores from the dry stack, (2) in situ measurements in the dry stack with a Guelph permeameter, and (3) laboratory permeameter measurements on packed fly ash obtained directly from the plant's precipitators. The variation in the averaged value of saturated hydraulic conductivity for these methods was about a factor of two. Two factors that could have caused such a range are spatial variability and different degrees of saturation within the different fly ash samples being tested.

CONTENTS

ILLUSTRATIONS

LIST OF SYMBOLS AND ABBREVIATIONS

Symbols

ρ	density (M/L^3)
η	porosity (-)
μ	dynamic viscosity (M/LT)
C_u	uniformity coefficient (-)
d	particle diameter (L)
ψ	potential representing negative pressure expressed in terms of an equivalent water column height (M/LT^2)
θ	water content (M/L^3)
$K(\theta)$	K as a function of water content (L/T)
K	hydraulic conductivity (L/T)
K_{SAT}	saturated hydraulic conductivity (L/T)
$K(\psi)$	K as a function of potential (L/T)
K_r	$K(\psi)/K_{SAT}$ or $K(\theta)/K_{SAT}$ = relative hydraulic conductivity (-)
$C(\theta)$	specific water capacity = $\gamma\theta/d\psi$ (1/L)
$D(\theta)$	$K(\theta)/C(\theta)$

Abbreviations

TVA	Tennessee Valley Authority
EPRI	Electric Power Research Institute
ASTM	American Society for Testing and Materials
AFBC	Atmospheric Fluidized Bed Combustion
FGD	Flue-Gas Desulfurization
SBM	Spent Bed Material
IDC	Initial Drainage Curve
MWC	Main Wetting Curve
MDC	Main Drainage Curve

1

INTRODUCTION

1.1 Objective and Scope

This report summarizes physical and hydraulic properties of fly ash from six Tennessee Valley Authority (TVA) power plants and of wastes produced from TVA Flue-Gas Desulfurization (FGD) and Atmospheric Fluidized Bed Combustion (AFBC) pilot plants. The report provides measured physical properties (e.g., specific gravity, bulk density), and measured hydraulic properties (moisture retention curves, saturated hydraulic conductivity, diffusivity) for the selected by-products and reviews the laboratory methods used to measure the properties. The laboratory-determined properties were validated with experimental data and numerical modeling. The information can be used to design a characterization study for fly ash, AFBC by-products, or FGD by-products.

1.2 Coal Combustion By-Products

The electric utility industry produces more than 80 million tons of coal-combustion wastes annually (ACAA, 1988). While carbon and some of the other elements in coal may be completely oxidized or volatilized during coal combustion, a large portion of the mineral matter is transformed into residual by-products. Residual by-products consist of noncombustible mineral matter initially present in the coal and to a lesser extent partly combusted coal. These by-products include slag, bottom ash, and fly ash.

Figure 1-1a is a schematic of a typical solid control system for the removal and collection of slag, bottom ash, and fly ash during coal combustion. Slag and bottom ash accumulate in the bottom of the boiler. Slag is a glassy, angular mostly non-crystalline material that accumulates as the coal residue melts to a viscous liquid and is quenched for removal. Bottom ash is the residue that exists in a solid granular form. Fly ash is the portion of the residue that becomes entrained with the flue gas. About 70 to 80 percent of the solid waste derived from the combustion of coal is fly ash (EPRI, 1979). Fly ash is primarily an aluminosilicate glass that contains oxides and salts of iron, calcium, sodium, magnesium and other metals. Typically 65 to 90 percent of fly ash is finer than 0.010 mm. The percentage depends upon the type of coal, removal system, and boiler (EPRI, 1979).

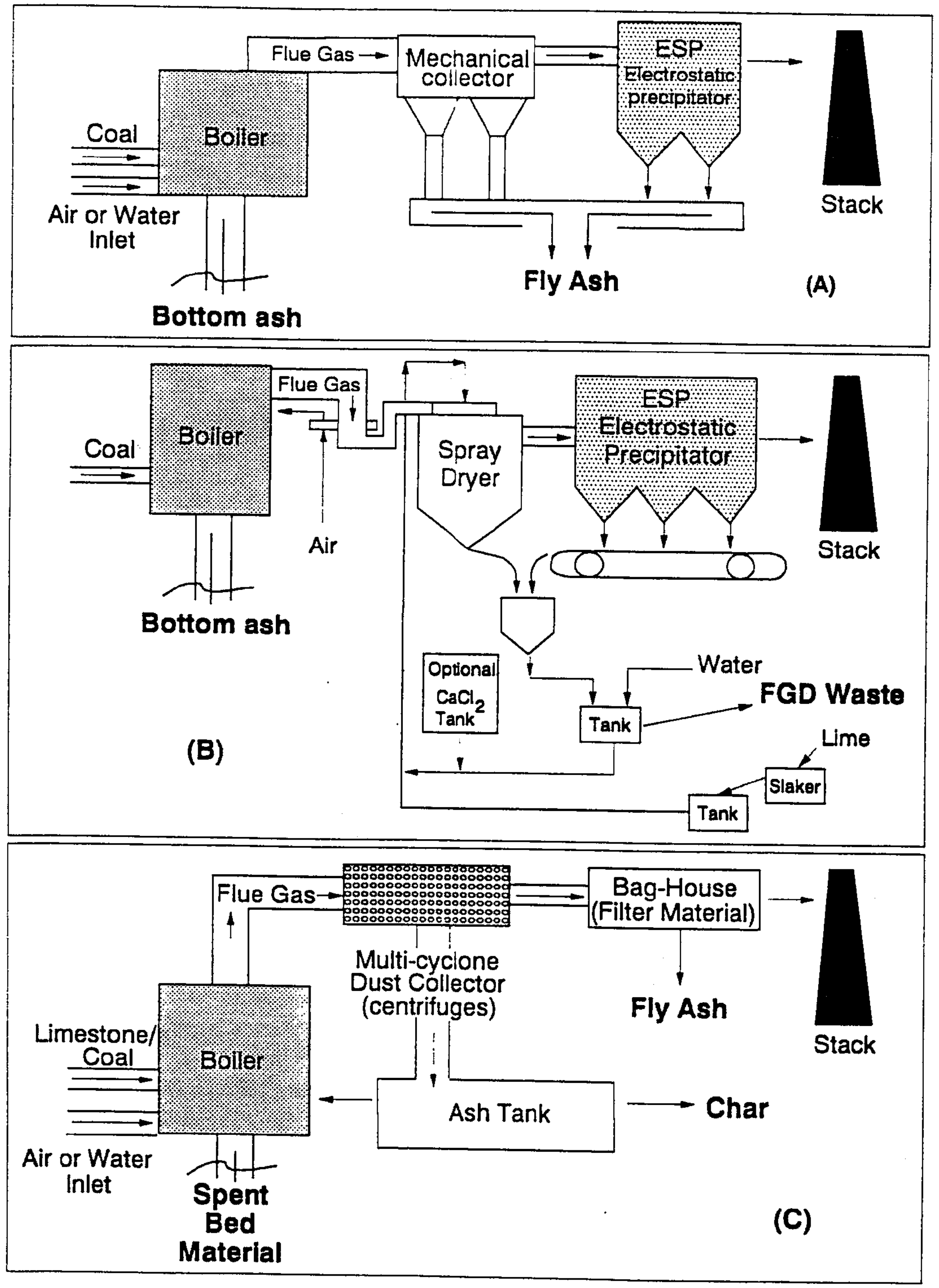

Figure 1-1. Schematics for Solid Control System For Removal of Coal-Combustion By-Products

Approximately 80 percent of fly ash is disposed in landfills or ponds (Simsiman et al., 1987). State and Federal regulations pertaining to groundwater quality protection encourage designing and operating disposal areas that have minimal environmental impact. To help minimize the impact of fly ash disposal on groundwater resources, the Tennessee Valley Authority (TVA) has converted from ponding to dry stacking fly ash at several of its plants. Since 1986, TVA has conducted a series of field and laboratory studies to assist in the design of the fly ash dry stacks. These studies have included fly ash from six different plants and by-products produced from pilot plant operations for Atmospheric Fluidized Bed Combustion (AFBC) and Flue-Gas Desulfurization (FGD). The purpose of AFBC and FGD is the reduction of atmospheric sulfur emissions.

Figure 1-1b is a schematic for a standard and a chlorine-enhanced FGD process. The FGD process includes spraying the flue gas with a fine mist of a calcium hydroxide solution ($Ca(OH)_2$) to remove sulfur dioxide from the flue gas. Studies have shown that the removal of atmospheric sulfur in the spray dryer is enhanced by adding chlorine to the calcium hydroxide enriched mist. The enhanced method is referred to as High-Chloride FGD. Table 1-1 lists the chemical composition for FGD and the High-Chloride FGD wastes characterized in this report.

Figure 1-1c is a schematic for the AFBC process. The AFBC process includes burning the coal with crushed limestone to inhibit the release of sulfur dioxide into the flue gas. Three wastes, spent bed material, char, and fly ash, are produced by the AFBC process. The AFBC spent bed material is a mixture of coal and limestone residue not entrained into the flue gas. The AFBC char is composed of the particulates that can be removed from the flue gas by a series of small centrifuges. The AFBC fly ash is composed of the fine particulates in the flue gas that cannot be collected by the centrifuges but can be collected by passing the flue gas through a fabric filter. Table 1-1 lists the chemical composition for the AFBC by-products used in this report.

TABLE 1-1

Chemical Composition for AFBC By-Products
and AFBC Wastes

	$CaSO_4$	CaO	$CaCO_3$	$CaSO_3$	$Ca(OH)_2$	Alumino-silicates	Carbon[+]	Water
FGD	9%	1%	11%	44%	15%	16%	–	4%
High-Chloride FGD	7%	4%	13%	48%	9%	15%	–	8%
AFBC								
Spent Bed Material	46-60%	22-40%	3-8%		–	–	4%	–
Char	26-30%	26-30%	5-10%		–	–	4-12%	–
Fly Ash	28-30%	26-35%	4-11%		–	–	5-9%	–

[+]primarily unburned coal

2

PARAMETERS AND METHODS

Laboratory tests were conducted to determine particle density (specific gravity), particle size distribution, dry bulk density, saturated hydraulic conductivity, moisture retention characteristic curves, and diffusivity for bulk samples of fly ash and other coal combustion by-products. Appendices A and B include the tabulated and graphical data for the measured parameters. Described herein are the laboratory methods used by Daniel B. Stephens & Associates to measure the reported results listed in the appendices.

2.1 Particle Density

Particle density is the density of a solid. It is expressed as the ratio of the total mass of the solid particles to the total volume occupied by the solids. Specific gravity is the ratio of the particle density to the density of water (i.e.,.1 g/cm^3) and is dimensionless. Knowledge of the particle density and the given bulk density of a soil allows the porosity of the bulk material to be calculated.

The water pycnometer method was used to determine particle densities for the fly ash. It is appropriate for determining particle density in most soils except those which contain extraneous matter (such as cement, lime, etc.), water soluble matter (such as sodium chloride), and soil containing matter with a specific gravity less than one. The fly ash is mainly aluminosilicate, but contains varying amounts of extraneous matter. Methods and procedures, outlined under ASTM Standard D854-83, are followed to determine the particle density of soils that pass through the No. 4 sieve using the water pycnometer method.

In the laboratory, a clean, dry pycnometer including its stopper is weighed. The pycnometer is a volumetric flask having a capacity of 250 ml. Initially, the soil sample is oven dried, then passed through a No. 10 sieve. Approximately 50 g of oven-dried soil is added to the pycnometer. Clay soil samples must be dispersed in distilled water following methods outlined in ASTM Standard D422 (Method of Particle Size Analysis of Soils). The outside and neck of the pycnometer are cleaned of any soil that may have spilled during transfer. The pycnometer, stopper, and contents are weighed. The pycnometer is then filled about half full with distilled water. Care is taken to wash any soil adhering to the inside of the neck into the flask. Any entrapped air is removed by gently boiling the soil/water solution for a minimum of 10 minutes with frequent gentle agitation of the contents. Distilled water is added to fill the pycnometer to a prescribed volume, and the outside is thoroughly dried. The pycnometer and its contents are weighed, and the temperature observed.

The soil/water mixture is removed from the pycnometer, and the flask is thoroughly washed. The weight of the pycnometer filled with distilled water at the observed temperature is determined from the calibration curve of the pycnometer.

Calibration curves are obtained for each pycnometer by obtaining at least three sets of temperature and weight measurements, about 4°C apart, within the temperature range of 20° to 30°C. Each set represents the coordinates for a point on the calibration curve. To obtain the calibration curve, a clean pycnometer is filled with de-aired distilled water so that the meniscus is at the calibration mark. Then, heat is applied to the pycnometer and the weight and temperature are recorded, making sure the water level is at the calibration mark. After several readings have been taken, temperature vs. weight of pycnometer and water are plotted. Then, a best fit curve is drawn through the points.

The particle density is calculated as follows:

$$\rho_s = \rho_w \frac{(M_s - M_a)}{(M_s - M_a) - (M_{sw} - M_w)}$$

where

ρ_s = particle density (g/cm^3)
ρ_w = density of water at observed temperature (g/cm^3)
M_s = mass of pycnometer plus oven-dried soil (g)
M_a = mass of pycnometer filled with air (g)
M_{sw} = mass of pycnometer filled with soil and water (g)
M_w = mass of pycnometer filled with water at observed temperature (g)

2.2 Dry Bulk Density

The dry bulk density of a soil sample is the mass of the oven dried soil per initial unit volume of soil. The dry bulk density increases as the sample is compacted. Knowledge of the particle density and bulk density allows for the calculation of porosity which, in turn, yields information concerning the consolidation of soils. Procedures described by Blake and Hartge (1986) and ASTM D4531-86 are followed to determine dry bulk density. Dry bulk density is calculated from the initial soil sample volume and oven dried mass of the soil sample. The sample mass is determined from methods outlined in ASTM D2216-80 (oven drying) or ASTM D4643-87 (microwave-oven drying).

The dry bulk density is calculated as follows:

$$\rho_b = \frac{M_d}{V_T}$$

where

ρ_b = dry bulk density (g/cm^3)
M_d = mass of oven dried soil sample (g)
V_T = total volume of soil sample (cm^3)

2.3 Particle Size Distribution

The distribution of soil particles in a sample is determined by standard sieve and hydrometer analysis. Methods and procedures outlined under ASTM D421-85 are followed to determine the particle size distribution of particles larger than 75 μm using the mechanical sieve technique. Distribution of particles smaller than 75 μm are determined using the hydrometer sedimentation analysis as outlined under ASTM D422-63(72).

2.3.1 *Dry Sieve Method*

A soil sample is separated into a series of fractions from 4.75 mm (No. 4) to 0.075 mm (No. 200) by mechanical sieve procedures. The sieve operates by means of lateral and vertical jarring motions shaking the soil sample through a series of finer sieves. Mechanical sieving is considered complete when less than 1 percent of the mass fraction passes a sieve during a one-minute hand sieving test.

A plot of the grain size accumulation curve is developed from the mass retained on each sieve and data from the hydrometer analysis. This plot is used to estimate the d_{10}, d_{16}, d_{30}, d_{50}, d_{60}, and d_{84} diameters (d_x is the diameter of a particle of which x percent of the sample mass is finer). These soil particle diameters are used to calculate the uniformity coefficient, Cu:

$$Cu = \frac{d_{60}}{d_{10}}$$

2.3.2 *Hydrometer Analysis*

Hydrometer analyses are performed in accordance to ASTM D-422-63(72). A soil sample of approximately 50 grams for silts and clays, or 100 grams for sands, is mixed for a minimum of 3 minutes in a solution of sodium hexametaphosphate. The mixture is then soaked for a minimum of 16 hours in a hydrometer jar. At the end of the soaking period, the sample is dispersed further by shaking the sample in the jar, then distilled water is added until the total volume is 1000 ml. The glass cylinder is turned upside down and back for one minute to complete agitation. Hydrometer readings are taken at ASTM-recommended times for a period of 24 hours.

The percentage of soil remaining in suspension at the level at which the hydrometer measures, P, is calculated as follows:

$$P = \frac{Ra}{W} x\ 100$$

where

P	=	percentage of soil remaining in suspension at the level at which the hydrometer measures the density of the suspension
R	=	hydrometer reading with composite correction applied
a	=	correction factor for particle density other than 2.65 applied to the readings of the 152H hydrometer [ASTM D 422-63 (72)]
W	=	oven-dried mass of the soil sample

The diameter of a particle corresponding to the above calculated percentage is calculated as follows:

$$d = K\sqrt{\frac{L}{T}}$$

where

d	=	diameter of the particle (mm)
K	=	a constant depending on temperature and specific gravity of the soil particles [ASTM D 422-63(72)]
L	=	distance from the suspension surface to the level where the suspension is being measured (cm)
T	=	time since the beginning of sedimentation (min)

A grain size accumulation curve is developed from the above data and data from the sieve analysis. However, only the points less than 75 μm diameter are plotted from the hydrometer data. This plot is used to estimate the d_{10}, d_{16}, d_{30}, d_{50}, d_{60}, and d_{84} diameters (d_x is the diameter of a particle of which x percent of the sample mass is finer). These soil particle diameters are used to calculate the uniformity coefficient, Cu.

2.4 Saturated Hydraulic Conductivity

Saturated hydraulic conductivity is a measure of a soil's capability to transmit water. It is dependent upon both the soil and fluid properties in question. Saturated hydraulic conductivity may be estimated as (Freeze and Cherry, 1979):

$$K_{sat} = \frac{Cd^2\rho g}{\mu}$$

where

K_{sat}	=	saturated hydraulic conductivity (cm/s)
C	=	constant
d	=	median grain diameter (cm)
ρ	=	fluid density (g/cm^3)
g	=	gravitational constant (cm/s^2)
μ	=	dynamic viscosity of fluid (g/cm/s)

The term "Cd^2" is a function of the soil, while μ and ρ are functions of the fluid. In natural soils, K_s varies over 13 orders of magnitude. An equation to describe saturated groundwater flow is Darcy's law (Freeze and Cherry, 1976):

$$Q = -K_{sat}A\ \frac{dh}{dl}$$

where

Q	=	volumetric discharge (L^3/T)
K_{sat}	=	saturated hydraulic conductivity (L/T)
A	=	cross-sectional area (L^2)
dh/dl	=	hydraulic gradient (L/L)

Sections 2.4.1 and 2.4.2 describe laboratory methods of determining K_s utilizing Darcy's law. Section 2.4.1 describes the constant head method outlined in ASTM D2434-68. Section 2.4.2 describes the falling head method outlined by Klute and Dirksen (1986).

2.4.1 *Constant Head Method*

The constant head permeameter is best suited for materials with a saturated hydraulic conductivity in the range of 1 to 10^{-5} cm/s which corresponds to soils from gravel to silty sand, respectively. At low flow rates (lower K soils), measurement error increases and the falling head method is utilized.

A soil sample, of length L and cross-sectional area A, is placed in a sample holder which prevents soil loss or volume change (Fig. 2-1). The soil sample is saturated with 0.01N $CaCl_2$ solution using vacuum flooding techniques. During the test a 0.01N $CaCl_2$ solution is used to maintain a constant head differential across the sample. Periodic readings of the volumetric outflow are taken until stable values for saturated hydraulic conductivity, K_s, are obtained.

The temperature of the water is measured with a thermometer. The kinematic viscosity of the fluid is corrected to 20°C and is then applied to the calculation of saturated hydraulic conductivity. Darcy's equation is used to calculate the saturated hydraulic conductivity as follows:

$$K_s = \left[\frac{Q}{A}\right] \left[\frac{\Delta L}{\Delta H}\right] \left[\frac{\nu_T}{\nu_{20}}\right]$$

where

- K_s = saturated hydraulic conductivity @ 20°C (cm/s)
- Q = volumetric outflow from soil sample (cm^3/s)
- A = cross-sectional area of the soil sample (cm^2)
- ΔL = length of the soil sample (cm)
- ΔH = head differential across the soil sample (cm)
- ν_T = kinematic viscosity of water at the measured temperature (m^2/s)
- ν_{20} = kinematic viscosity of water at 20°C (m^2/s)

2.4.2 *Falling Head Method*

Saturated hydraulic conductivity determined by the falling head method is based on a boundary value problem that describes one-dimensional transient flow across a soil sample. Due to constraints on the apparatus size and time, the falling head method is best suited for

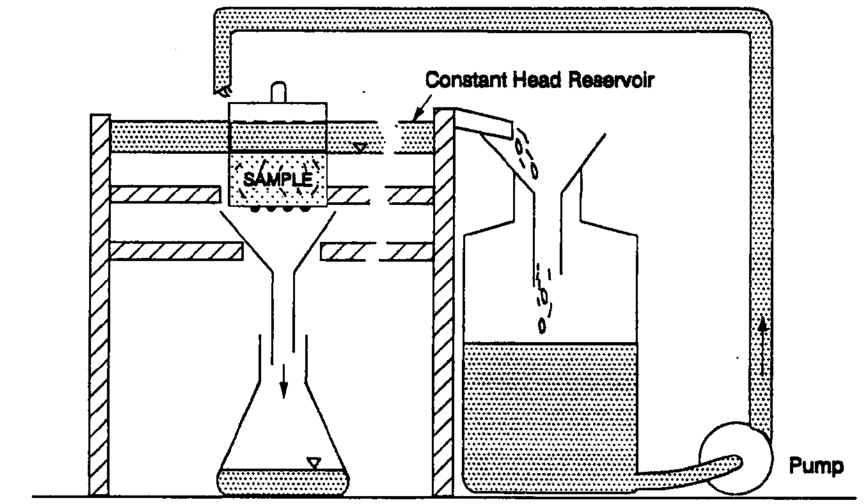

Figure 2-1. Constant Head Apparatus for Saturated Hydraulic Conductivity (Modified from Klute and Dirksen, 1986)

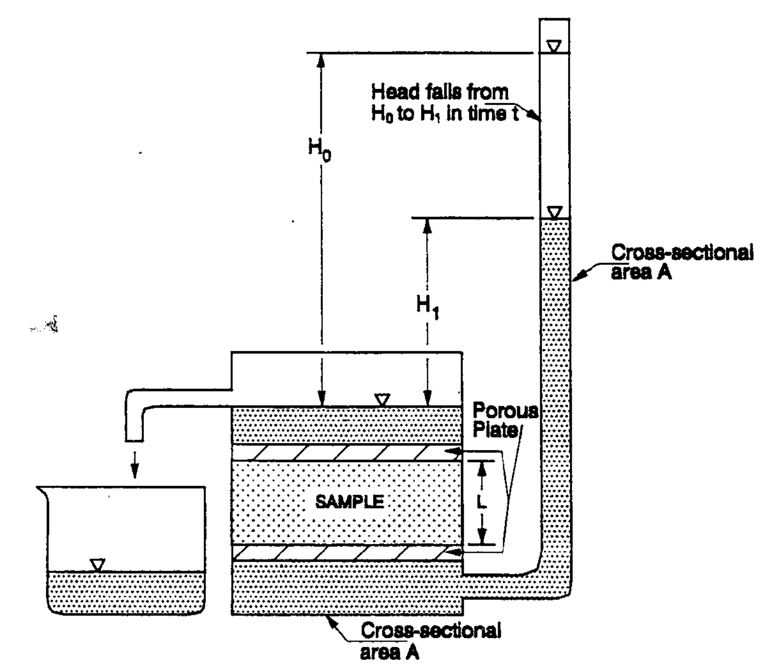

Figure 2-2. Falling Head Apparatus for Saturated Hydraulic Conductivity (Modified from Klute and Dirksen, 1986)

soil with a saturated hydraulic conductivity in the range of 10^{-3} to 10^{-7} cm/s which corresponds to soils from sand to clay, respectively.

A soil sample, of length L and cross-sectional area A, is placed in a sample holder, which prevents soil loss or volume change (Fig. 2-2). The soil sample is saturated in a 0.01N $CaCl_2$ solution using vacuum flooding techniques. The same 0.01N $CaCl_2$ solution is used throughout the test. After saturation, a standpipe is connected, and the rate of water drop in the standpipe is recorded.

The temperature of the water is measured with a thermometer. The kinematic viscosity of the fluid is corrected to 20°C and is then applied to the calculation of saturated hydraulic conductivity.

The head measured in the standpipe, of cross-sectional area A, is allowed to fall from H_0 to H_1 during time t (Fig. 2-2). The saturated hydraulic conductivity is calculated as follows:

$$K_s = \left[\frac{aL}{At}\right]_{\ell n} \left[\frac{H_0}{H_1}\right] \left[\frac{\nu_T}{\nu_{20}}\right]$$

where

- K_s = saturated hydraulic conductivity at 20°C (cm/s)
- a = cross-sectional area of the standpipe (cm^2)
- L = length of the soil sample (cm)
- A = cross-sectional area of the soil sample (cm^2)
- t = time for head to fall from H_0 to H_1 (s)
- H_0 = head at experiment start (cm)
- H_1 = head at experiment end (cm)
- ν_T = kinematic viscosity of water at the measured temperature (cm^2/s)
- ν_{20} = kinematic viscosity of water at 20°C (cm^2/s)
- ℓn = natural log

2.5 Moisture Characteristic Curves

Moisture retention characteristic curves describe the relationship between soil/water content and soil/water potential. Reeve and Carter (1991) states moisture retention curves: (1) indicate the ability of a soil to store water; (2) indicate the aeration status of a drained soil; and (3) in non-swelling soils, are used to estimate the pore size distribution.
Because the moisture characteristic curves reflect the pore geometry of the soil, which largely determines the hydraulic transport properties, the moisture characteristic curves can be used to estimate the unsaturated hydraulic conductivity function.

Two laboratory methods, the hanging column and pressure plate, are generally used to determine the moisture characteristic curves. The hanging column is used in the potential range from zero to approximately 200 cm of water while pressure plates extend the relationship to 15 bars.

2.5.1 Hanging Column Method

The key component of the hanging column apparatus for measuring the retention of water at different pressure heads or pore size distributions is a fritted glass porous plate (Fig. 2-3). The plate conducts water but, when wet, is impermeable to air at low pressures. Fritted glass plates have an air-entry pressure of about 300 to 400 cm of water. These plates are affixed to a glass funnel, which is connected to a burette with a stopcock by means of flexible tubing. A soil sample is placed on the plate and potential (ψ) is applied to the sample by positioning the fluid in the burette at different levels below the center of the sample. Water flows out of the sample, into the burette, until equilibrium is achieved. The potential is again increased or decreased to obtain another state of equilibrium between water held by capillary forces in the sample and the applied potential.

To make a measurement, air is first removed from the porous plate by allowing de-aired water to pass continuously through it for 24 hours. The funnel with the porous plate, and the burette are supported on vertical rods by means of clamps. A saturated soil sample within its sample ring is then placed on the porous plate, assuring that good hydraulic contact is established between the soil particles and the plate. With the stopcock of the burette closed, the initial level of the water in the burette is recorded.

The burette is then lowered a small increment to about 10 to 15 cm below the center of the soil sample. When the stopcock is opened, the soil will begin to desaturate, and the drainage will flow into the burette. After 24 hours, the drainage is assumed to have ceased. The stopcock is closed and the water level in the burette is recorded, along with the weight of the sample and the vertical distance from the bottom of the meniscus of the water in the burette to the middle of the soil sample. The procedure is repeated in a stepwise manner until the maximum potential desired (up to 200 cm) is reached. A reversal of the process is used to gather data on the wetting behavior of the sample. The laboratory procedures are similar to those described by Klute (1986).

Saturated water content (volume percent) is calculated as follows:

$$\theta_{sat} = \frac{M_{sat} - M_{dry}}{V_T \; x \; \rho_w} \; x \; 100$$

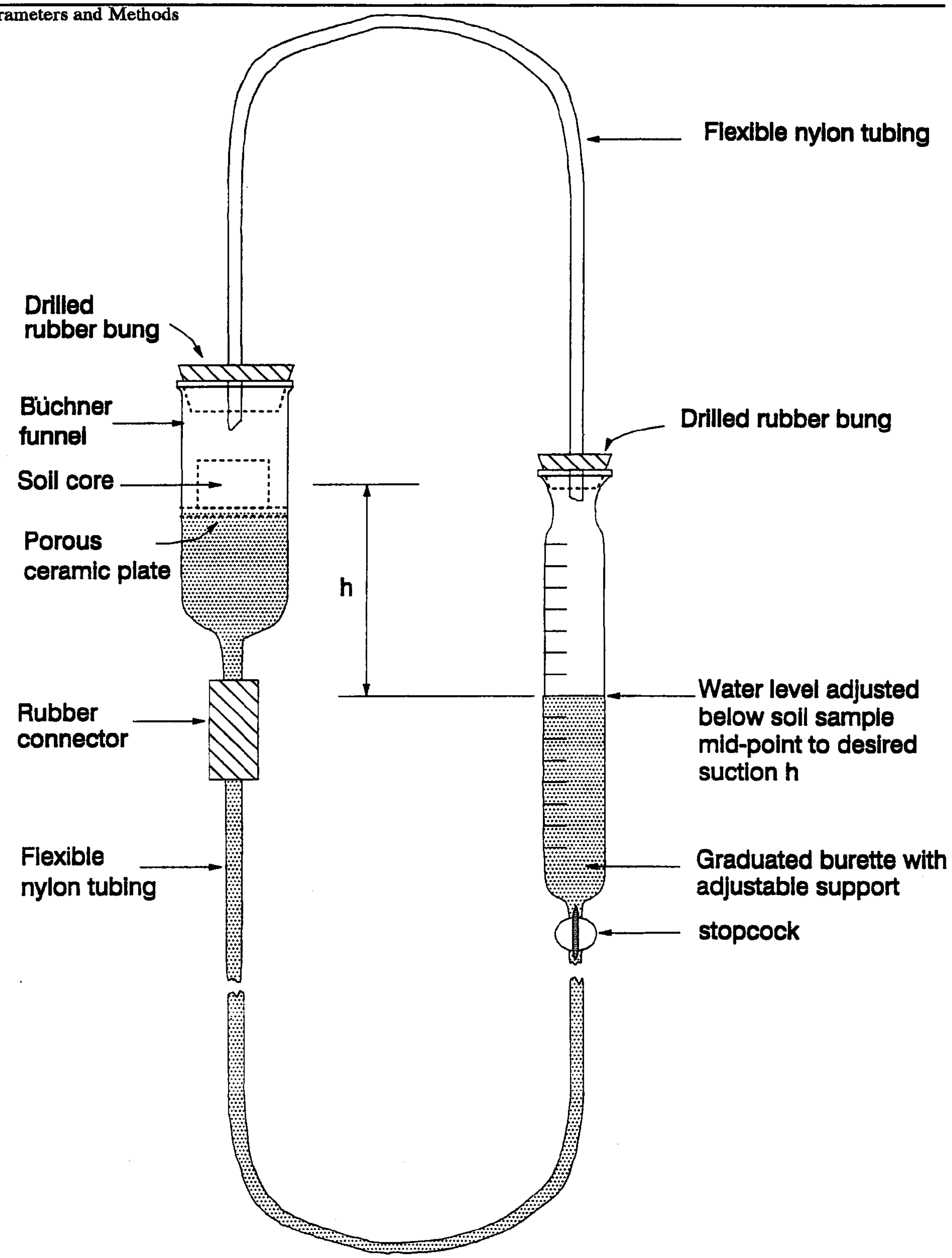

Figure 2-3. Hanging Column Apparatus for Measuring Moisture Retention Curves (Modified from Klute, 1986)

where

θ_{sat} = saturated volumetric water content (%, cm^3/cm^3)
M_{sat} = mass of sample, saturated (g)
M_{dry} = mass of sample, oven dried to a constant weight (g)
V_T = volume of the sample (cm^3)
ρ_w = density of the water at temperature when saturated mass was determined (g/cm^3)

The quantity $[M_{sat} - M_{dry}]/\rho_w$ is the volume, in cubic centimeters, of water initially contained in the sample volume. The drainage is subtracted from the initial volume of water, and then divided by the sample volume, to arrive at the water content in percent volume at the given value of potential.

$$\theta_\psi = \frac{V_i - V_D}{V_T} x \ 100$$

where

V_i = initial volume of water (cm^3)
V_D = cumulative volume of water drained from sample (cm^3)
V_T = volume of sample (cm^3)
θ_ψ = water content at the potential value ψ (%cm^3/cm^3)

This then gives a paired set of values of potential, or pressure head, versus volumetric water content.

2.5.2 *Pressure Plate Method*

Methods and procedures outlined under ASTM D2325-68 (81) and ASTM D3152-72 are followed to determine the moisture retention characteristics in the 1- to 15-bar suction range. Moisture retention characteristics are obtained using a pressure plate extractor (Soil Moisture Inc., Santa Barbara, CA, Model 1500), with a 1-, 3-, or 15-bar ceramic plate. Pressure is provided by high pressure nitrogen from cylinders.

A porous ceramic plate of the desired suction range is placed in a shallow pan with de-aired distilled water and allowed to saturate overnight. The ceramic plate is then removed from the pan and placed in the pressure plate extractor. De-aired distilled water is poured over the plate to slightly submerge the plate. The pressure plate is sealed and pressure brought to 50 percent of the plate's maximum rated pressure. This pressure is maintained until outflow ceases. The extractor is opened and any excess water around the plate is removed.

Up to 10 soil samples in their sample rings are then placed on the plate, while assuring that good hydraulic contact is established. The extractor is sealed and the pressure step is imposed. The pressure is maintained until outflow ceases. The extractor is then opened and the samples weighed quickly on an electronic top-loading balance. Subsequently, the samples are returned to the extractor, and the pressure is increased to the next increment. Figure 2-4 is a schematic for a typical pressure plate set-up.

The decrease in the water volume in the sample during a period of applied pressure is used to calculate the water content at that pressure as follows:

$$\theta_p = \frac{V_i - \Sigma V_w}{V_T} \; x \; 100$$

where

θ_p = water content at pressure p (% vol)
V_i = initial volume of water in the sample (cm^3)
ΣV_w = cumulative water volume change (cm^3)
V_T = total volume of the sample (cm^3)

2.6 Diffusivity

Measurements of diffusivity are used extensively in evaporation studies and are an indirect means of estimating the unsaturated hydraulic conductivity function. It is defined as

$$D(\theta) = \frac{K(\theta)}{C(\theta)} = K(\theta)\frac{d\psi}{d\theta}$$

where

$D(\theta)$ = hydraulic diffusivity at θ (L^2/T)
$K(\theta)$ = hydraulic conductivity at θ (L/T)
$C(\theta)$ = specific water capacity at θ = $(d\theta)/(d\psi)$ (L^{-1})

Here, hydraulic diffusivity describes the mass flow of water and should not be confused with the diffusive transfer of components in the gaseous and liquid phases as in the classical concept of diffusivity. An advantage of using hydraulic diffusivity, however, is that its range of variation is much smaller than that of hydraulic conductivity. Diffusivity generally ranges over 3 to 4 orders of magnitude, from near 1 cm^2/day to 10^4 cm^2/day (Hillel, 1971).

Methods and procedures outlined by Klute and Dirksen (1986) and Bruce and Klute (1956) are followed to determine diffusivity. Air-dried soil of known water content, is packed into a 30-cm long sectioned plastic column with a diameter of approximately 2.5 cm (Fig. 2-5).

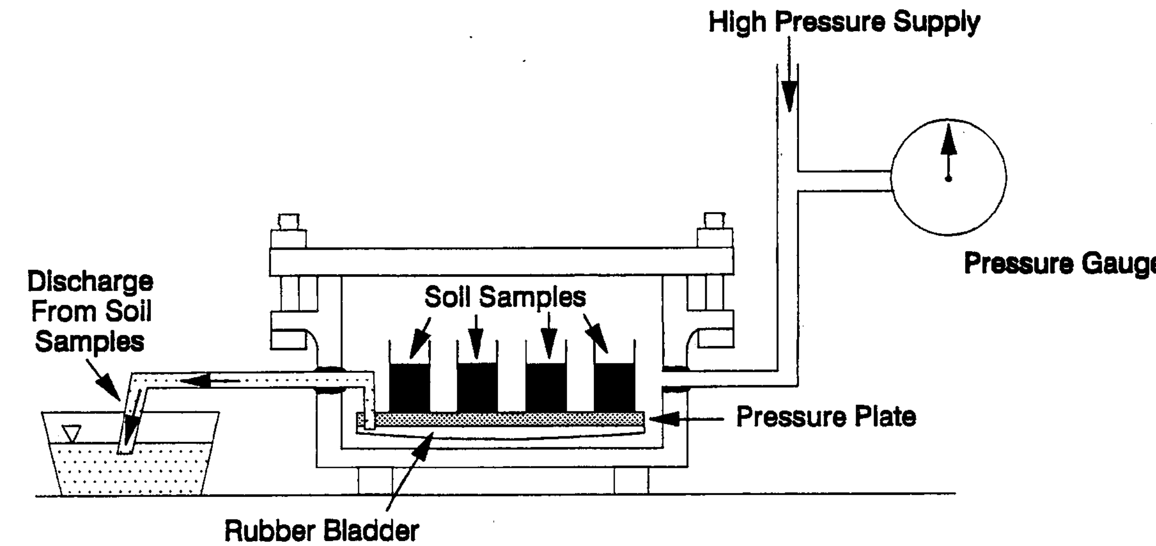

Figure 2-4. Experimental Set-Up for the Pressure Plate Method (Modified from Klute, 1986)

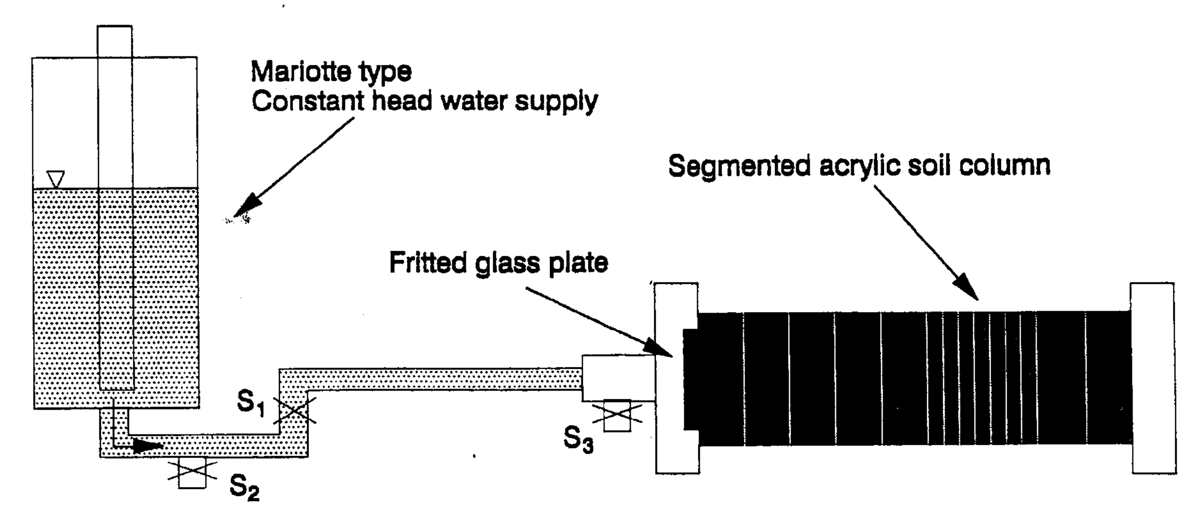

Figure 2-5. Hydraulic Diffusivity Apparatus (Modified from Klute and Dirksen, 1986)

The soil is compacted by continued vibrations while the soil column is being filled. The column is capped and placed in a horizontal position. Water is supplied at one end of the soil column under a slight potential using a Mariotte bottle. The water is allowed to infiltrate, while time and distance to the wetting front are recorded. When the wetting front reaches the desired position, the flow of water is stopped and the column quickly sectioned. Each soil section is weighed and oven dried to determine the bulk density and water content.

Hydraulic diffusivity measurements assume the use of an effectively semi-infinite one-dimensional flow field and the diffusivity form of the flow equation is assumed to be valid. Two experimental approaches can be used: (1) the experiment can be stopped at an arbitrary time, and the soil water content measured as a function of distance from the source; or (2) water content can be measured at a known distance from the source, as a function of time. The Boltzman variable allows the transformation of both time and distance into one variable in the following form:

$$\lambda(\theta) = xt^{-1/2}$$

where

- $\lambda(\theta)$ = the Boltzman composite variable
- x = horizontal distance from the source to a particular value of θ
- t = time since infiltration began

The Boltzman variable allows the transformation of Richard's equation for one-dimensional horizontal flow to an ordinary differential equation. The initial and boundary conditions for the experiment are that the soil is initially at a uniform water content and, after infiltration begins, the water content at the point of water entry maintains constant. Using the above conditions, a solution for diffusivity is developed in the following form:

$$D(\theta') = -\frac{1}{2}\left(\frac{d\lambda}{d\theta}\right)_{h=\theta'} \int_{\theta_o}^{\theta'} \lambda(\theta)\, d\theta$$

where

- $D(\theta')$ = the diffusivity at θ'
- $d\lambda/d\theta$ = the slope of a λ vs θ at θ'
- $\int_{\theta_o}^{\theta'} \lambda(\theta)\, d\theta$ = the area under the $\lambda(\theta)$ curve between θ_o and θ'

Graphing the θ vs $x^{-1/2}$ relationship determined by the laboratory experiment allows the slope and the integral of the θ vs λ relationship to be determined.

3

PHYSICAL AND HYDRAULIC PROPERTIES

3.1 Particle Density and Bulk Density

Particle densities for the fly ash ranged from 2.11 g/cm^3 to 2.44 g/cm^3. Particle densities are tabulated in Appendix A.

Particle density results were almost certainly affected by the presence of cenospheres, which are hollow spherical fly ash bodies that contain entrapped air. Typically, they range in diameter from 10 to 100 μm, and may constitute up to 20 percent of the fly ash by volume (Hecht and Duvale, 1975). Some (always less than 1 percent v/v) of these cenospheres floated at the air/water interface in the pycnometer. The pycnometer method, yielding biased data due to dead-end pore space (cenospheres), shows the expected pattern of particle densities of less than 2.65 g/cm^3 for mineral components expected to be 2.65 g/cm^3 or greater. In terms of hydraulic properties, however, the parameters, as measured, are most useful for determining available porosity.

3.2 Particle Size Distribution

Most fly ash is well-sorted material due to the combustion and collection processes employed. Figure 3-1 includes particle size distributions for four soils (Mualem and Dagan, 1976), six fly ashes, and FGD and AFBC by-products. The mean particle diameters (d_{50}) vary from 9 μm on Kingston fly ash to 34 μm on Johnsonville fly ash (Appendix B). The Shawnee spent bed material had a measured mean diameter of 870 μm.

Because of their hollow structures, cenospheres sink at a rate less than predicted by the standard application of Stokes Law. As a result, the use of the hydrometer method will produce a bias in the grain-size distribution where cenospheres are most abundant (i.e., 10 to 100 μm). This bias will skew the data to suggest a higher fraction of smaller particles than is present. Therefore, the material may be even more sorted by size than indicated by the plotted particle size distributions. Given that fly ash d_{10}'s are approximately half of the lower range of common cenosphere diameters, low cenosphere density could result in the d_{10} estimate being too small.

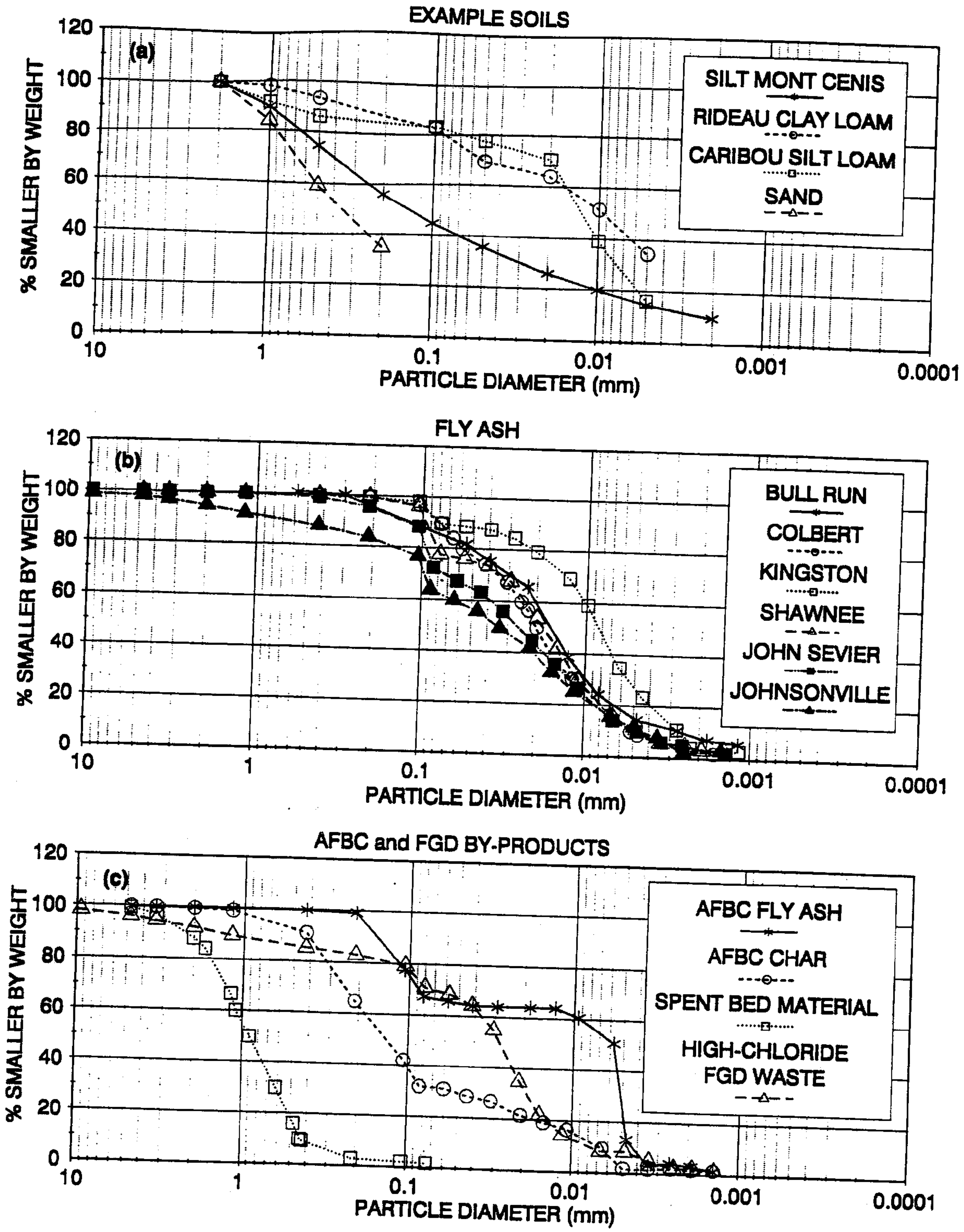

Figure 3-1. Grain Size Accumulation Curves: (a) Example Soils (Mualem, 1976); (b) Fly Ashes; and (c) AFBC and FGD By-Products

Uniformity coefficients (d_{60}/d_{10}) for the fly ash varies from 3 to 14 (Appendix B). This index is used mostly with coarse grained materials. A C_u value of 1 implies a single particle size (extremely well-sorted). Soils, generally being better graded, typically show larger values. Materials with small C_u's typically show a sharper break on ψ-θ plots due to a narrow pore size distribution associated with a narrow particle size distribution.

Data for the ash material analyzed and several soils from a catalog compiled by Mualem and Dagan (1976) are plotted on a textural triangle in Figure 3-2, to give a broader context to the data obtained. All fly ashes analyzed herein plot as a silty loam, as does the AFBC fly ash and FGD High Chloride waste. The larger spent bed material (SBM) plots as a sand, while the intermediate char plots as a sandy loam.

3.3 Saturated Hydraulic Conductivity

Saturated hydraulic conductivities for six silty loams selected from Mualem's catalog were in the 10^{-4} to 10^{-5} cm/s range. Fly ash saturated hydraulic conductivities were similar, while AFBC fly ash had a 2 order of magnitude lower conductivity of approximately 10^{-7} cm/s. The AFBC fly ash and the spent bed material were exothermic upon the addition of water. A white precipitate was eluted from the spent bed material during conductivity testing. Both the spent bed material and the AFBC fly ash were found to be cemented after oven drying. We speculate that the cementation probably reduced measured hydraulic conductivities below values expected from particle size analysis alone.

A simple internal comparison can be run on the particle size and hydraulic conductivity data for a well-sorted material like fly ash. Hazen (1892) developed the empirical relationship

$$d_{10}^{\ 2} = K_{sat}$$

where

d_{10} = mm
K_{sat} = cm/s

The equation is probably the most widely used relationship between conductivity and particle size distribution. Hazen's formula is fairly reliable for well-sorted coarser materials with small uniformity coefficients. Figures 3-3a and 3-3b show the relationship between measured conductivity and conductivity calculated from Hazen's formula for fly ash and non-fly ash, respectively. The fly ash values in Figure 3-3a show good agreement with the Hazen relationship. The two outliers in Figure 3-3b were likely caused by cementation among the particles. Cementation would reduce the conductivity expected on a purely physical basis

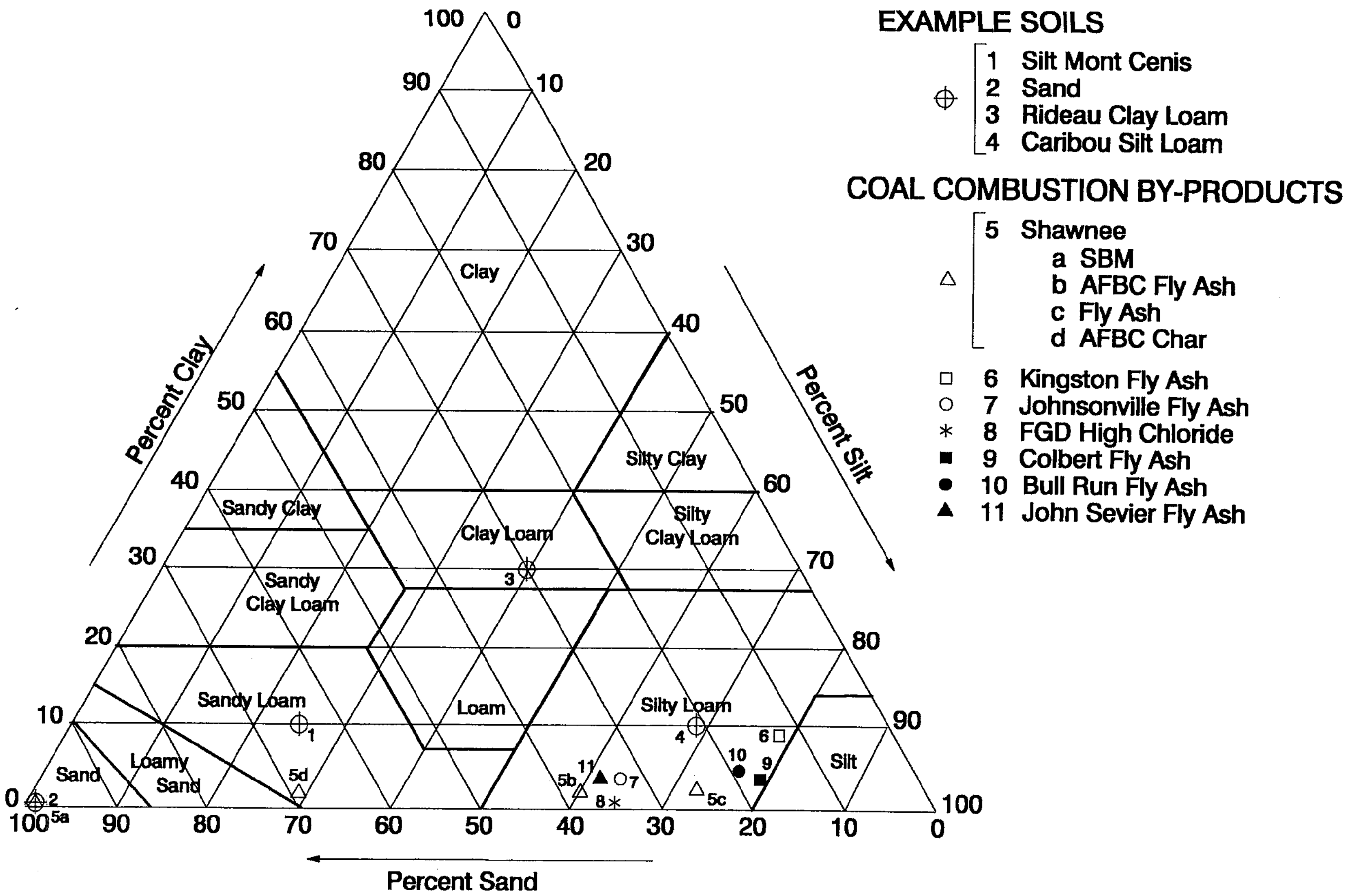

Figure 3-2. Textural Triangle Mapping Example Soils and Coal-Combustion By-Products

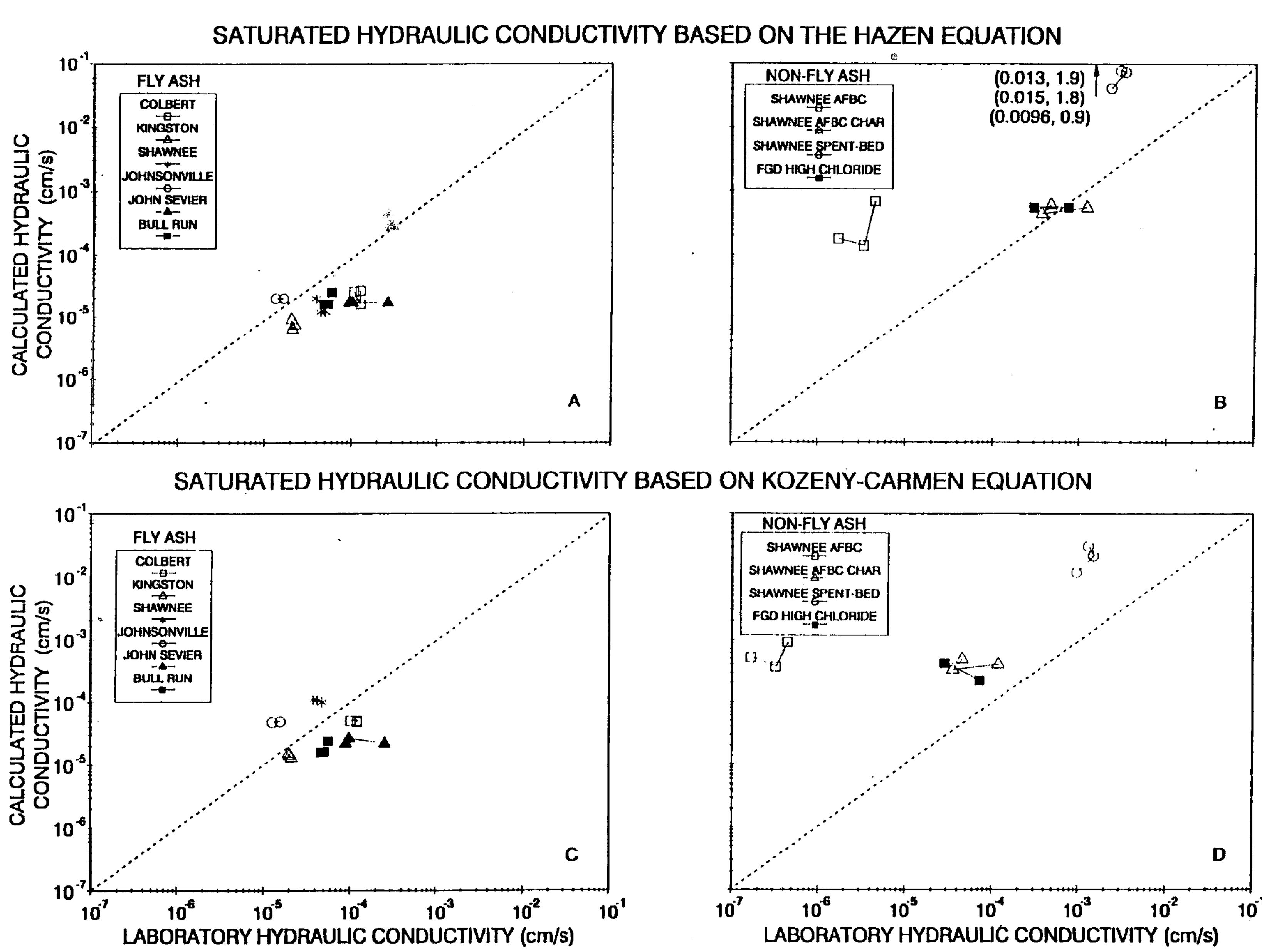

Figure 3-3. Saturated Hydraulic Conductivity Based on the Hazen and the Kozeny-Carmen Equations for Coal-Combustion By-Products

Physical and Hydraulic Properties

(i.e., particle size distribution) and result in outliers occurring above the 1:1 line as seen in Figure 3-3b.

Another commonly used relationship between particle size distribution and K_{sat} is the Kozeny-Carmen equation (Carmen, 1937). The original equation relates specific surface to permeability. Modifications of this equation have tied specific surface to an 'average' particle diameter because of the ready availability of particle size distributions. The d_{10} value, for example, is used in our comparisons. The relationship is

$$k = \frac{\rho g}{\mu}\left[\frac{n^3}{(1-n)^2}\right]\frac{d_{10}^{\ 2}}{180}$$

where

- k = permeability (L/T)
- ρ = density (M/L^3)
- μ = viscosity (M/LT)
- n = porosity

Figures 3-3c and 3-3d show K_{sat} estimated from the Kozeny-Carmen equation for the fly ash and non-fly ash, respectively. Accounting for the porosity in the Kozeny-Carmen equation slightly improves the fit to measured K_{sat}. The same two outliers are noted in both Figures 3-3b and 3-3d comparing calculated with measured saturated hydraulic conductivities of non-fly ash materials.

Because of the good comparisons offered by the Hazen (1892) and the Kozeny-Carmen (Carmen, 1937) equations, several recent equations were applied to the data (Figures 3-4 and 3-5). The modified Hazen method is a result of performing a linear regression to optimize the power to which d_{10} is raised. For the modified Hazen equation, a power of 1.81 was used instead of 2.0. In Figures 3-4 and 3-5, the average values are reported for each set of analysis. Of the six methods, the Sieler and the modified Hazen equations appear the most appropriate for estimating saturated hydraulic conductivity from grain-size data.

3.4 Moisture Retention Characteristic Curves

Figure 3-6 is a generalized moisture characteristic curve for the wetting and drying of a soil sample. It shows the hysteretic nature of most soils in which the water content at a given potential is less for the wetting than the drying of the soil. Hysteresis can occur because of varying pore size, different soil/water contact angles for wetting and drying, entrapped air, and shrinking/swelling of the sample (Reeve and Carter, 1991). The scanning curves in

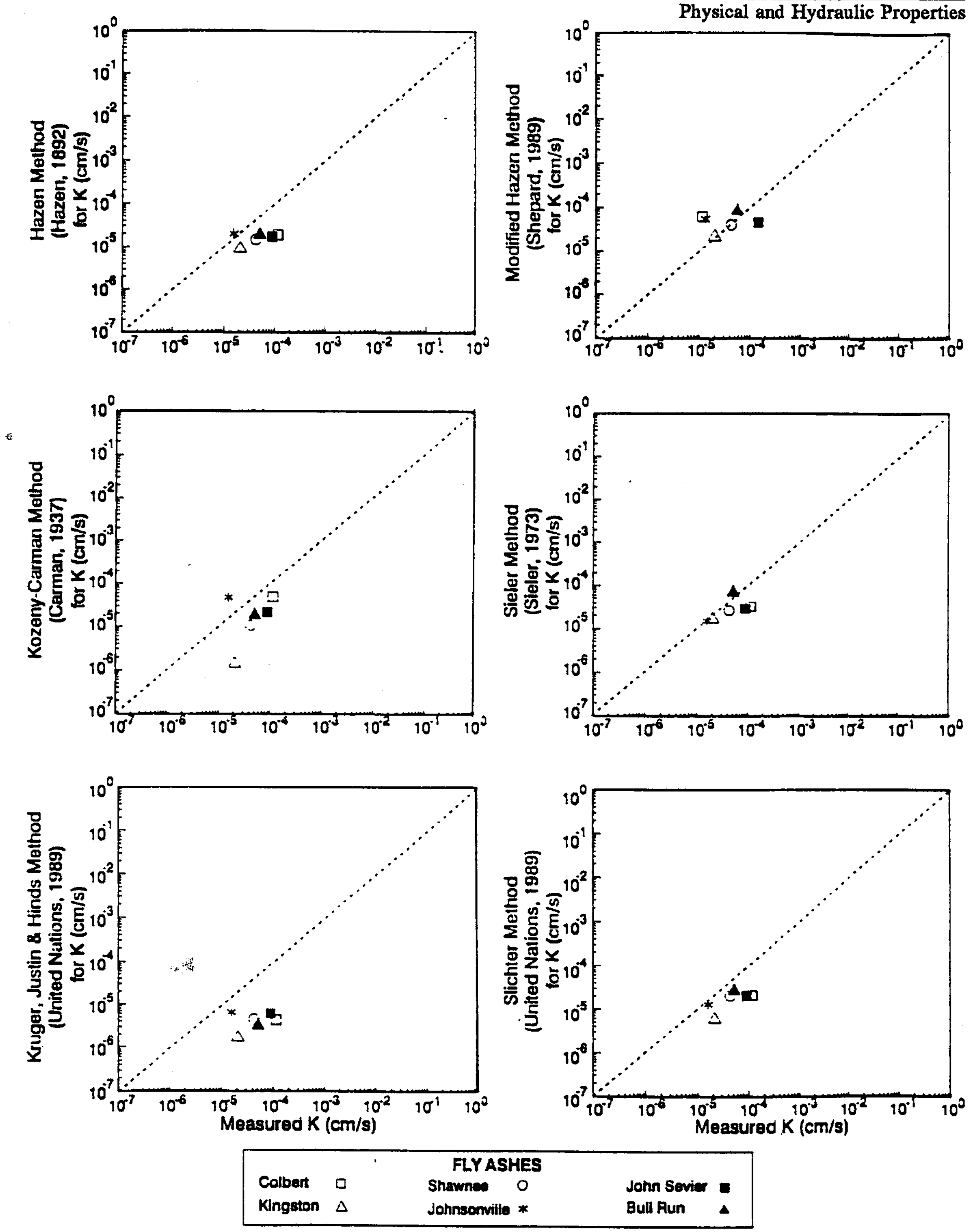

Figure 3-4. Comparison of Methods for Calculating Saturated Hydraulic Conductivity from Particle-Size Distribution for Fly Ash

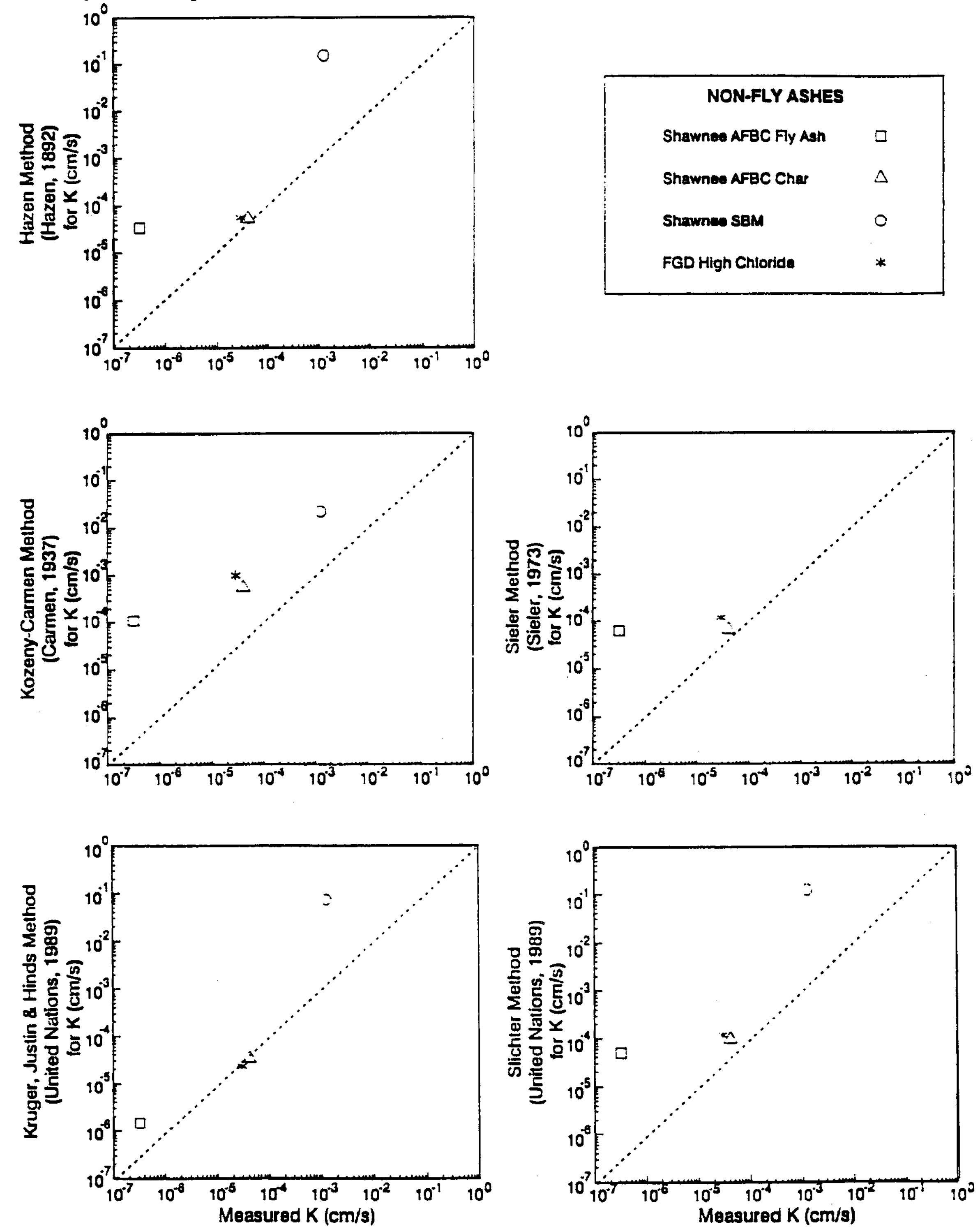

Figure 3-5. Comparison of Methods for Calculating Saturated Hydraulic Conductivity from Particle-Size Distribution for Non-Fly Ash Coal-Combustion By-Products

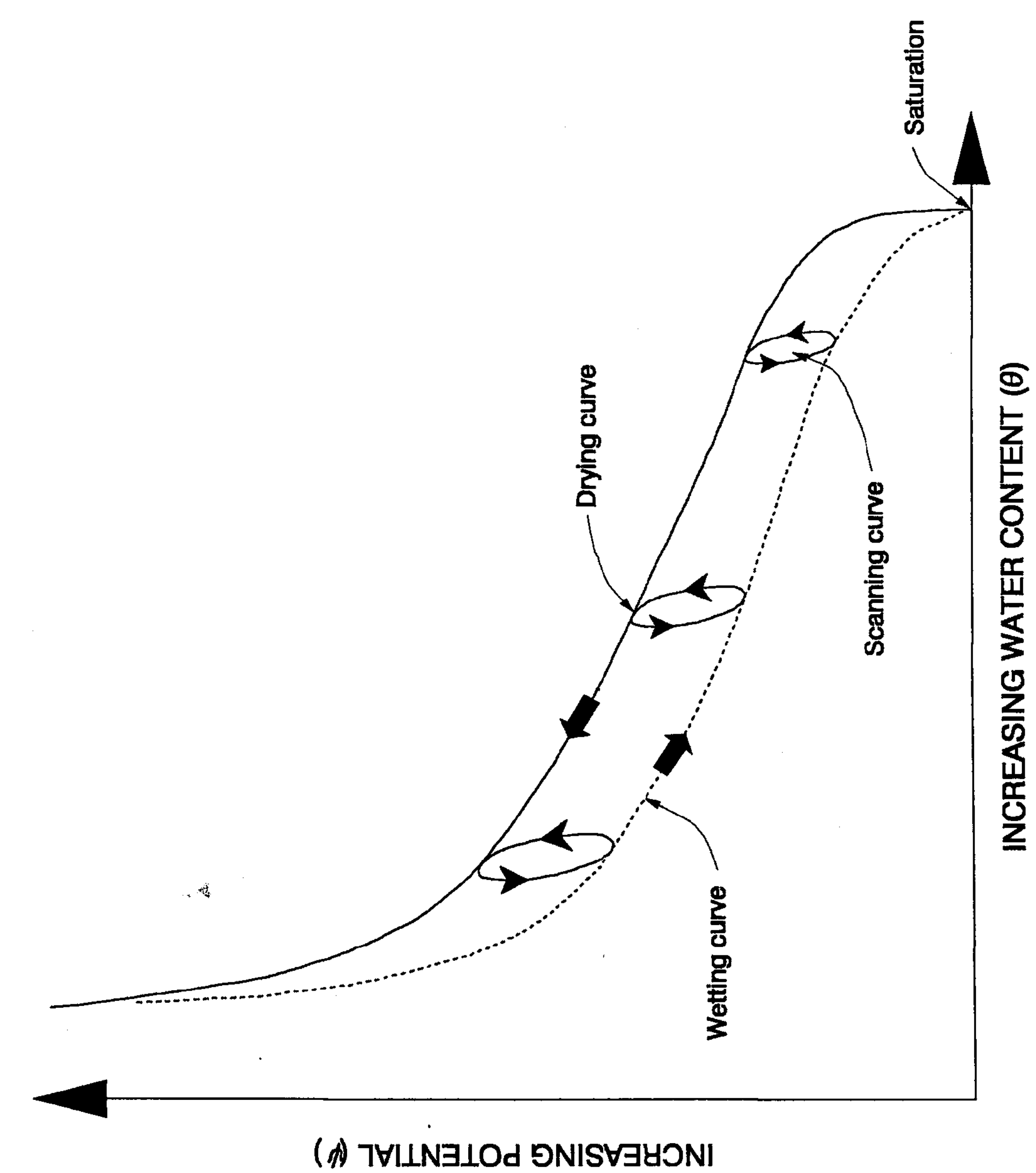

Figure 3-6. Hypothetical Moisture Characteristic Curve Showing Hysteresis From Wetting and Drying

Figure 3-6 show the effects of partial wetting and drying on the relationship between soil/water content and potential.

One approach to characterize hysteresis is to measure the Initial Drainage Curve (IDC), the Main Wetting Curve (MWC), and the Main Drainage Curve (MDC) sequentially on the same sample. Using a single sample for all three curves assures that the transitions among the different curves are continuous--that is, one curve begins where another ends. However, the use of a single sample can be time-consuming. For improved efficiency, another approach is to have on-going measurements to simultaneously measure one of the three main curves (i.e., IDC, MWC, MDC). With the latter approach, differences in the curves include not only effects of hysteresis but also of different soil packing, wetting/drying histories, and small-scale heterogeneities among the soil samples. Depending on the purpose of the measurements, the inclusion of other effects on the moisture retention curves may or may not be desirable.

Primarily because of the need to characterize the moisture retention curves on a timely basis, different samples were used to develop the IDC, MWC, and the MDC curves. Because of this approach, some of the transitions among several of the curves are discontinuous. It is believed that these discontinuities are not necessarily bad because, they are a measure of the error and uncertainty associated with the moisture retention curves which the geohydrologist should be aware. Figures 3-7 and 3-8 show selected plots from Appendix A of the moisture retention curves for the fly ash and the example soils.

Fly ashes are generally better sorted than the example soils. The extraction of the ash from the flue gas is physically analogous to aeolian separation of particle sizes in nature. Dune sands and loess are formed by this process. The result is that all the fly ashes studied consist of more than 90 percent silt-size particles, except for Johnsonville. In comparison to the example soils, the fly ashes tend to exhibit a higher air-entry value, which is the point where a soil begins to release moisture with increasing potential, and a sharper "break" in water content, where much of the desorption and absorption occurs in a small pressure increment. The sharper "break" is characteristic of well-sorted materials. Materials with a narrow range in particle size distribution tend to have a narrow pore size distribution. The narrow range in particle size and sharp break in the θ-Ψ curve suggest a quite uniform pore size distribution for most fly ash.

The high air entry, ranging from ~100 cm potential (Colbert) to nearly 400 cm potential (John Sevier) may be attributed to small pore size and capillarity. However, attendant with the man-made nature of fly ash, the high air entry values may be partially a result of chemical properties such as CEC, specific surface, and/or hygroscopic compounds like calcium oxide. When compared to soils, the fly ashes show characteristics of both silts and clays (high air-entry) and sands (sharp drainage and imbibition over small $\Delta\psi$). While particle size analysis suggests the fly ash should be classified as silt loam, they tend to release more water, more steeply, once the air-entry value has been attained.

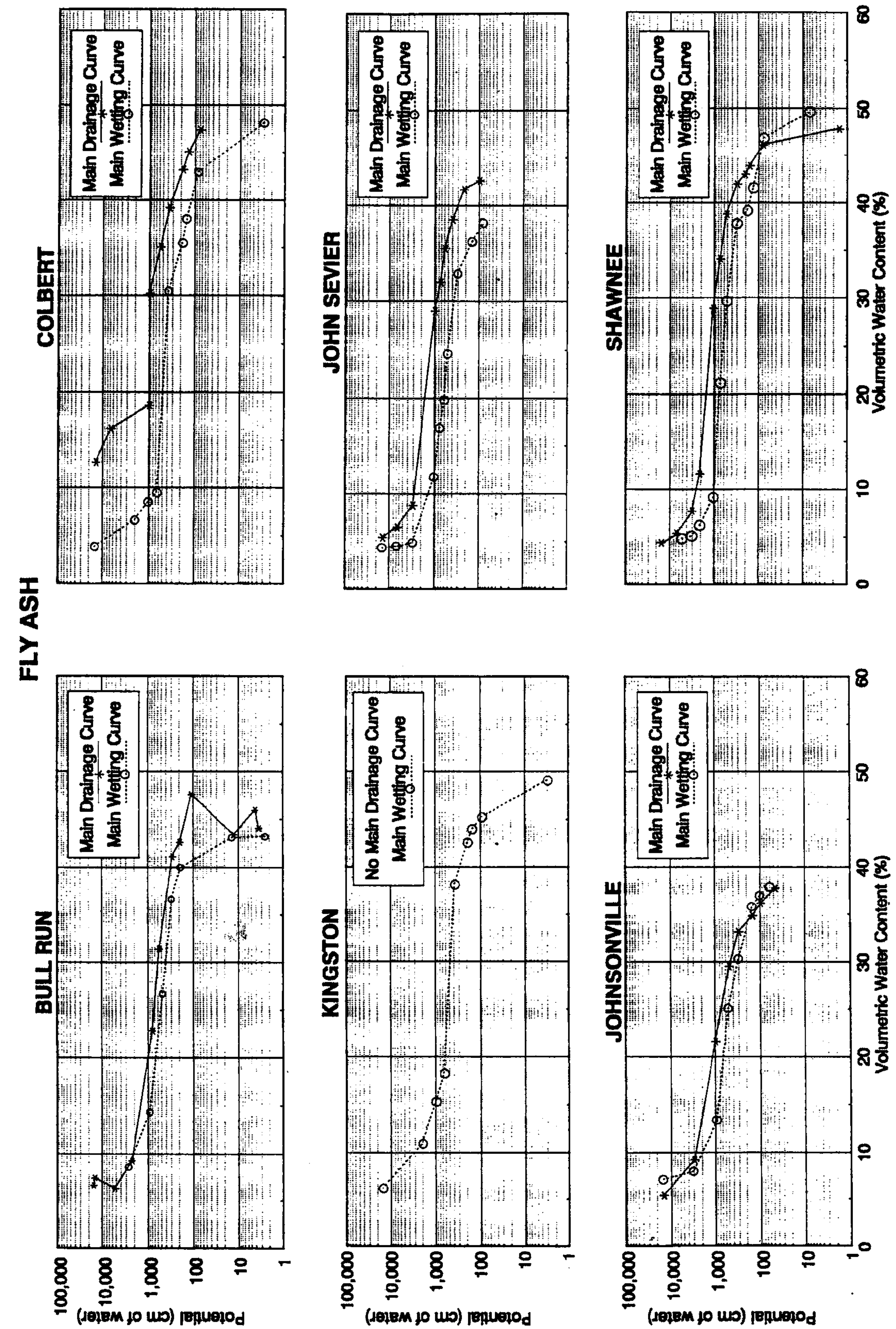

Figure 3-7. Moisture Retention Curves for Wetting and Drying for Different Fly Ashes

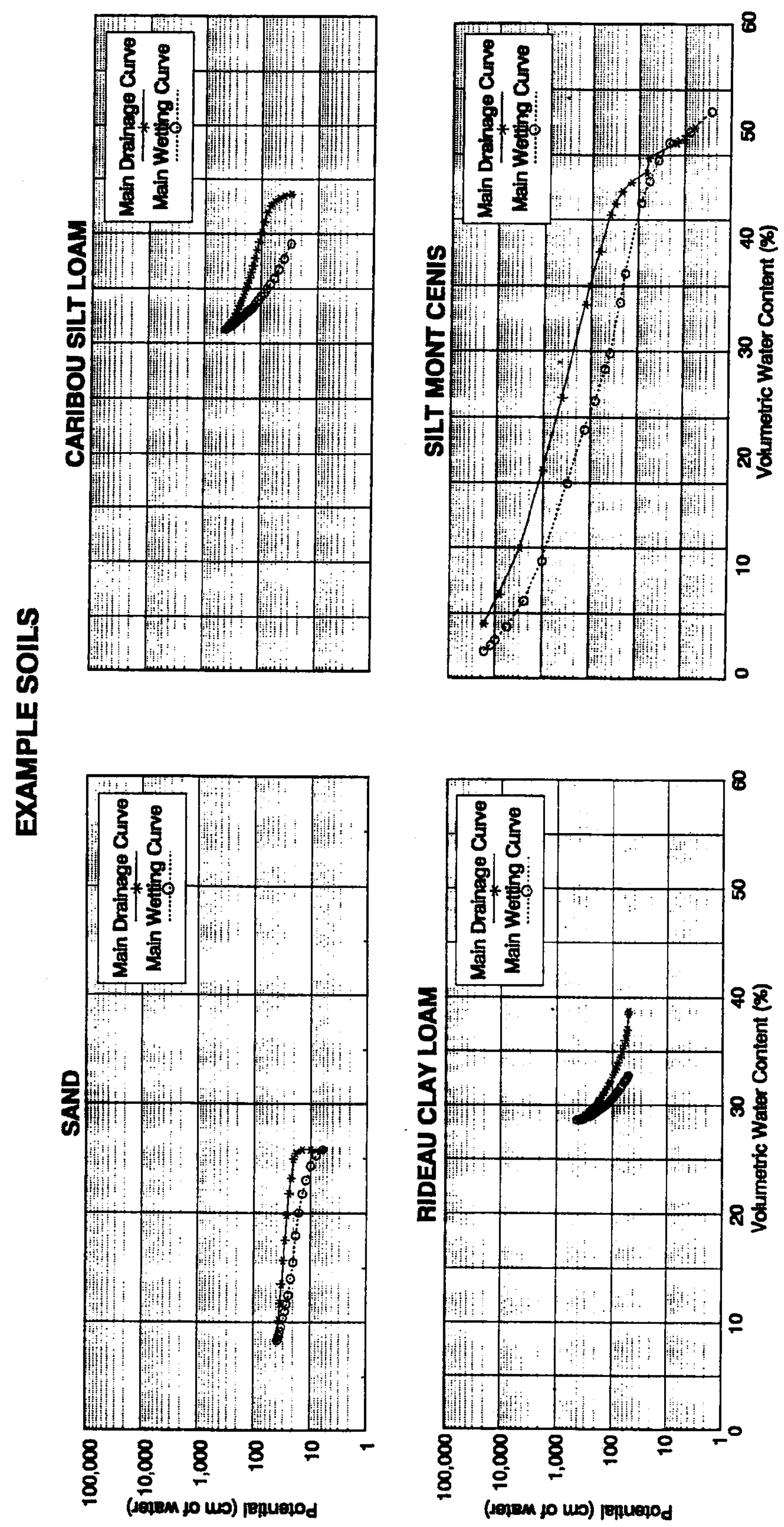

Figure 3-8. Moisture Retention Curves for Wetting and Drying for Example Soils

According to Reeve and Carter (1991), moisture characteristic curves are "not generally unique for either a group of similar soils, or even a soil type." The shape and position of the curve is mainly dependent upon soil properties, as well as the wetting and drying history (hysteresis). This appears true for the fly ash. Although the moisture characteristic curves have similar shapes, one could expect some variability in moisture characteristic curves between samples from the same fly ash and greater variability between the types of fly ash. As mentioned briefly in Section 2.5, hysteresis is the tendency of a soil's equilibrium water content to be dependent upon the soil's wetting and drying history. It can be of major importance with regard to hydraulic studies. Sand (4107) from Mualem's catalog (1976), for example, shows significant hysteresis. However, from Figure 3-7 it appears that fly ash exhibits varying degrees of hysteresis. It is significant that over the moisture range of interest (~10-30 percent volumetric water content) for most water budget studies, the fly ash exhibits the greatest hysteresis. For instance, the John Sevier sample exhibits a water content of approximately 20 percent at 2 bars during draining and approximately 0.6 bars during wetting.

3.5 Diffusivity

Figures 3-9 and 3-10 include selected plots from Appendix A of diffusivity versus water content for the fly ashes and the FGD and AFBC by-products. It appears that the fly ashes can be separated into at least two groups based on the plots of laboratory-determined diffusivity. The Johnsonville and John Sevier fly ashes are similar in that they exhibit a greater capacity to absorb water at a particular water content than the remaining fly ashes. Both the Johnsonville and John Sevier samples have a particle size distribution extending further into the sand fraction than most of the other fly ashes. Correspondingly, the relative diffusivity is larger at a particular water content. The Bull Run samples present an outlier to the discussion, exhibiting a relatively large grain size with narrow distribution, but relatively low $D(\theta)$ values for a particular water content. It is possible, but unlikely, that the Bull Run samples will show the distribution of aggregates and not single particulates. Another possibility is that dual porosity exists in the Bull Run samples leading to a smaller than expected diffusivity at a particular water content. The relatively low values of saturation for the Johnsonville and John Sevier fly ashes may be due to entrapped air during infiltration. In any case, it is apparent that although similarities exist in the laboratory $D(\theta)$ versus θ plots, a different relationship between the diffusivity and water content exists for each fly ash.

Figures 3-9 and 3-10 include the theoretical fits of $D(\theta)$ versus θ calculated by van Genuchten's analysis using Mualem's coefficients plotted with laboratory values. The theoretical values for $D(\theta)$ are generally one order of magnitude lower at a particular water content than laboratory determined values. The Bull Run laboratory, and calculated, diffusivities appear to be best correlated. The Shawnee theoretical fit approaches the lab values in the wet range, but diverges in the dry range. In general, the slopes of the theoretical and laboratory curves are similar, although the curves appear to be shifted relative

TVA-00011533

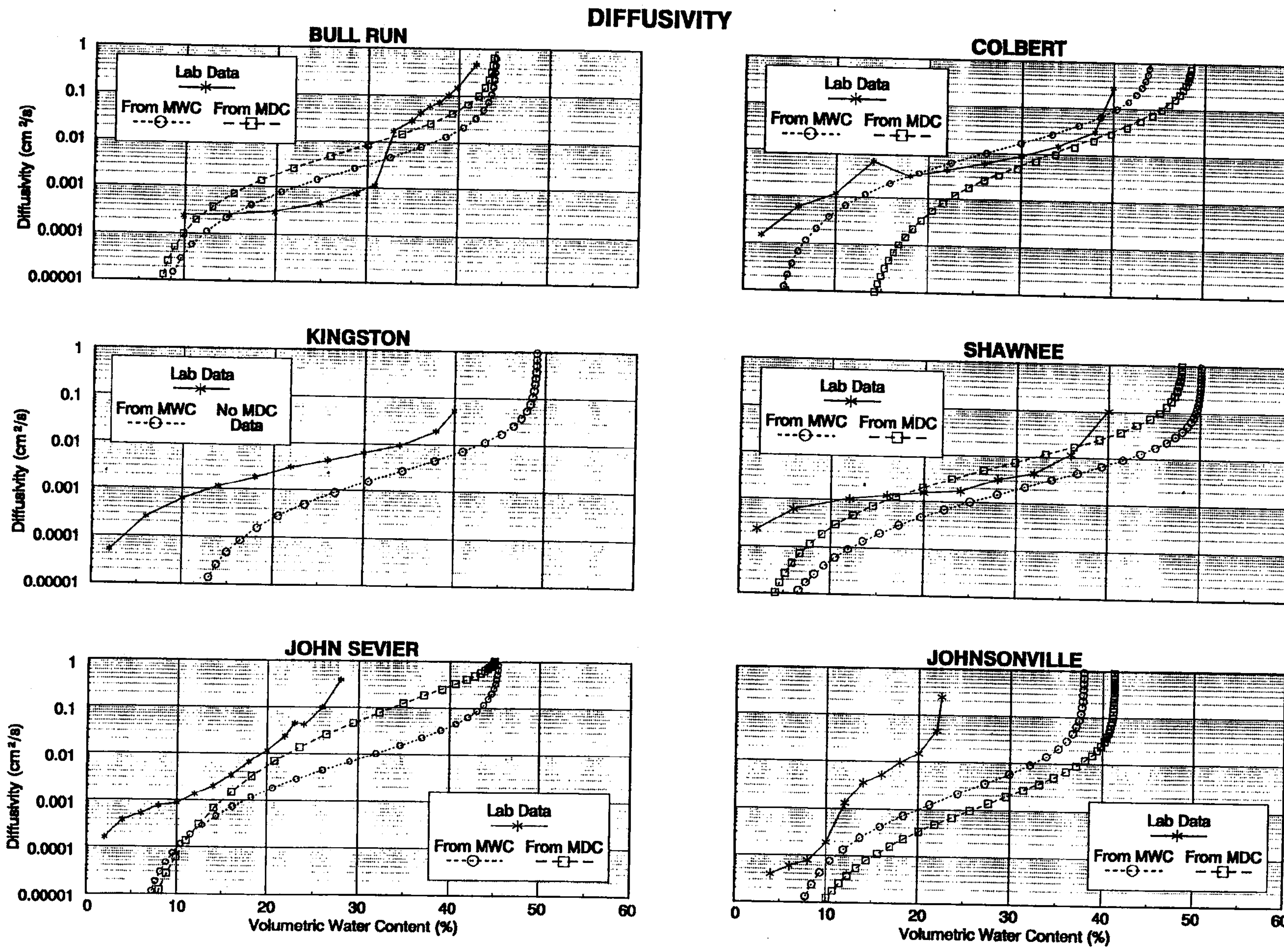

Figure 3-9. Diffusivity for Different Fly Ashes

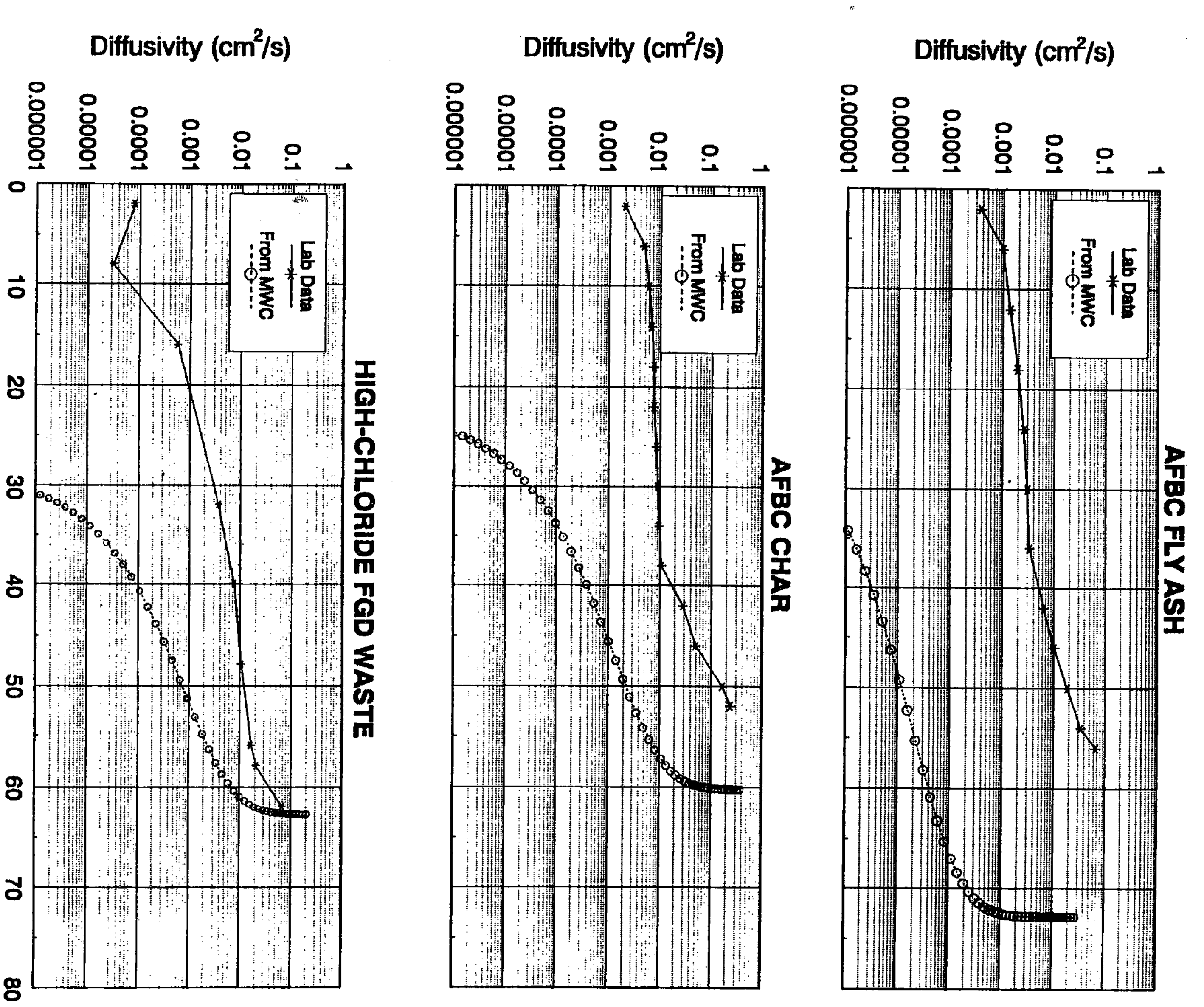

Figure 3-10. Diffusivity for Non Fly Ash Coal-Combustion By-Products

to each other. There are likely several causes for the discrepancy between the predicted and the measured diffusivity curves; such as differences in boundary conditions, chemical reactions between the water and fly ash, and sample preparation.

The influence of different boundary conditions is attributed to differences in the set-up used to obtain laboratory data for computing diffusivity. The laboratory values of diffusivity are determined from the distribution of moisture produced by water infiltrating into a horizontal air-dried soil column after a period of several hours. The moisture retention relationships are determined by slowly draining a saturated soil sample (MDC) and by the rewetting of a relatively dry soil sample that was initially saturated but has been equilibrated with -15 bars potential. For most of the MWC and MDC data, the tests required several weeks to months.

Clothier et al. (1983) provide reasons and data to illustrate the shortcomings of the method of Bruce and Klute (1956) for diffusivity related to different boundary conditions. In addition, Clothier et al. (1983) show that there are problems with calculating diffusivity from the horizontal column imbibition experiment at low and high water contents because the slopes of the $\lambda(\theta)$ data approach zero near low water content and become very large near saturation. Another concern with equating the results in Figures 3-9 and 3-10 is that the laboratory diffusivity curves are calculated from relationships measured during a transient flow test, whereas the moisture retention data and the corresponding van Genuchten diffusivity curves are calculated from relationships measured during equilibrium conditions. In interpreting data from different experimental regimes, the assumptions regarding issues such as entrapped air and hystersis affect the reliability of the results.

An implicit assumption of the van Genuchten method for calculating diffusivity is that capillarity is the primary mechanism affecting water retention. No allowances can be made for the influence of chemical reactions. Chemical reactions affect the bonding of water to the soil particles and can affect the physical properties of water. Of particular concern is hydration of fly ash and especially of AFBC by-products that contain CaO and other similar materials. These concerns are summarized by Selim et al., (1970): "one would expect the diffusion equation to hold for many conditions except the following: whenever a significant solute-water-particle surface interaction exists, whenever soil swells upon wetting, or whenever the physical properties of the soil water change within the soil during infiltration caused by inorganic and/or organic solutes affecting wetting angles, viscosity, vapor transfers etc..."

Clearly, in situations where chemical reactions are known to significantly affect the movement of water (such as the AFBC by-products) some type of direct measurement of diffusivity is preferred over diffusivity values from a van Genuchten analysis. However, where chemical reactions may not significantly affect the movement of water, the advantage of using laboratory determined diffusivity values or van Genuchten diffusivity values is unclear. The question of which method more closely approximates the field depends upon the application and the processes of most interest. It may be the case, that the errors

inherent in using either method are of similar magnitude. Additional studies are required to investigate the significance and the cause of the order-of-magnitude variations in the calculated diffusivity values.

3.6 Mualem's Coefficients

Knowledge of diffusivity as a function of volumetric water content is needed as input for evaporation studies and for estimation of unsaturated hydraulic conductivity. Laboratory methods are more reliable for fine-textured rather than coarse materials. Unfortunately, laboratory methods are also time consuming. Therefore, it is often convenient to estimate diffusivity from moisture retention data. A closed form analytical solution to calculate diffusivity as a function of water content from the moisture retention characteristic curve was developed by van Genuchten (1978). His approach is based in part upon a theoretical model by Mualem (1976). The equation derived by Mualem is used to predict the relative hydraulic conductivity (K_r) using the measured moisture retention characteristic $\theta(\psi)$

$$K_r = \theta^{1/2} \left[\frac{\int_0^\theta \frac{1}{\psi(x)dx}}{\int_0^1 \frac{1}{\psi(x)dx}} \right]^2$$

where

ψ = pressure head at θ, $\psi(\theta)$
x = dummy variable
θ = dimensionless water content defined by $\Theta = \frac{\theta - \theta_r}{\theta_s - \theta_r}$
θ_s = saturated water content
θ_r = residual water content

To determine the relative hydraulic conductivity as a function of water content or pressure head, the above equation is combined with the following equation, which represents a best fit through measured θ and ψ data:

$$\theta = \left[\frac{1}{1 + (\alpha\psi)^N} \right]^m$$

where α and N are fitting parameters that depend on the shape of the moisture retention curve. The α coefficient is generally viewed as inversely proportional to the air-entry value, while N has been related (Brooks and Corey, 1966) and reaffirmed (Sakellariou-Makrantonaki et al., 1987) to the pore size distribution in natural soils. As N increases, the pore size is generally viewed as becoming more uniform. The m parameter is related to N by

$$m = 1 - \frac{1}{N} \qquad (0 < m < 1, \; N > 1)$$

Using the $D(\theta)$ - $K(\theta)$ relationship discussed in Section 2.6, the following equation was developed:

$$D(\theta) = \frac{(1 - m)K_s}{\alpha m(\theta_s - \theta_r)} \theta^{1/2 - 1/m} \left[(1 - \theta^{1/m})^{-m} + (1 - \theta^{1/m})^{m} - 2\right]$$

A closed form analytical equation by van Genuchten (1980) was used to summarize the moisture characteristic information. Representative α and N values for the fly ash are tabulated in Appendix B. The α and N parameters obtained can be used to estimate capillary effects, unsaturated hydraulic conductivity, and diffusivity. Stephens et al. (1987) calculated α and N for the soils of Mualem's catalog (Appendix C). They found α to range from 0.0042 for silt loam G.E. 3 (3310) to 0.12 for Crab Creek sand (4117). The values of α suggest a two order of magnitude difference in air entry for the two soils. The silt loam G.E. 3 with the α of 0.004, an N of 2.1, a θ_r of 0.13, and a K_{sat} of 5.7×10^{-5} cm/s is nearly indistinguishable from the fly ash properties presented in Appendices A and B. However, a particle size distribution was not available for this soil. Fly ash α values range from approximately 0.001 to 0.004 (Appendix B). In comparison of the α's calculated by Stephens et al. (1987), the α values for fly ash are approximately an order of magnitude lower than most silty loam soils. The fly ash α values are more typical of finer textured soils.

Calculated N values for fly ash range from 1.5 to 3.1 (Appendix B). N's from Stephens et al. (1987) ranged from 1.18 for Ida silt loam (3306) to 5.8 for a sorted Plainfield sand (4104). Most soils appear to have N values ranging from 1 to 4. As stated earlier, according to Mualem's theory (1976), N increases as the soil pore size distribution becomes more uniform. Fly ash N values fall within the broad boundaries of soil N values.

4

LABORATORY AND FIELD EXPERIMENTS

A concern with laboratory methods for characterizing hydraulic properties of soils is whether the laboratory-determined properties are representative of field conditions. One problem is that soil sampling and preparation may alter the soil structure. Another problem is that the small laboratory sample may not be representative of the field, because of larger scale spatial variability within the fly ash deposit. Because of strict quality control measures imposed on the combustion of coal and in the stacking of fly ash, fly ash dry stacks should be considerably less complex to characterize than most natural soils. However, less complexity does not insure the representativeness of laboratory measurements to field conditions. Specifically, there is a need to document the spatial variability in a dry stack and to check the laboratory-determined hydraulic properties with independent field and laboratory experiments. The need to check the adequacy of laboratory measured parameters has been partially satisfied by studies that TVA conducted at the Bull Run Fossil Plant, and with fly ash from the Bull Run, Kingston, and Colbert Fossil Plants.

4.1 Bull Run Fly Ash Dry Stack

The Bull Run Fossil Plant has a maximum capacity of 990,000 kilowatts, which is generated by one unit. Approximately 1,000 million kg of coal are burned each year. In 1983, dry stacking of fly ash began. During normal operations, about 0.35 million kg of fly ash are added to the dry stack daily. Dry stacking consists of: (1) wetting the fly ash to an averaged gravimetric water content between 14 and 16 percent; (2) transporting the fly ash by truck in 0.013 to 0.018 million kg loads to the stack; (3) spreading the fly ash with bulldozers to a thickness of 8 to 13 cm; and (4) compacting the fly ash with a steam roller. Approximately one hectare of the dry stack is worked daily.

The fly ash dry stack at Bull Run Fossil Plant has been extensively studied to improve TVA's capability to model water budgets. Extensive field studies that included installing a 0.76-meter H-flume to measure runoff; installing 24 mini-lysimeters to measure evaporation, and drilling five sets of boreholes through and beneath the stack to measure the vertical moisture profile has been performed by Young (1989; 1992). Also, Young and Beard (1989) and Young and Velasco (1991) have modeled the water budget of the dry stack and compared it to a water budget estimated from field studies. These reports address the suitability and representativeness of the laboratory-determined physical and hydraulic properties, in detail. For this report, only the information most relevant to documenting spatial variability in the dry stack and checking representativeness of the laboratory-determined hydraulic properties with independent field and laboratory experiments is presented.

4.1.1 *Dry Bulk Density*

Because the structural condition of a soil affects its hydraulic properties, dry bulk density is a physical property whose spatial variability is of interest. During design and early development stages of the dry stack, TVA's Construction Materials Laboratory determined that the maximum dry bulk density and optimum water content from the Proctor test for the fly ash was 1.29 g/cm³ and 26 percent. The construction design specifications require the fly ash to be compacted to at least 90 percent of the maximum dry bulk density. Based on these specifications, the average dry bulk density in the dry stack should lie between 1.15 and 1.29 g/cm³.

In 1987, several grab samples of fresh fly ash were collected and analyzed by Dr. Arnold Klute to determine the properties listed in Appendix A. The laboratory analysis produced a maximum dry bulk density and optimum water content of 1.26 g/cm³ and 26 percent, respectively. These values are in good agreement with the results from TVA's Construction Materials Laboratory tests conducted on fly ash produced several years prior. In 1987 and 1988, 25 undisturbed samples of fly ash were collected from the upper 10 meters of the dry stack via Shelby tubes during drilling with a hollow-stem auger. The mean and standard deviation of the density measurements were 1.22 and 0.11 g/cm³, respectively (Young, 1989). These results suggest: (1) that the dry bulk density values in the dry stack exhibit relatively little variability; and (2) that the packing of fly ash samples in the laboratory can be based on the construction specifications for the dry stack.

4.1.2 *Porosity and Particle Density*

Porosity calculations were made for 23 of the 25 Shelby-tube samples collected from the dry stack in 1987 and 1988. The porosity of each sample was calculated from the dry density of the undisturbed sample and the particle density of the fly ash from the sample. For 12 of the samples, a second method was used to calculate the porosity based on the weights of the saturated and the dried undisturbed samples. Except for one sample, the two porosity values were within an absolute value of 0.5 percent of each other. The mean and standard deviation for the 23 porosity values were 42.3 percent and 6.8 percent. The mean is in good agreement with the laboratory value of 42 percent (Appendix B) calculated from recompacted fly ash.

Figure 4-1 shows a relationship among porosity, particle density, and dry bulk density for the Shelby-tube samples taken from the Bull Run dry stack. The porosity values range from

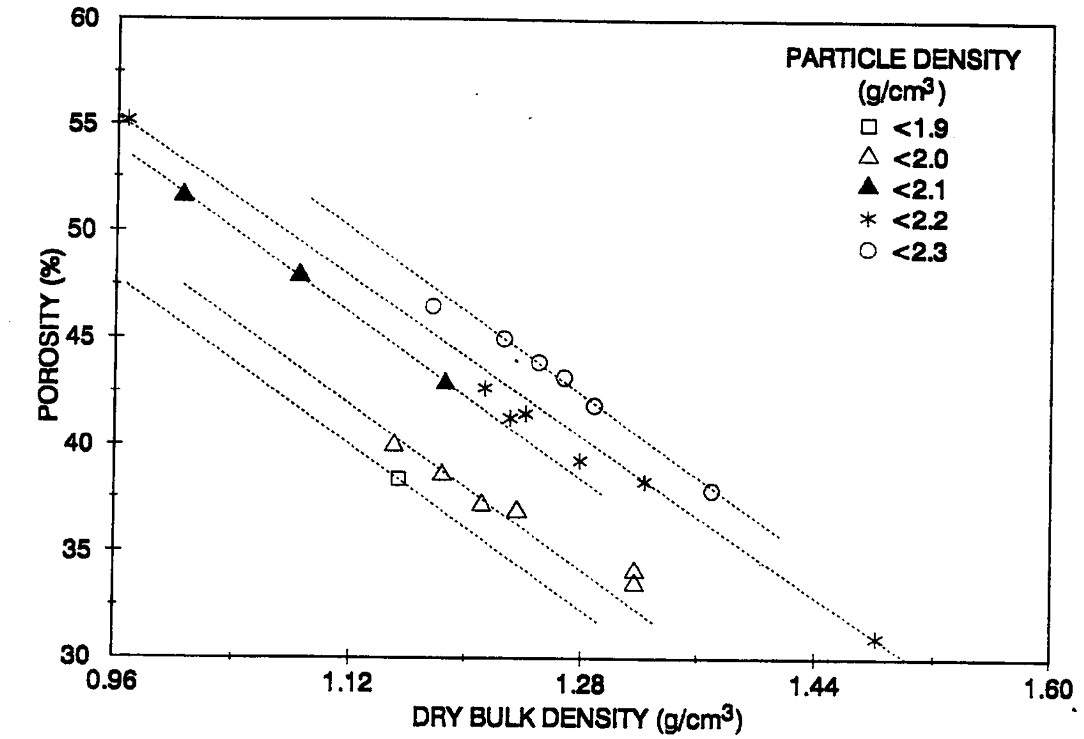

Figure 4-1. Distribution of Values for Porosities, Dry Bulk Density, and Particle Density Among the Shelby-Tube Samples

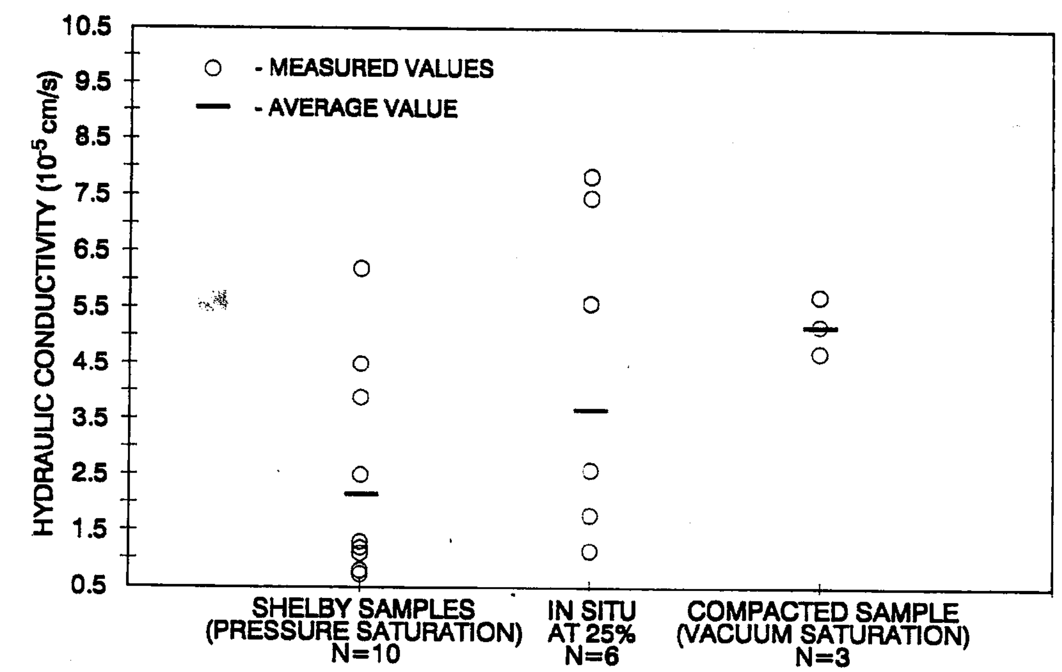

Figure 4-2. Comparison of Saturated Hydraulic Conductivity Measurements

30 to 55 percent. The large range has occurred because of the differences in the particle density and the packing of the fly ash. As shown in Figure 4-1, for a given particle density, the porosity is inversely proportional to the bulk density. Similarly, for a given bulk density, the porosity is inversely proportional to the particle density.

4.1.3 Saturated Hydraulic Conductivity

Three methods were used to estimate the saturated hydraulic conductivity of the dry stack material. They included laboratory permeameter measurements on undisturbed cores (i.e., Shelby tubes), *in-situ* measurements with a Guelph permeameter, and laboratory permeameter measurements on fresh fly ash compacted in the laboratory. Geological Associates measured the hydraulic conductivity of the previously mentioned undisturbed Shelby samples in triaxial cells at their laboratory in Knoxville, TN. The tests were performed in accordance with ASTM procedures and guidelines presented by Lambe (1953). In October 1987, TVA personnel used a Guelph permeameter (Reynolds and Elrick, 1986; Elrick and Reynolds, 1986) to measure the *in-situ* hydraulic conductivity. Three Guelph permeameter measurements were made at depths of 0.45 and 1.5 meters, where the average gravimetric water content of the fly ash was approximately 25 percent. TVA collected fresh Bull Run fly ash and sent it to Dr. Arnold Klute, who packed three samples at dry densities between 1.12 and 1.20 g/cm^3 and tested the samples with a falling-head apparatus after saturating the samples by a vacuum saturation technique.

The averaged saturated hydraulic conductivity values for the permeameter tests on "undisturbed" samples from the field, the permeameter tests on fly ash compacted in the laboratory, and the *in situ* Guelph permeameter measurements are 2.1 10^{-5} cm/s, 3.7 10^{-5} cm/s, and 5.2 10^{-5} cm/s, respectively (Figure 4-2). Two factors that contribute to the differences are spatial variability and degree of saturation. Spatial variability is evident in the different dry bulk densities and the specific gravities calculated for the undisturbed cores. The degree of saturation is caused by different amounts of entrapped air. Entrapped air effects were probably greatest and least for the *in-situ* and laboratory measurements, respectively. The effects of entrapped air have been shown to reduce the true saturated hydraulic conductivity by as much as 50 percent (Bouwer and Jackson, 1974; Stephens et al., 1984). Based on the good comparison of the mean value for the three different methods, it appears that the laboratory testing on properly packed samples of fresh fly ash can provide reasonable values for saturated hydraulic conductivity.

4.1.4 Unsaturated Hydraulic Conductivity

Two approaches can be used to calculate the relationship between unsaturated hydraulic conductivity and potential. One approach is to backcalculate $K(\psi)$ using moisture retention curves diffusivity $D(\theta)$ and saturated hydraulic conductivity, K_{sat} (see Section 2.6). The

second approach is to measure the hydraulic conductivity of an unsaturated soil column using the elaborate equipment set-up and methods described by Klute and Dirksen (1986). For the Bull Run fly ash, Dr. Arnold Klute performed sufficient tests to calculate $K(\psi)$ via both approaches. Figure 4-3 shows that both approaches indicate that $K(\psi)$ remains relatively constant at $5.2x10^{-5}$ cm/s between 0 and 300 cm. Beyond 350 cm, there is not enough information to compare the two approaches. At high potentials (e.g., >350 cm), numerous problems with the method of Klute and Dirksen (1986) occurred because of pressure leaks in the equipment, so that only a few measurements could be obtained. Overall, the test results suggests that the two approaches provide comparable results, and that appreciable declines in the $K(\psi)$ values do not occur until ψ is greater than the air entry value.

4.2 Laboratory Evaporation Experiment

As part of its environmental assessment activities, TVA has used the hydraulic properties in Appendix A with groundwater flow models to predict the water budgets of fly ash dry stacks. Predictions with different fly ash (Young and Beard, 1989; Lindquist and Young, 1989; and Lindquist et al., 1991) consistently show runoff and evaporation to be less than 5 percent and greater than 65 percent of precipitation, respectively. Although these estimates are consistent with available field data (Young, 1989), the estimates are not readily accepted by regulatory agencies because they differ substantially from simulations using hydraulic properties for natural soils as input. In order to demonstrate the validity of its groundwater models and the high evaporation rates from fly ash, TVA conducted a series of evaporation experiments (Foust and Young, 1992). For this report, sufficient information is given to support using the laboratory-determined properties in Appendix A to predict evaporation rates from different fly ash.

4.2.1 Experimental Set-Up

The experiments focused on measuring cumulative evaporative losses from cylinders of fly ash that have no flow boundaries at the bottom and sides boundaries and a constant evaporation potential at their surface. The evaporation potential was established primarily with electric fans and quartz halogen dichroic mirror lamps (Figure 4-4). The meteorological instrumentation included sensors for humidity, temperature, net solar radiometer, and wind speed. This instrumentation is not shown in Figure 4-4.

Two experiments were conducted with the Kingston and Colbert fly ashes under almost identical meteorological conditions. Figure 4-5 shows the continuous record for the meteorological data for the first experiment. Abrupt shifts in the continuous record for several meteorological parameters are evident. These shifts do not represent changes in meteorological conditions. The shifts represent changes in the location of the monitoring

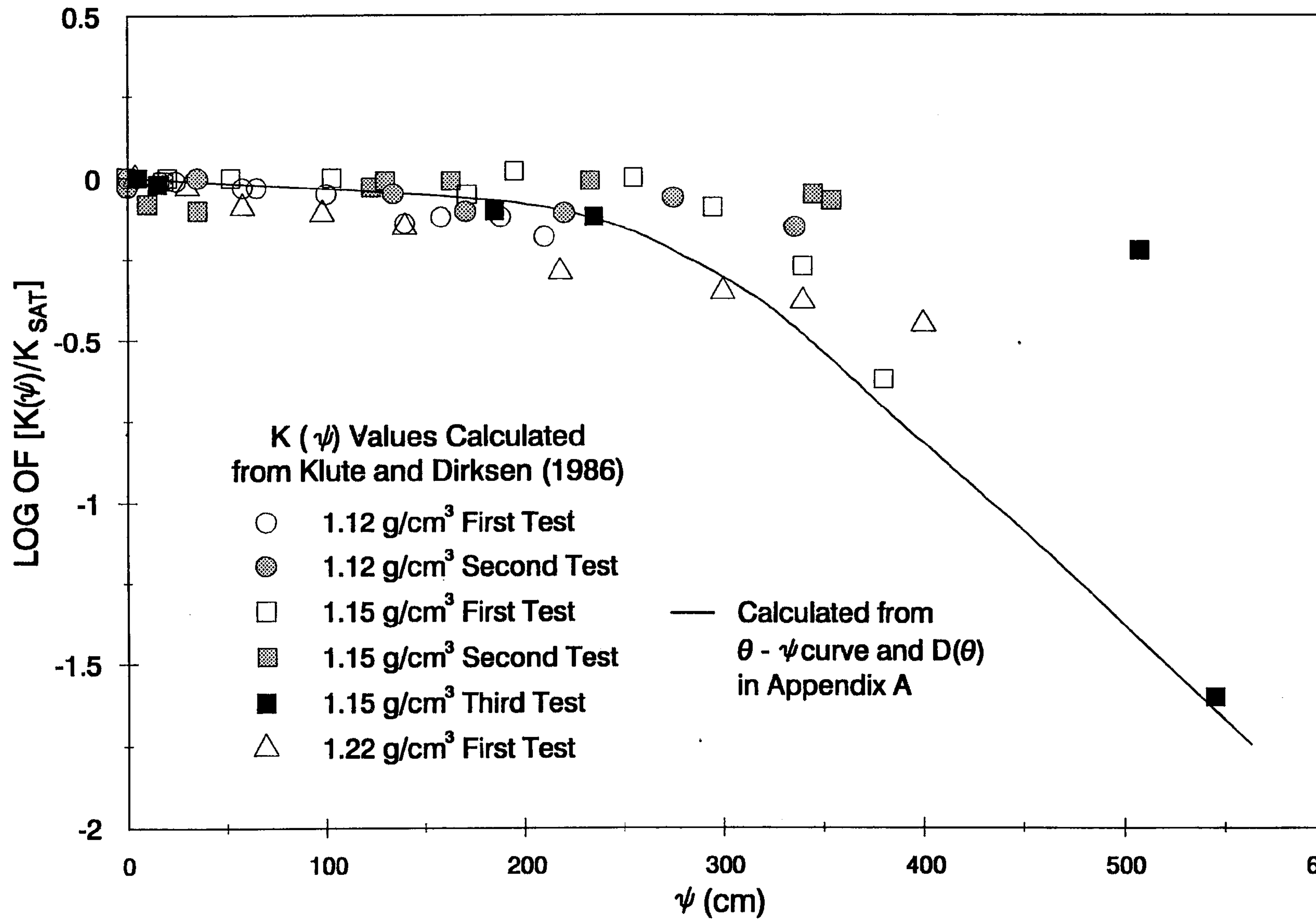

Figure 4-3. Comparison of Measured K(ψ) Values and Those Calculated From Measured θ-ψ and D(θ) Data

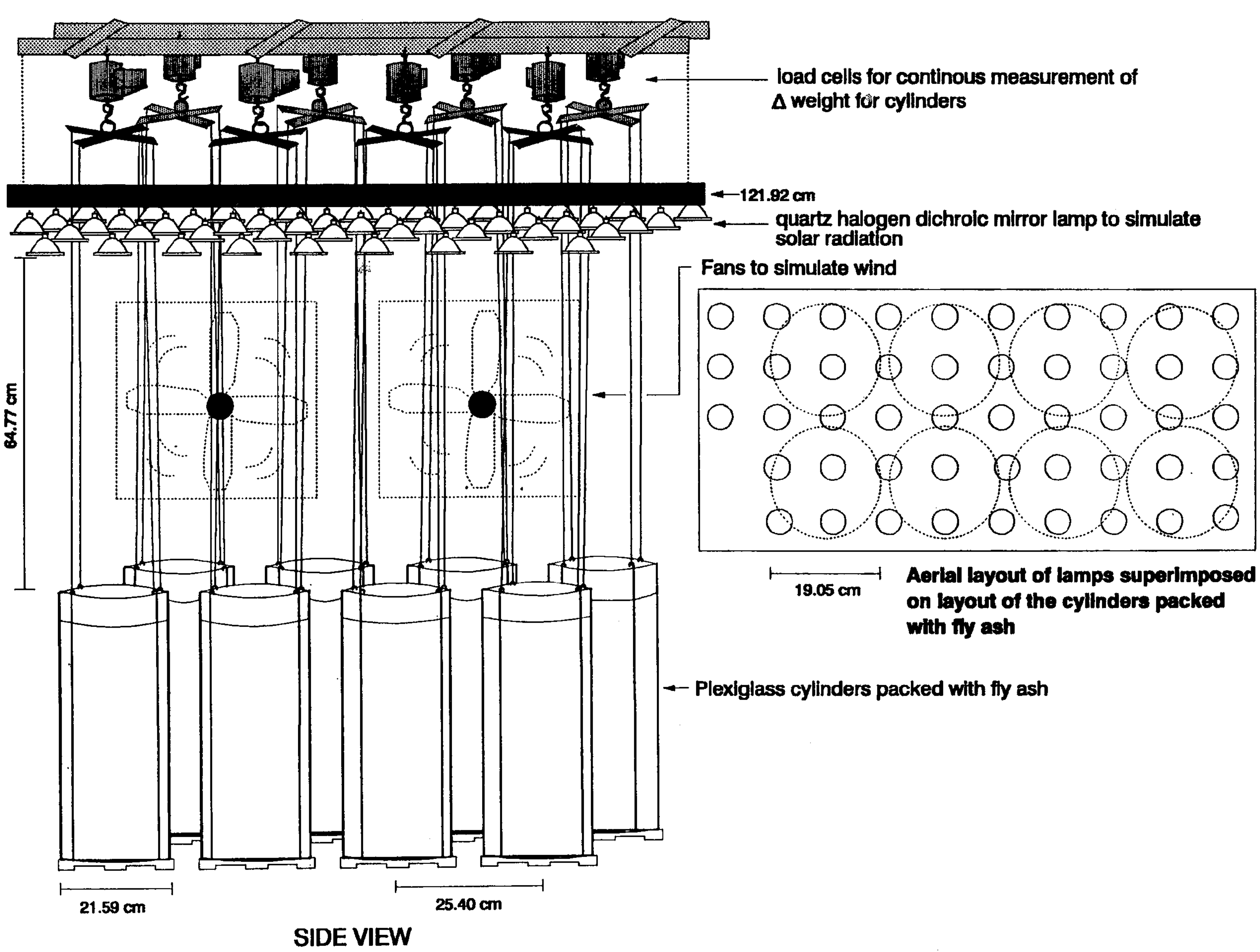

Figure 4-4. Equipment Set-Up for Laboratory Evaporation Experiments

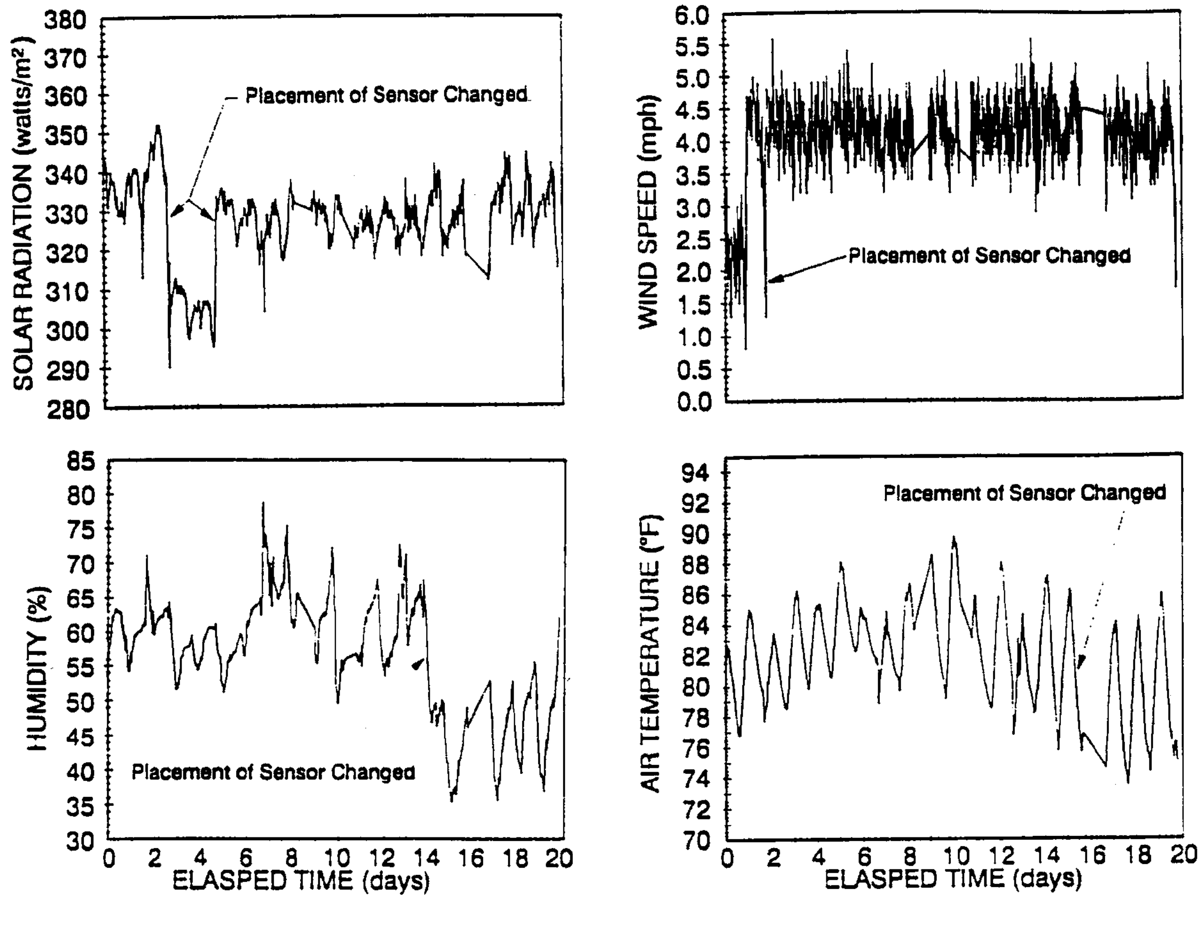

Figure 4-5. Twenty-Day Meteorological Data Set During Evaporation Test 1

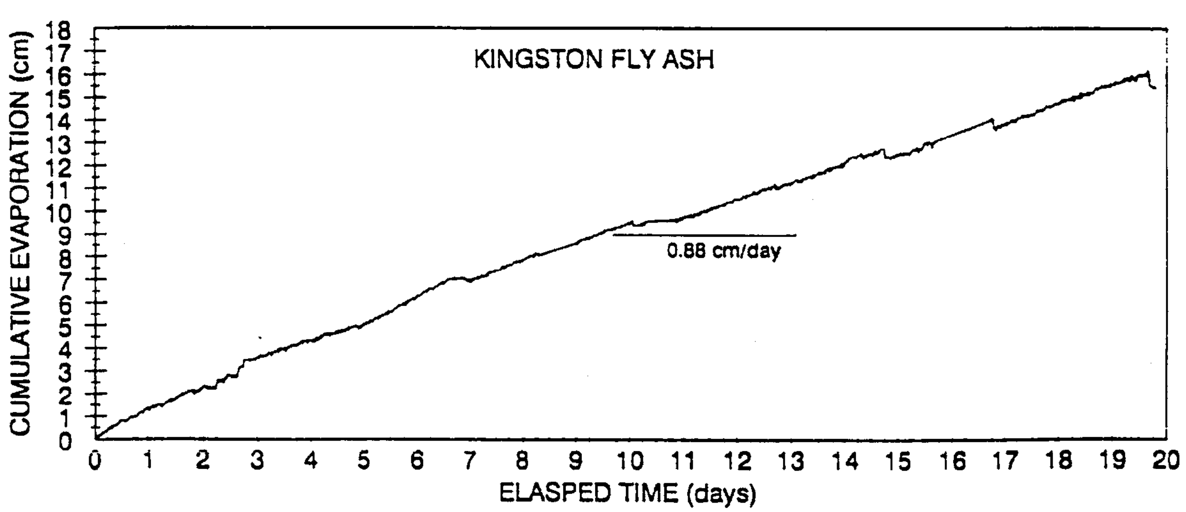

Figure 4-6. Cumulative Evaporation from Continually Saturated Kingston Fly Ash for Evaporation Test 1

sensors that occurred when the fly ash cylinders were removed and manually weighed to check the accuracy of the load cells.

The meteorological variable that primarily determines the evaporation potential is the solar radiation. Throughout most of the tests, the solar radiation values ranged between 320 and 350 watts/m^2. The 10 percent fluctuations is caused by the daily changes in the lighting patterns for the larger area in which the experimental set-up is located. Daily patterns are especially evident in the temperature and relative humidity measurements. As should be expected, the changes in the humidity and temperature values are inversely related.

A primary objective of the first experiment was to directly measure the evaporation potential. To accomplish this objective, specially-built cylinders were filled with saturated fly ash. These cylinders were designed such that water could easily flow into them from a known water source to replenish any evaporative losses. The measured evaporation rates from these cylinders ranged from 0.8 to 0.9 cm/day. Figure 4-6 shows the evaporation losses from a cylinder filled with saturated Kingston fly ash. The data indicates a relatively constant evaporation potential of 0.88 cm/day, the value used for the modeling of the results of the second experiment.

A primary objective of the second experiment was to measure the evaporation losses from fly ash uniformly compacted and moistened to represent averaged field conditions of about 20 percent volumetric moisture. Foust and Young (1992) describe the compaction procedure. The cylinders used in the second experiment had 17.8-cm diameters and were 46 cm long. Figure 4-7 shows the cumulative evaporation losses from cylinders packed with Kingston and Colbert fly ashes. For both the Kingston and the Colbert cylinders, the initial evaporation rate was nearly 0.88 cm/day.

At the onset of the second experiment, the initial volume of water in each cylinder was estimated from gravimetric moisture values and weight of the wetted fly ash. At the end of the second experiment, the fly ash was removed from each cylinder, weighed, dried in an oven, and reweighed. By combining the water losses measured after the experiment and during the experiment, the initial volume of water was calculated for each cylinder. In turn, an initial averaged volumetric water content was then calculated based on the known volume of water and dimension for each cylinder.

4.2.2 Modeling Results

The WF (Clapp, 1982) and the EFLOW (EPRI, 1988) models were used to simulate the evaporation results. Input into the numerical models were hydraulic properties from a three-parameter Brooks-Corey fit (Clapp and Hornberger, 1978) to the approximate information from Appendix A (Figure 4-8), a 0.88 cm/day evaporation potential, and a uniform initial volumetric water content of 23 and 24 percent for the Kingston and the Colbert fly ashes,

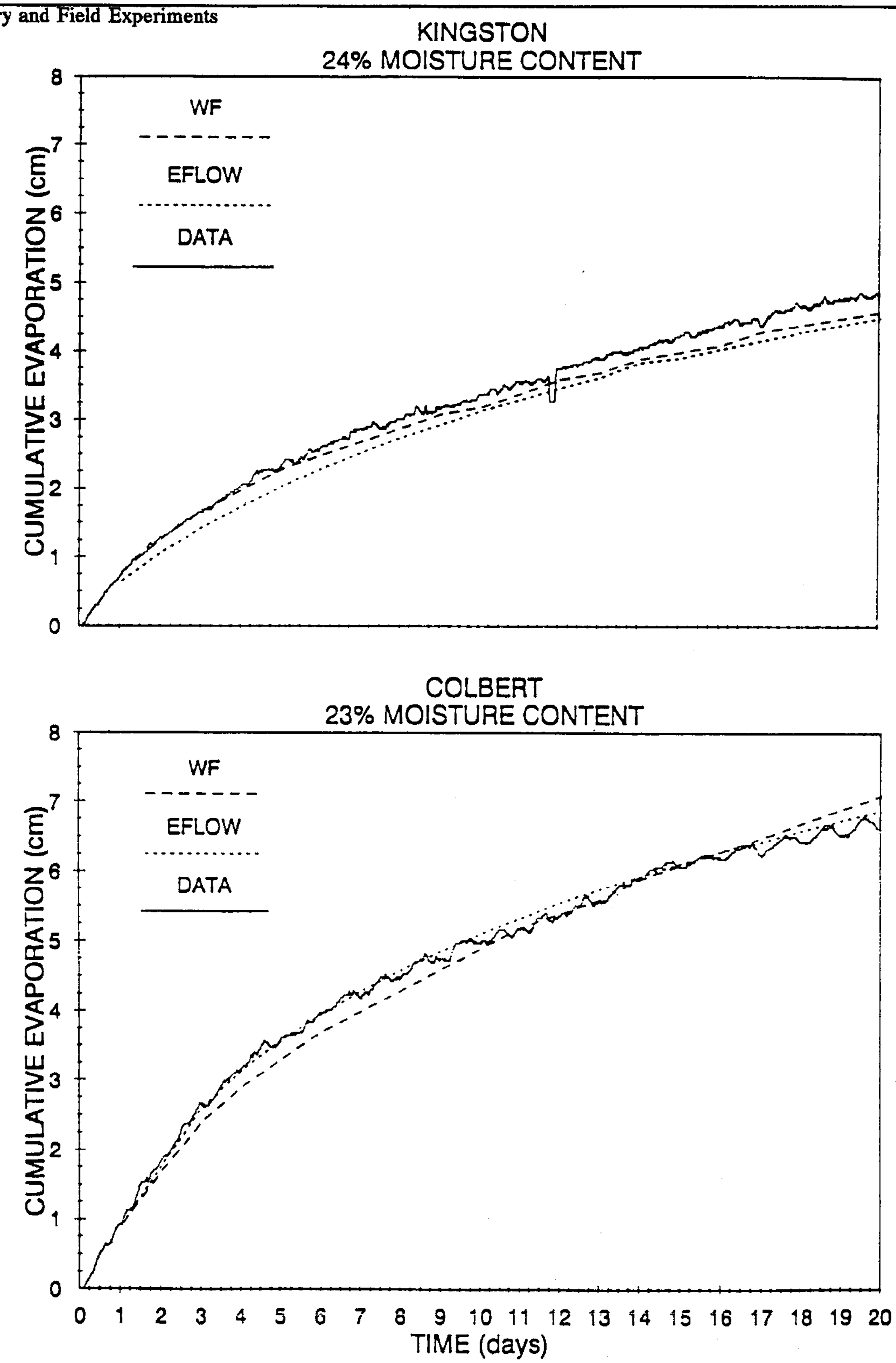

Figure 4-7. Measured and Predicted Losses for Evaporation Test 2

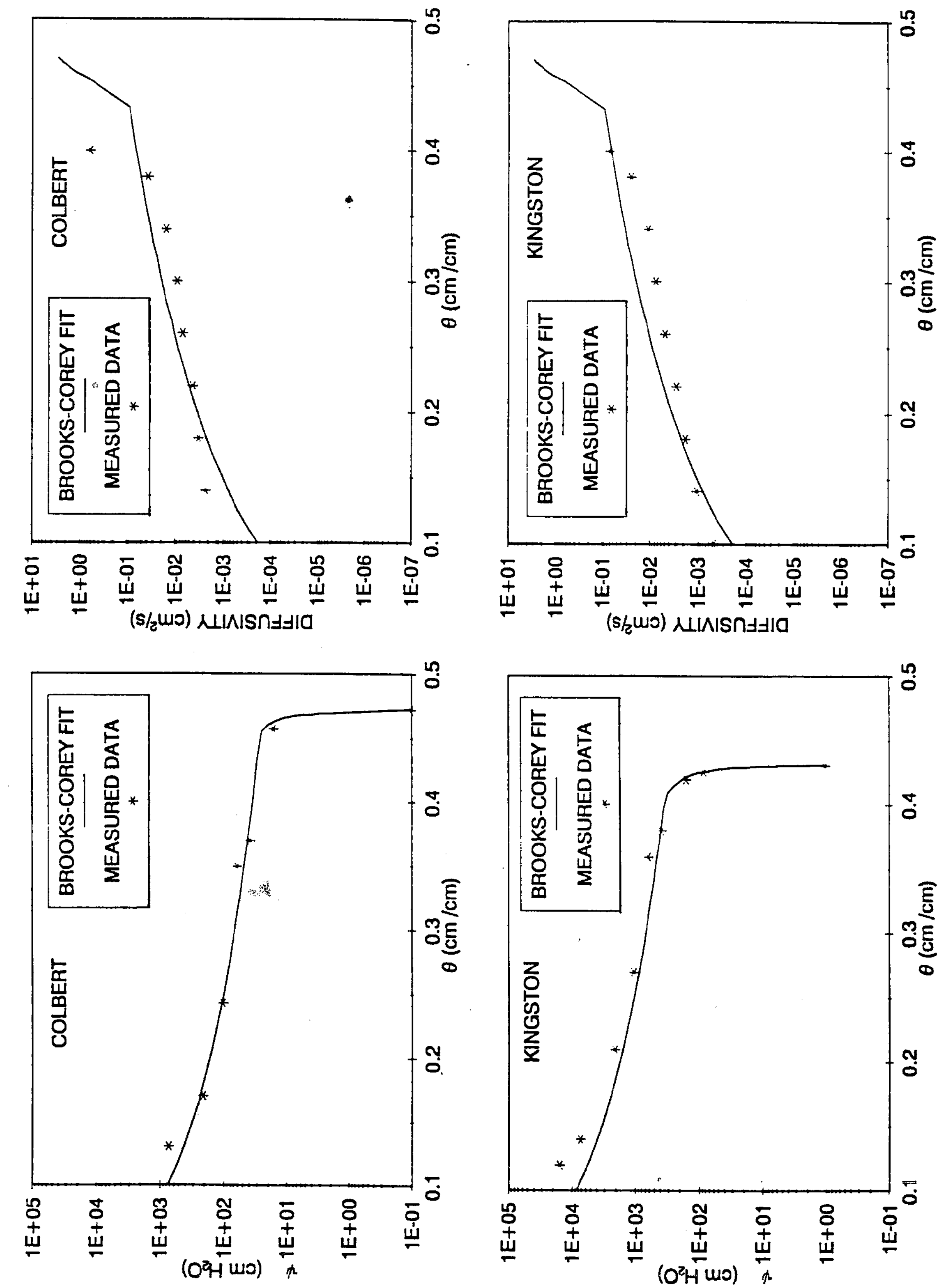

Figure 4-8. Three-Parameter Brooks-Corey Fit to Measured Moisture-Retention and Diffusivity Data

respectively. The water contents were based on the results of the mass balance conducted at the end of the experiments. The Brooks-Corey fit was used because the WF model was initially written to accept only Brooks-Corey coefficients. In order to run EFLOW a pressure of -10000 cm was input as the minimum pressure for the uppermost element. Figure 4-7 shows that the WF and EFLOW models provide results that are in excellent agreement with the laboratory values. The excellent agreement suggests that the laboratory-determined properties in Appendix A are appropriate for predicting unsaturated flow in compacted fly ash.

5

SUMMARY

The electric utility industry produces more than 80 million tons of coal-combustion wastes annually (ACAA, 1988). To help minimize the impact of coal-combustion by-products on groundwater resources, the Tennessee Valley Authority (TVA) has converted from ponding to dry stacking of coal-combustion by-products at several of its plants. Since 1986, TVA has performed a series of field and laboratory studies to assist in the design of dry stacks. These studies include six different fly ashes and by-products produced from pilot plant operations for Atmospheric Fluidized Bed Combustion (AFBC) and Flue-Gas Desulfurization (FGD).

The report reviews the laboratory methods for characterizing the physical and hydraulic properties of coal-combustion by-products, and provides the measured properties for six fly ashes and several AFBC and FGD by-products. The physical and hydraulic properties are compared to natural soil properties and to the results of several semi-empirical predictive formulas. Several studies are presented in which the laboratory-determined fly ash properties compare favorably with field measurements or are used in numerical models to simulate an evaporation experiment.

Primary sources for the development and refinement of methods for measuring the physical and hydraulic properties of soils are the American Society of Testing and Materials (ASTM) and the American Society of Agronomy (ASA). The physical measurements described and presented are particle density, dry bulk density, and particle size distribution. The hydraulic measurements described and presented are saturated hydraulic conductivity, moisture retention curves, and diffusivity.

For the purpose of discussion, the test results are grouped into fly ash and FGD and AFBC by-products. The grouping is necessary because the by-products have distinctly different physical and chemical characteristics from the fly ash. Most notably, the by-products have high percentages of calcium and sulfur oxides that are reactive with water. Reactions such as hydration and cementation affect the measurement of selective hydraulic properties.

5.1 Fly Ash

All of the fly ash plot on a textural triangle as a silty loam. Most are well-sorted; the uniformity coefficient ranges from 3 to 14. Particle densities range from 2.11 g/cm^3 to 2.44 g/cm^4. The lower particle densities occur partly because of cenospheres, which are hollow spherical fly ash bodies that contain entrapped air. Because of their hollow structures, cenospheres sink at a rank less than predicted by the standard application of Stokes Law. As a result, the hydrometer method will produce a bias in the grain-size distribution where cenospheres are most abundant (i.e., 10 to 100 um). This bias will skew the data to suggest that a higher fraction of smaller particles is present.

The extraction of ash from the flue gas is physically analogous to aeolian separation of particle sizes in nature. As a result, fly ashes are generally better sorted than most natural soils. The combination of being well-sorted and relatively fine-grained gives fly ash a higher air-entry value than most natural soils. The air-entry values range from 100 cm to 400 cm potential. Although the moisture characteristic curves have similar patterns among the fly ashes, there is considerable differences among the magnitudes and trends.

For five fly ashes, the initial drainage curve (IDC), main drainage curve (MDC), and main wetting curve (MWC) were measured. The results showed significantly different degrees of hysteresis. Briefly, hysteresis is the tendency of a soil's equilibrium water content to be dependent upon the soil's wetting and drying history. Several of the fly ashes exhibited significant hysteresis. One fly ash, for example, has a water content of approximately 20 percent at 2 bars during drainage and at 0.6 bars during wetting.

Mualem coefficients α and N were calculated by fitting an analytical equation to moisture retention curves. The coefficients are useful for comparing fly ash properties to those of natural soils. The values of α and N can be considered measures of the air entry values and sorting, respectively. Tabulated values for α show that they vary from 0.0042 for silt loam to 0.12 for sand. The α for fly ash range from approximately 0.001 to 0.004. Compared to the α values for silty loam, the fly ash values are approximately an order of magnitude lower and therefore more typical of a finer textured soil. The tabulated N values for fly ash ranges from 1.18 for a silt loam to 5.8 for a sand. The calculated N values range from 1.5 to 3.1 and thus fall within the broad range of N values calculated for natural soils.

The porosity values for the fly ash ranges from 42 percent to 51 percent. The values for saturated hydraulic conductivity range from 1 x 10^{-5} cm/s to 1 x 10^{-4} cm/s. Both the porosity and the permeability values are in the range expected for silty loam. Several equations exists in the soil literature that predict saturated hydraulic conductivity based on particle size data. Several of these equations were applied to the fly ash data. Two of the equations provided good predictions. The equations were the Sieler equation (Sieler, 1973) and a modified Hazen equation (Hazen, 1892) using 1.81 instead of 2 as the exponent.

Between the water content values of 20 to 30 percent--the range of the average moisture content in TVA fly ash dry stacks--the $D(\theta)$ for a given fly ash typically changed less than an order of magnitude. Within the same water content range, however, the values of $D(\theta)$ among different fly ashes at a particular water content varied up to three-orders of magnitude. Although some of the trends in the $D(\theta)$ versus θ plots were similar among the fly ashes, only one generalization exist. That is, no general trends are evident within the laboratory-determined diffusivity values for all six fly ashes.

For each fly ash, theoretical fits of $D(\theta)$ versus θ were calculated using van Genuchten's analysis based on Mualem's coefficients. The theoretical values for $D(\theta)$ are generally one order of magnitude lower at a particular water content than laboratory-determined values. There are likely several causes contributing to the discrepancy between the predicted and the measured $D(\theta)$ values; such as, differences in boundary conditions, chemical reactions, and sample preparation. Several of these are discussed.

5.2 FGD and AFBC By-Products

Most of the FGD and AFBC by-products include coarser material than fly ash. Their textural classifications include sandy loam, clay loam, and silty loam. Some are well-sorted; some are poorly-sorted. The uniformity coefficient ranges from 3 to 23. The particle densities range from 2.51 to 2.72. Unlike fly ash, the FGD and AFBC by-products have particle densities consistent with their mineralogical composition. No cenospheres were discovered in any of the FGD or AFBC by-products.

Limited moisture retention data was collected for the FGD and AFBC by-products. Most of them had only the main wetting curve characterized. Both the AFBC fly ash and char had saturated and residual water contents near 60 and 20 percent, respectively. The high-chloride FGD has a saturated and residual water content near 50 and 26 percent. All three of these by-products have high percentages of calcium and/or sulfur oxides. Hydration of these oxides undoubtedly causes the high residual moisture contents and contributes to the high saturation values.

Mualem coefficients α and N were calculated by fitting an analytical equation to the moisture retention curves. The values for α range between 0.0019 and 0.019. The tabulated values for N have a narrow range between 1.68 and 1.80. The range lies below the lowest N value calculated for the fly ash. All of the calculated residual water content θr for the Mualem fit are above 20 percent. The low N values and high θr values are not consistent with the trends in natural soils with similar particle size distributions. The discrepancy is partly attributed to the affects of the chemical reactions between the oxides and the water.

The porosity values for the by-products ranged from 24 to 70 percent. The values for the saturated hydraulic conductivity ranged from 3 x 10^{-7} to 1 x 10^{-3} cm/s. Several equations exists in the soil literature that predict saturated hydraulic conductivity based on particle size data. Most of the equations worked well with the fly ash data. Although several of the equations worked satisfactorily with the FGD high-chloride and the AFBC char data; no equation worked well with either the AFBC fly ash or the AFBC spent bed material. The reason attributed for the two outliers is cementation among the particles.

For each of the by-products, $D(\theta)$ versus θ was determined in the laboratory. This relationship was compared to that predicted using van Genutchen's analysis based on Mualem's coefficients. The theoretical values for $D(\theta)$ were typically at least three-orders of magnitude lower than the laboratory-determined values. The van Genutchen analysis has no allowances for the influence of chemical reactions, which are important with many types of FGD and AFBC by-products. Clearly, in situations where chemical reactions are known to significantly affect the movement of water, some type of direct measurement of diffusivity is required.

5.3 Laboratory and Field Experiments

A concern with laboratory methods for characterizing hydraulic properties is whether laboratory-determined properties are representative of field conditions. Because of strict quality control measures imposed on coal combustion and in operating a dry stack, fly ash dry stacks should be considerably less variable than most natural soils. However, less complexity does not insure the representativeness of laboratory measurements to field conditions. The need to check the adequacy of laboratory measured parameters has been partially satisfied by investigations at the fly ash dry stack at TVA's Bull Run Fossil Plant and by numerical simulation of laboratory evaporation experiments.

The studies at TVA's Bull Run Fossil Plant provided field data on bulk density, porosity, and hydraulic conductivity. During the design and early development stages of the stack, the maximum dry bulk density and optimum water content was 1.29 g/cm^3 and 26 percent, respectively. Four years later in 1987, grab samples of fly ash were collected for laboratory testing. Laboratory testing provided a dry bulk density and optimum water content of 1.26 g/cm^3 and 26 percent. The good comparison between the two sets of values reflects the consistency in the fly ash properties.

In 1987 and 1988, 25 undisturbed samples of fly ash were collected from the upper 10 meters of the dry stack via Shelby tubes. The mean and standard deviation of these dry bulk density measurements were 1.22 and 0.11 g/cm^3. These values are in excellent agreement with the expected range of 1.15 and 1.29 g/cm^3 based on the design specifications. The mean and standard deviation for the porosity measurements on 23 Shelby tubes was 42.3 and 6.8 percent, respectively. The laboratory-determined porosity was 42 percent.

Three methods were used to calculate the saturated hydraulic conductivity of the Bull Run fly ash. The methods were (1) laboratory permeameters measurements on the Shelby-tube cores taken from the dry stack, (2) in-situ measurements in the dry stack with a Guelph permeameter, and (3) laboratory permeameter measurements on packed fly ash obtained directly from the electrostatic precipitators. The variation in the averaged value of saturated hydraulic conductivity for these methods was about a factor of two.

The comparison between the field and laboratory data for the averaged values for dry bulk density, porosity, and saturated hydraulic conductivity are very favorable. The favorable comparison indicates that the laboratory tests provided results reflective of field conditions.

In order to demonstrate the high evaporation rates for fly ash, TVA conducted a series of evapofation experiments. The experiments focused on measuring cumulative evaporative losses from cylinders of fly ash that have no flow boundaries at the bottom and sides, and a constant evaporation potential at the surface. Using the a Brooks-Corey relationship fit to the laboratory-determined hydraulic properties, two separate numerical models were used to accurately simulate a 20-day evaporation test for two different fly ashes. The accurate numerical predictions support the transferability of laboratory-determined properties to field problems.

6

REFERENCES

American Coal Ash Association, 1988. Annual Ash Production and Utility Survey Data.

American Society for Testing and Materials, 1991. Soil and Rock; Dimension Stone; Geosynthetics. Vol. 4.08.

Battelle and GeoTrans, 1988. "FASTCHEM Package; User's Guide to EFLOW, The Groundwater Flow Code," Palo Alto, CA, Electric Power Research Institute, EPRI EA-5870, Vol. 2.

Blake, F.R., and K.H. Hartge, 1986. Bulk Density. In *Methods of Soil Analysis, Part 1*, Klute ed., American Society of Agronomy, Madison, WI. 9:363-367.

Bouwer, H., and R.D. Jackson, 1974. "Determining Soil Properties, Drainage for Agriculture," J. van Schilfgaarde (ed)., Agronomy, No. 17, pp 611-672, American Society of Agronomy, Madison, WI.

Brooks, R.H., and A.T. Corey, 1966. "Properties of Porous Media Affecting Fluid Flow." J. Irrig. Drain., ASCE, 92:61-88.

Bruce, R.R., and A. Klute, 1956. "The Measurement of Soil Moisture Diffusivity." Soil Sci. Soc. Am. Proc., 20:458-462.

Carmen, P.C., 1937. "Fluid Flow Through a Granular Bed," Trans. Inst. Chem. Eng. London, 15:150-156.

Clapp, R.B., 1982. "The Wetting Front Model of Soil Water Dynamics," Ph.D. Dissertation, Dept. of Environmental Science, University of Virginia, Charlottesville, VA.

Clapp, R.B., and G.M. Hornberger, 1978. "Empirical Equations for Some Soil Hydraulic Properties," Water Resour. Res., 14:601-604.

Clothier, B.E., D.R. Scotter, and A.E. Green, 1983. "Diffusivity and One-Dimensional Absorption Experiments." SSSAF, 47:641-644.

Clothier, B.D., and R.A. Wooding, 1983. "The Soil Water Diffusivity Near Saturation," SSSAJ, 47: 636-640.

Electric Power Research Institute (EPRI), 1979. Coal Ash Disposal Manual, FP-1257 Research Project 1404-1, 347 p.

Elrick, D.E., and W.E. Reynolds, 1986. "An Analysis of the Percolation Test Based on Three-Dimensional Saturated-Unsaturated Flow From a Cylindrical Test Hole," Soil Science, 142(5):308-321.

Foust, D.D. and S.C. Young, 1992. "Column Evaporation Studies With Fly Ash for the Evaluation of Numerical Water Budget Models," TVA Report WR28-1-520-181, Tennessee Valley Authority, Norris, TN.

Freeze, R.A., and J.A. Cherry, 1979. Groundwater. Prentice-Hall, Inc. 604 pp.

Hazen, A., 1892. "Experiments Upon the Purification of Sewage and Water at the Lawrence Experiment Station," Massachusetts State Board of Health, 23rd Annual Report.

Hecht, N.L., and S.S. Duvale. 1975. "Characterization and Utilization of Municipal and Utility Sludges and Ashes. Vol. II: Utility Coal Ash." University of Dayton, Dayton, OH. Publication No. PB-244312.

Hillel, D., 1971. Soil and Water: Physical Principles and Processes. Academic Press, New York, 285 pp.

Klute, A., 1986. Water Retention: Laboratory Methods. In *Methods of Soil Analysis, Part 1*, Klute ed., American Society of Agronomy, Madison, WI. 9:637-639.

Klute, A., and C. Dirksen, 1986. "Hydraulic Conductivity and Diffusivity: Laboratory Methods," in *Methods of Soil Analysis, Part 1*, Physical and Mineralogical Methods, American Society of Agronomy, Madison, WI.

Lambe, T.W., and R.V. Whitman, 1979. Soil Mechanics, SI Version. John Wiley and Sons, New York. 553 pp.

Lambe, T.W., 1953. "The Permeability of Fine-Grained Soils," ASTM Special Publication 163, pp 57-67.

Lindquist, K.F. and S.C. Young, 1989. "Colbert Dry Stack Groundwater Evaluation," Technical Report WR28-1-37-103, Tennessee Valley Authority, Norris, TN.

Lindquist, K.F., C.E. Bohac, and S.C. Young, 1991. "Shawnee Groundwater Assessment, Phase II," Technical Report WR28-1-35-112, Tennessee Valley Authority, Norris, TN.

Malik, R.S., A. Laroussi, and L.W. DeBacker, 1979. "Physical Components of the Diffusivity Coefficient," SSSAJ, 43:633-637.

Mather, B., 1961. "Nature and Distribution of Particles of Various Sizes in Fly Ash." Corps of Engineers, Vicksburg, MS. Technical Report 6-583.

Mualem, Y., 1976. "A New Model for Predicting the Hydraulic Conductivity of Unsaturated Porous Media." Water Resources Research, 12(3):513-522.

Mualem, Y., and G. Dagan, 1976. A catalog of the hydraulic properties of unsaturated soils. Technical Report. 100 pp. Technion Israel Inst. of Tehnol., Haifa.

OCR Report, 1972. Mineral Matter and Trace Elements in U.S. Coal. Office of Coal Research. Research and Development Report No. 61. Pittsburgh, PA.

Reeve, M.J., and A.D. Carter, 1991. Water Release Characteristic. In *Soil Analysis: Physical Methods*. K.E. Smith and C.E. Mullins ed. Marcel Dekker, Inc. NY.

Reynolds, W.D., and D.E. Elrick, 1986. "A Method of Simultaneous In-Situ Measurement in the Vadose Zone of Field-Saturated Hydraulic Conductivity, Sorptivity, and the Conductivity-Pressure Head Relationships," Ground Water Monitoring Review, 6:84-95.

Sakellariou-Makrantonaki, M.C. Tzimopoulds, and D. Gouliaras, 1987. "Analysis of a Closed-Form Analytical Model to Predict the Hydraulic Conductivity Function," Journal of Hydrology, pp 289-300.

Seiler, K.P., 1973. "Durchlassigkeit, Porositat and Kornverteilung quartarer Keis-Sand-Ablagerunger des bayerischen Alpenvorlandes," Gas-und Wasserfach, 114(8):353-400.

Selim, H.M., Don Kirkham, and M. Amemiya, 1970. "A Comparison of Two Methods for Determining Soil Water Diffusivity," SSSAP, Vol. 34.

Simsiman, G.V., G. Chesters, and A.W. Andren, 1987. "Effect of Ash Disposal Ponds on Groundwater Quality at a Coal-Fired Power Plant," Water Resources, 21(4):417-426.

Shepherd, Russell, 1989. "Correlations of Permeability and Grain Size," Ground Water, 27(5):15-20.

Stephens, D.B., K. Lambert, and D. Watson, 1984, "Influence of Entrapped Air on Field Determination of Hydraulic Properties in the Vadose Zone," Proc. Conf. Characterization and Monitoring of the Vadose Zone, National Water Well Association, Worthington, OH, pp 57-76.

Stephens, D.B., K. Lambert, and D. Watson, 1987. "Regression Models for Hydraulic Conductivity and Field Test of the Borehole Permeameter," Water Res. Res., 23:2207-2214.

United Nations Report, 1989. Ground Water Software: Part One Database and Utilities--User's Manual. United Nations Department of Technical Cooperation for Development, Water Resources Branch.

van Genuchten, M.T., 1978. "Calculating the Unsaturated Hydraulic Conductivity With a New Closed-Form Analytical Model, 78-WR-08, Water Res. Program, Dept. of Civil Eng., Princeton Univ., Princeton, New Jersey.

van Genuchten, M.T., 1980. "A Closed-Form Equation for Predicting the Hydraulic Conductivity of Unsaturated Soils," Soil Sci. Soc. Am. J., 44:892-898.

Young, S.C., 1989. "Leachate Generation from Dry Stacked Fly Ash at the Bull Run Fossil Plant, Part I: Field Experiments," Technical Report WR28-1-49-102, Tennessee Valley Authority, Norris, TN.

Young, S.C., 1992. "Vertical Moisture Profiles in the Bull Run Dry Stack and Implications to Leachate Generation," Technical Report WR28-1-49-109, Tennessee Valley Authority, Norris, TN.

Young, S.C., and L.M. Beard, 1989. "An Assessment of the Phase II Fly Ash Dry Stacking at the Bull Run Fossil Plant," Technical Report WR28-1-49-104, Tennessee Valley Authority, Norris, TN.

Young, S.C., and R.B. Clapp, 1989. "The Importance of Climatological Variability and the Rate at Which Waste is Added to Modeling Water Budgets of Landfills," Presented at the National Water Well Association Conference, Indianapolis, IN.

Young, S.C., and M.L. Velasco, 1991. "Water Budget Predictions for an Active Fly Ash Dry Stack Using the HELP2 Model," Technical Report WR28-1-49-106, Tennessee Valley Authority, Norris, TN.

APPENDIX A

Physical and Hydraulic Properties for Coal Combustion By-Products

BULL RUN FLY ASH*

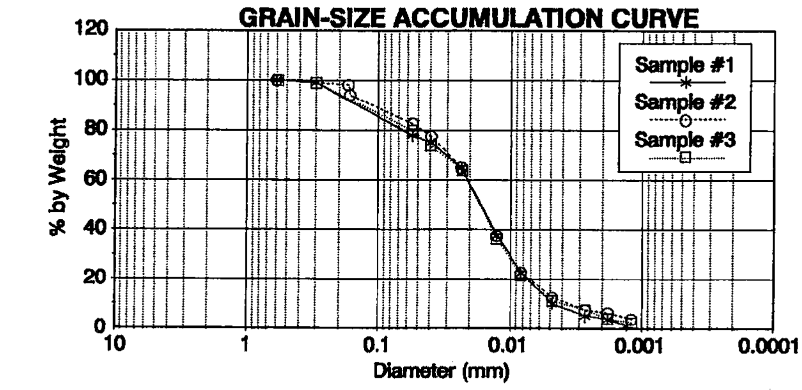

	Sample #1	Sample #2	Sample #3
Particle Density (g/cm^3)	2.10	2.11	2.12
Optimum Water Content (%,g/g)	26.0	—	—
Maximum Bulk Density (g/cm^3)	1.26	—	—
Saturated Hydraulic Conductivity (cm/s)	5.80E-05	4.70E-05	5.20E-05

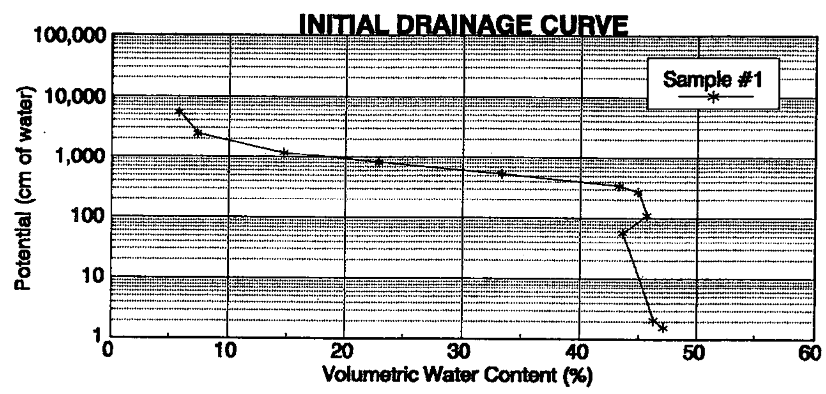

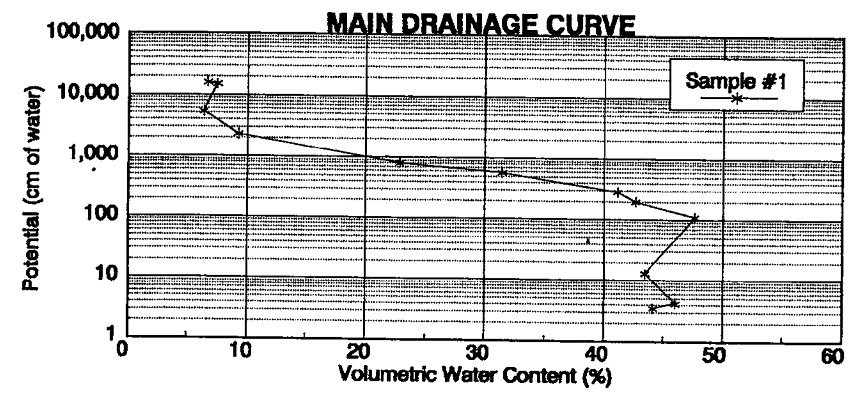

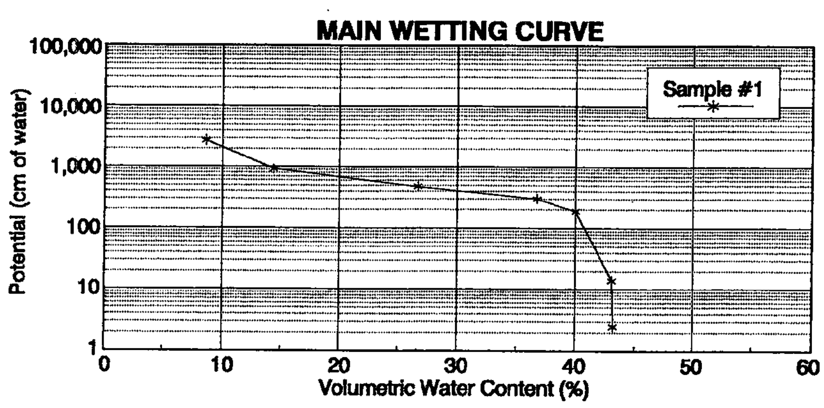

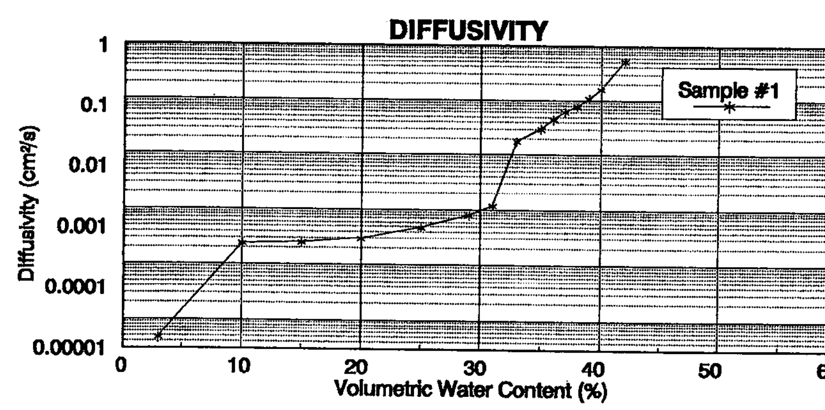

* Testing by Dr. Arnold Klute, Fort Collins, CO.

COLBERT FLY ASH*

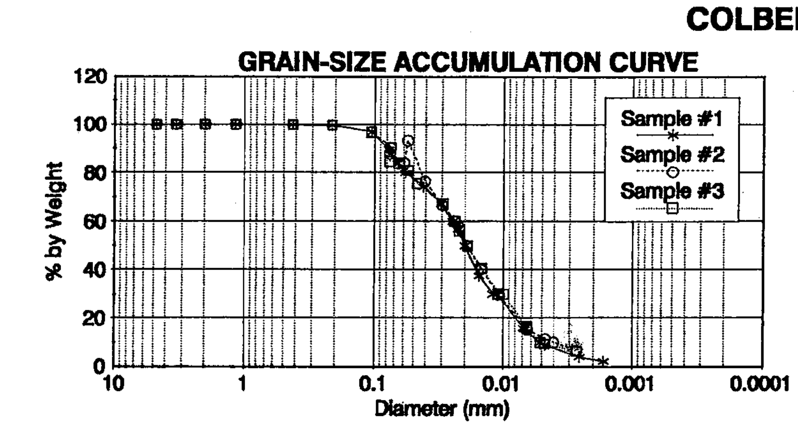

	Sample #1	Sample #2	Sample #3
Particle Density (g/cm^3)	2.34	2.33	2.34
Optimum Water Content (%,g/g)	27.5	26.5	27.0
Maximum Bulk Density (g/cm^3)	1.23	1.27	1.29
Saturated Hydraulic Conductivity (cm/s)	1.25E-04	1.3E-04	1.04E-04

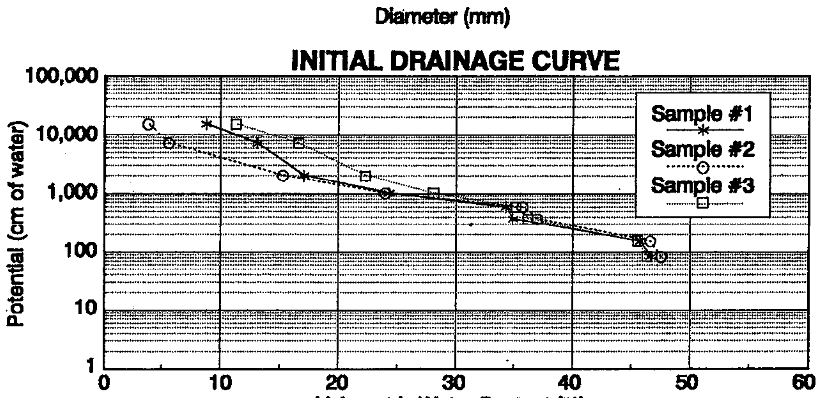

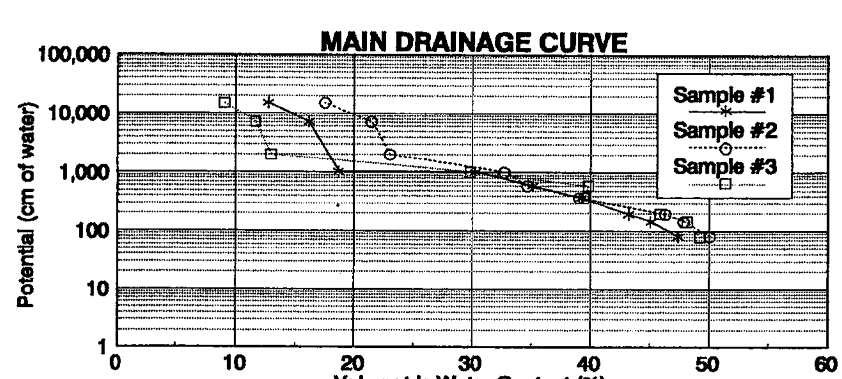

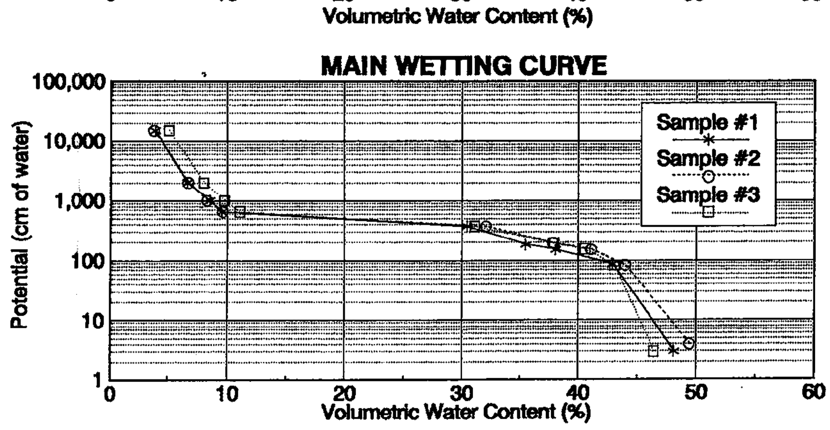

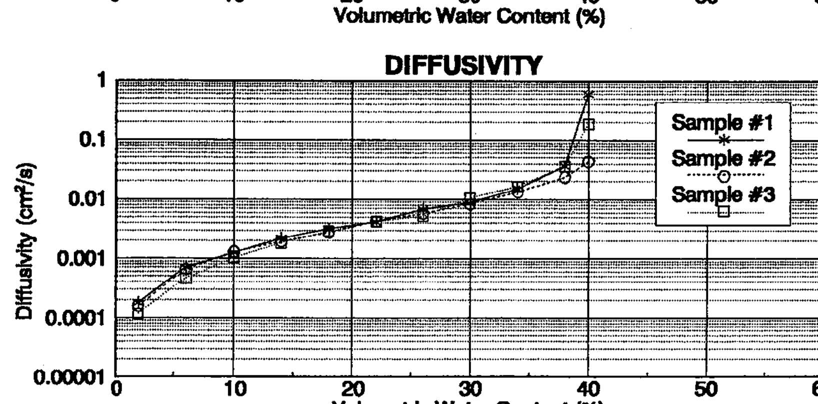

* Testing by Daniel B. Stephens and Associates, Inc., Albuquerque, NM.

JOHNSONVILLE FLY ASH*

GRAIN-SIZE ACCUMULATION CURVE

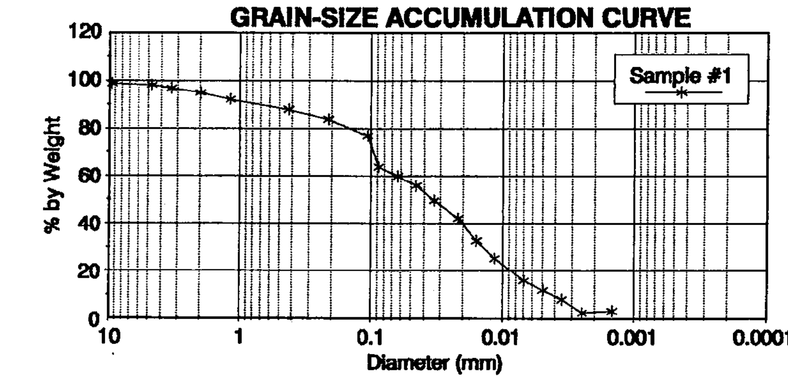

	Sample #1	Sample #2	Sample #3
Particle Density (g/cm^3)	——	——	——
Optimum Water Content (%,g/g)	21.4	——	——
Maximum Bulk Density (g/cm^3)	1.48	——	——
Saturated Hydraulic Conductivity (cm/s)	1.60E-05	1.60E-05	1.30E-05

INITIAL DRAINAGE CURVE

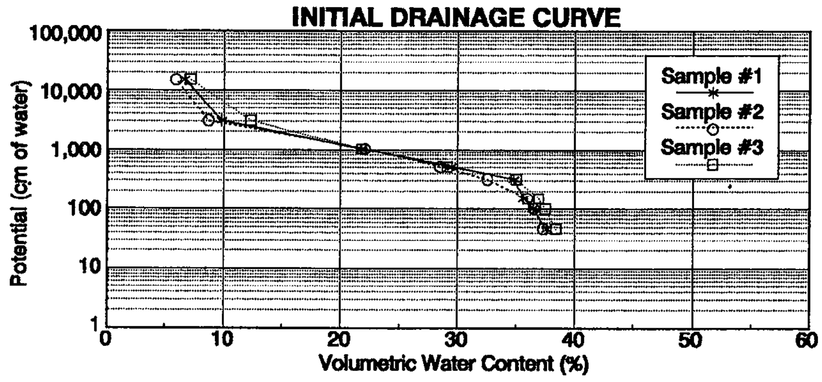

MAIN DRAINAGE CURVE

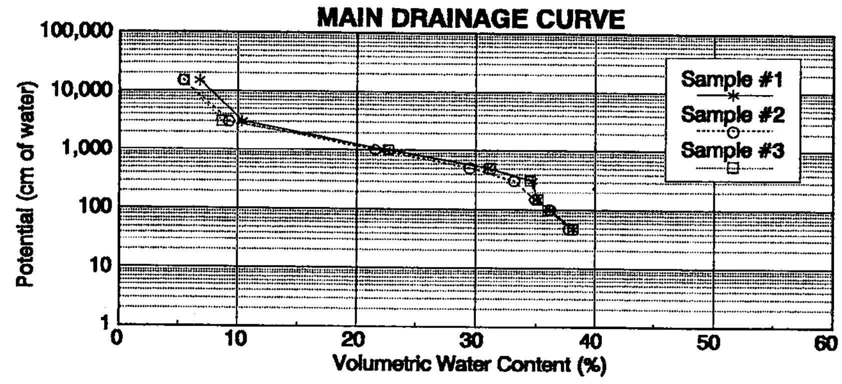

MAIN WETTING CURVE

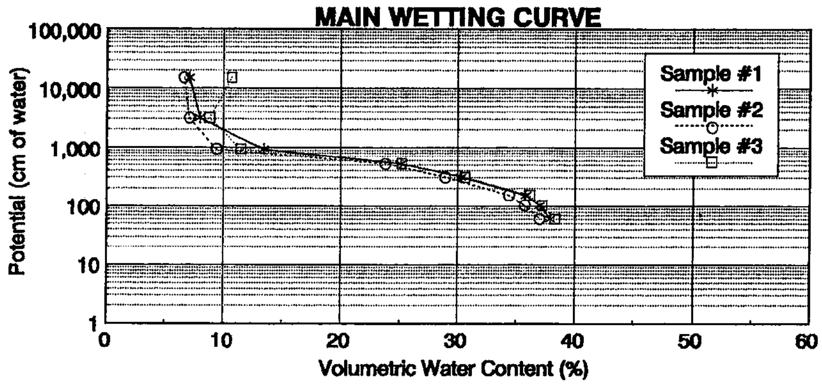

DIFFUSIVITY

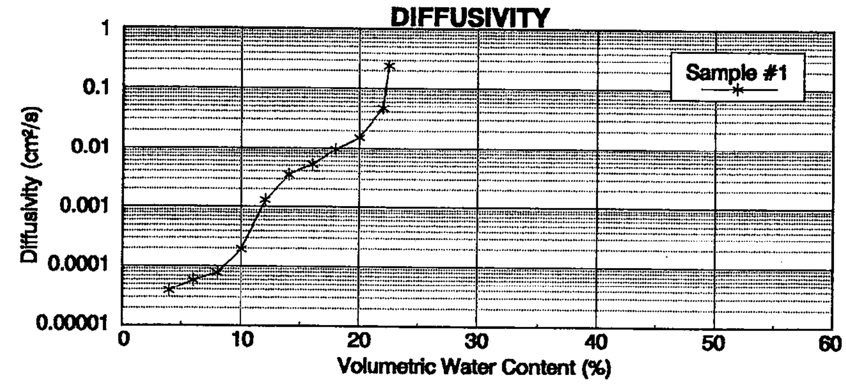

* Testing by Daniel B. Stephens and Associates, Inc., Albuquerque, NM.

JOHN SEVIER FLY ASH*

GRAIN-SIZE ACCUMULATION CURVE

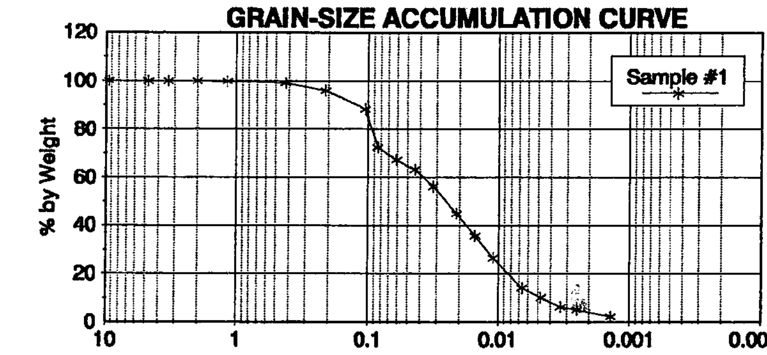

	Sample #1	Sample #2	Sample #3
Particle Density (g/cm^3)	2.35	——	——
Optimum Water Content (%,g/g)	24.0	——	——
Maximum Bulk Density (g/cm^3)	1.33	——	——
Saturated Hydraulic Conductivity (cm/s)	9.20E-05	1.00E-04	2.60E-04

INITIAL DRAINAGE CURVE

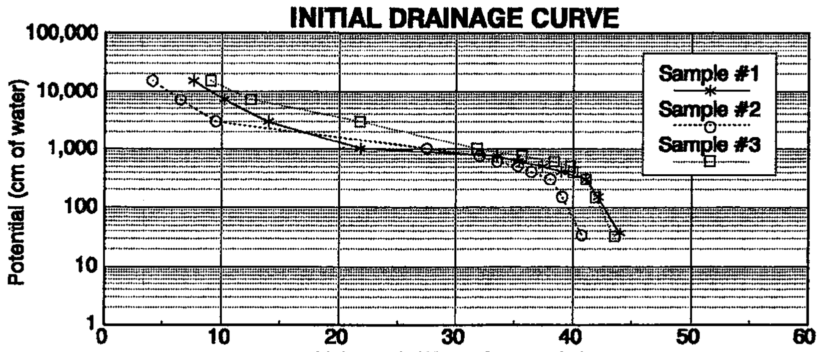

MAIN DRAINAGE CURVE

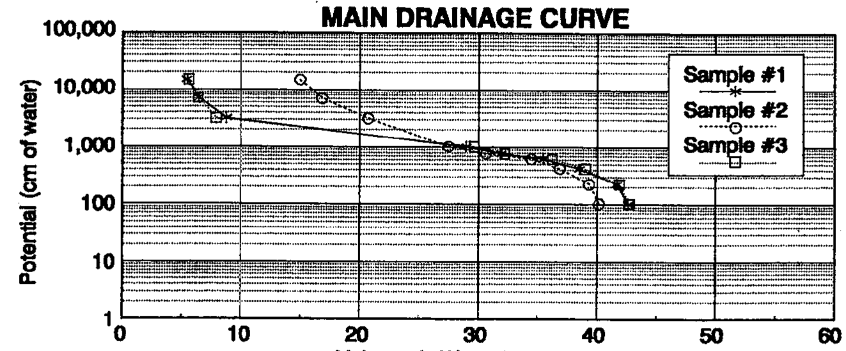

MAIN WETTING CURVE

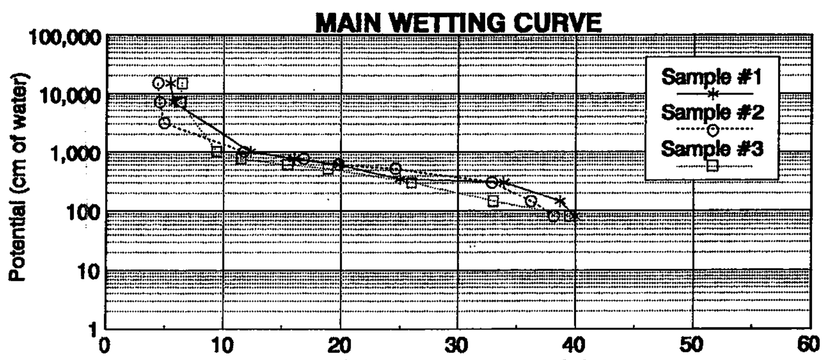

DIFFUSIVITY

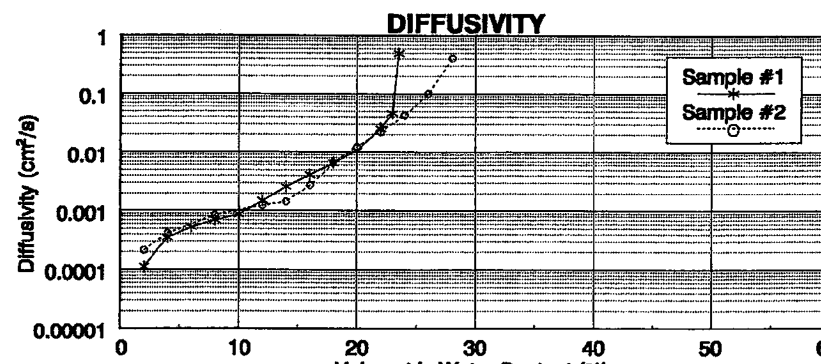

* Testing by Daniel B. Stephens and Associates, Inc., Albuquerque, NM.

KINGSTON FLY ASH*

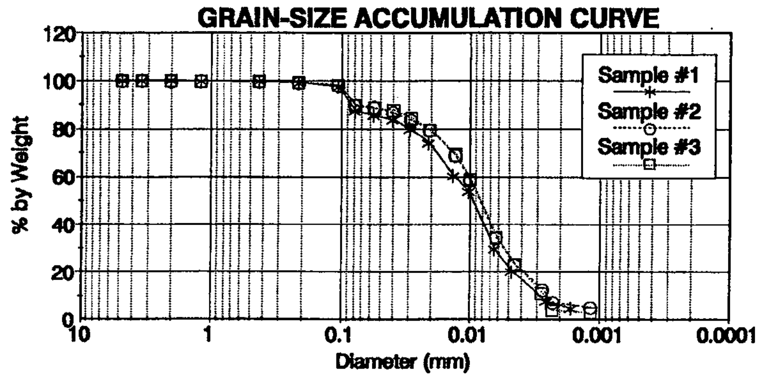

	Sample #1	Sample #2	Sample #3
Particle Density (g/cm³)	2.44	2.42	2.38
Optimum Water Content (%,g/g)	25.5	25.5	25.0
Maximum Bulk Density (g/cm³)	1.35	1.34	1.36
Saturated Hydraulic Conductivity (cm/s)	2.00E-05	2.1E-05	2.17E-05

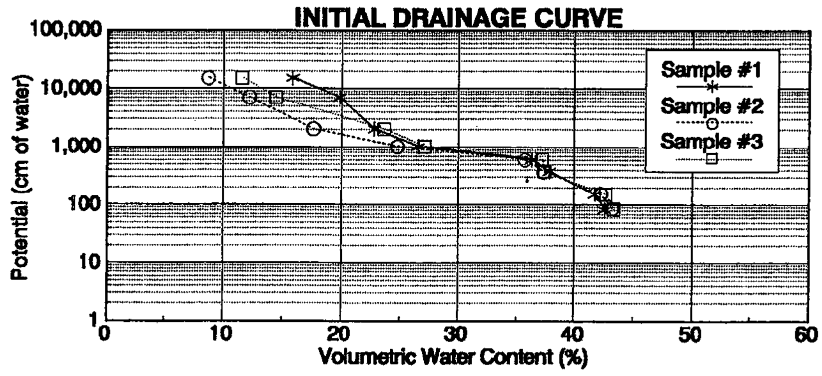

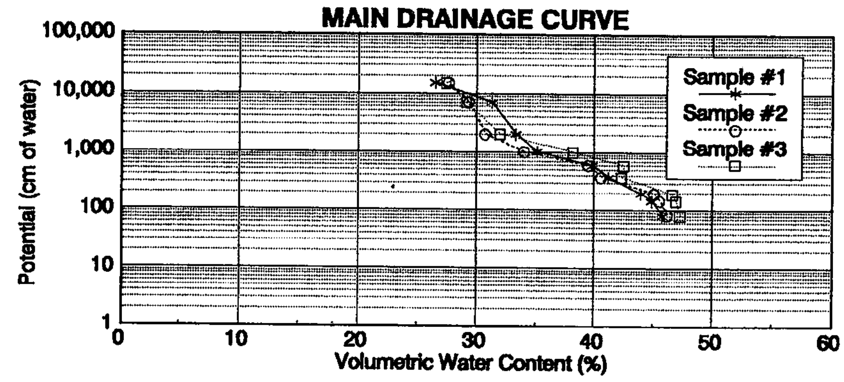

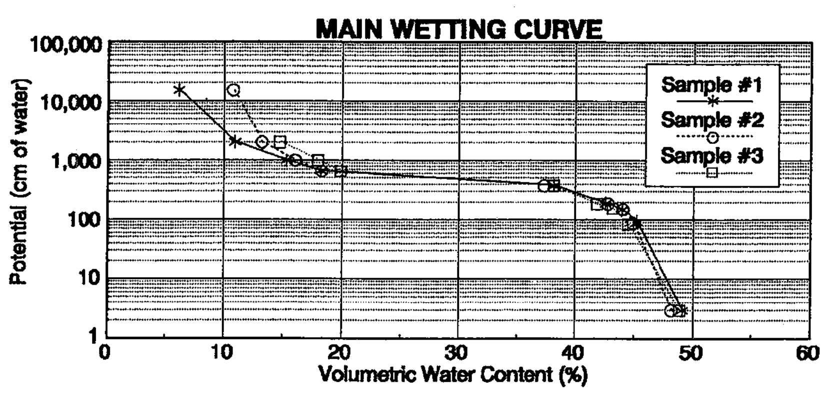

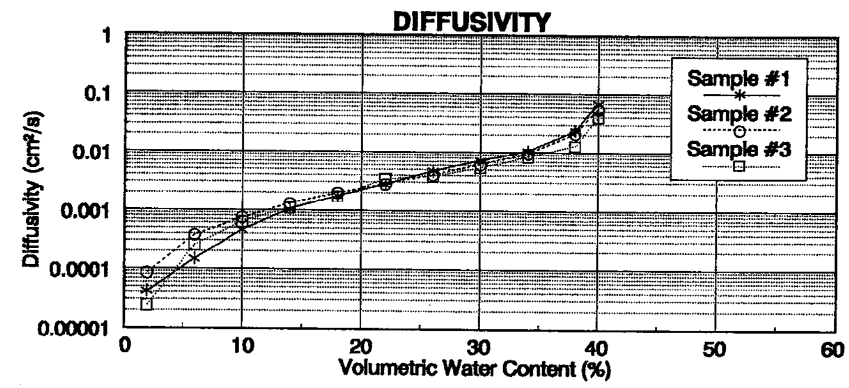

* Testing by Daniel B. Stephens and Associates, Inc., Albuquerque, NM.

SHAWNEE FLY ASH*

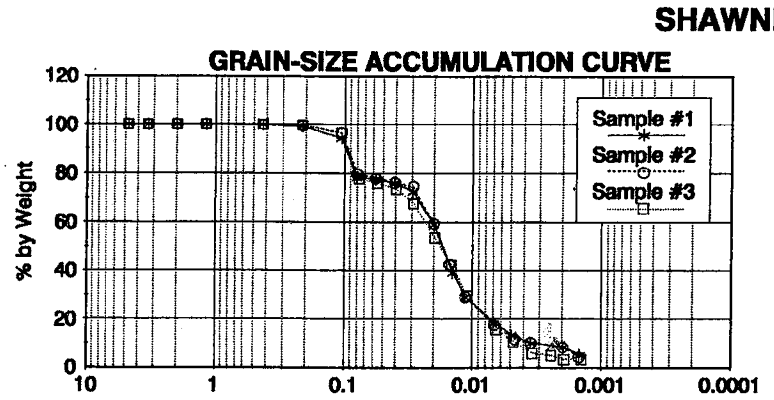

	Sample #1	Sample #2	Sample #3
Particle Density (g/cm³)	———	———	———
Optimum Water Content (%,g/g)	33.5	———	———
Maximum Bulk Density (g/cm³)	1.17	———	———
Saturated Hydraulic Conductivity (cm/s)	4.30E-05	4.90E-05	3.80E-05

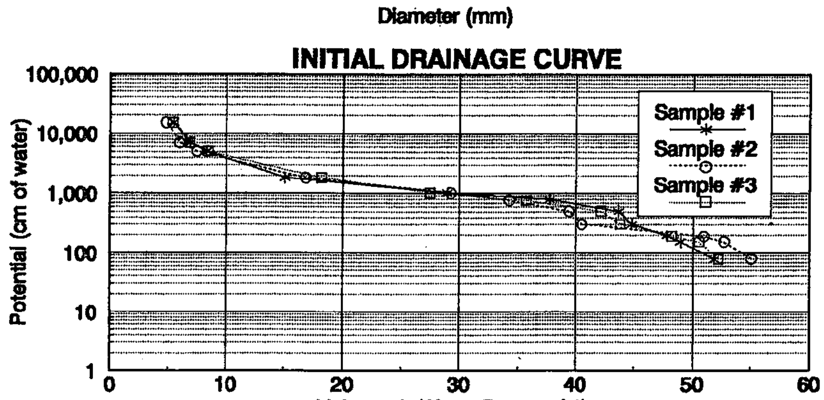

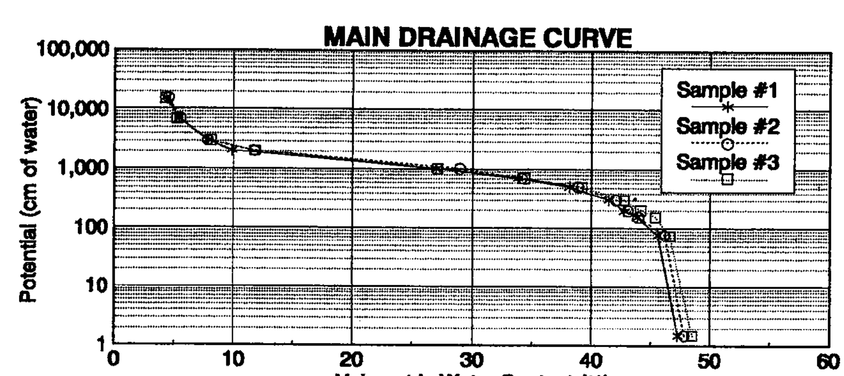

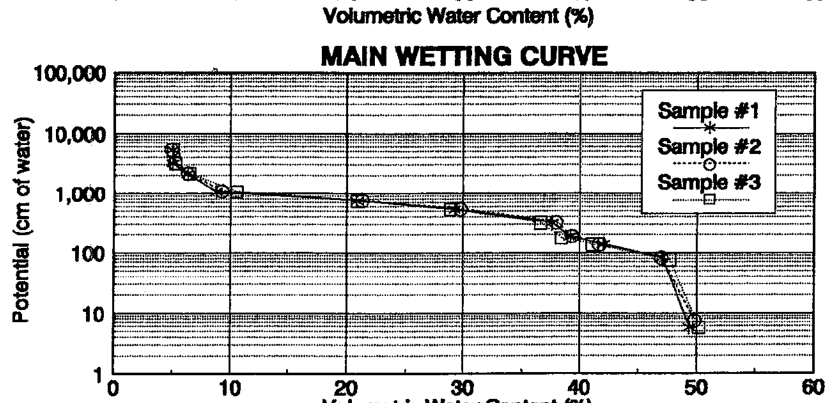

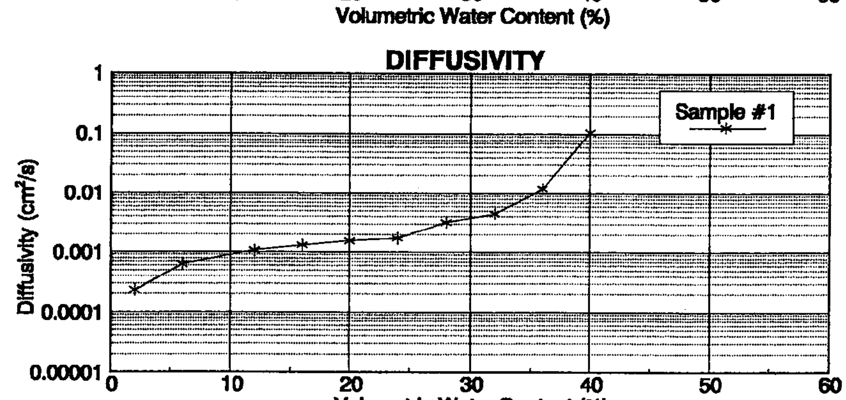

* Testing by Daniel B. Stephens and Associates, Inc., Albuquerque, NM.

SHAWNEE
AFBC CHAR*

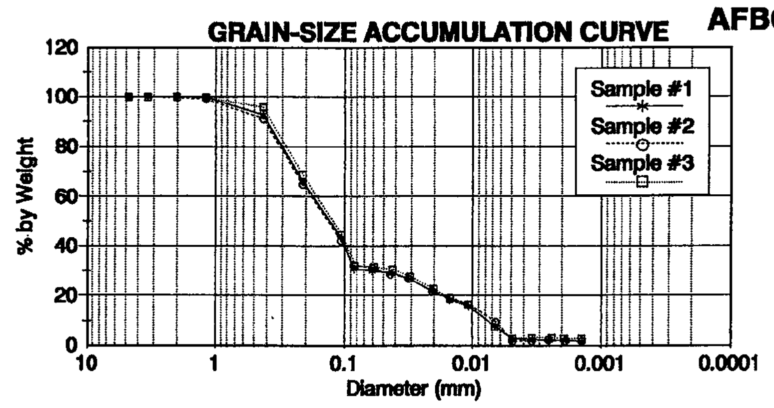

	Sample #1	Sample #2	Sample #3
Particle Density (g/cm^3)	——	——	——
Optimum Water Content (%,g/g)	38.3	——	——
Maximum Bulk Density (g/cm^3)	1.18	——	——
Saturated Hydraulic Conductivity (cm/s)	4.60E-05	3.60E-05	1.20E-04

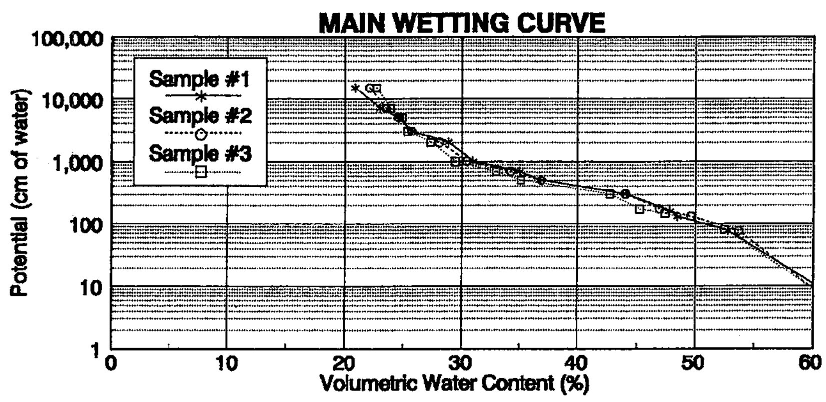

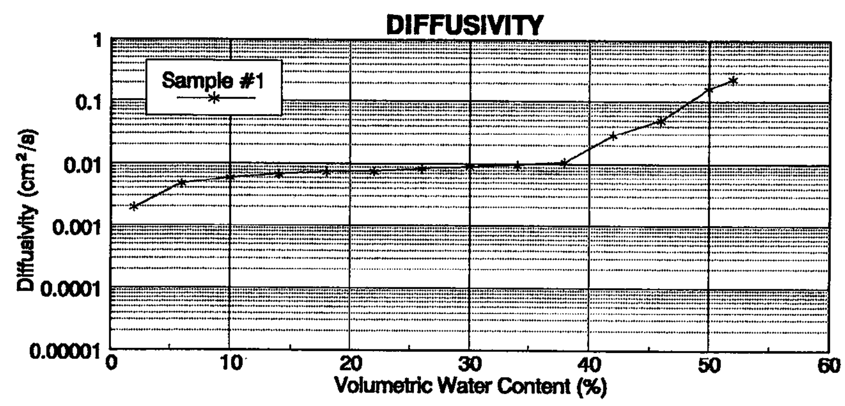

* Testing by Daniel B. Stephens and Associates, Inc., Albuquerque, NM.

SHAWNEE
AFBC FLY ASH*

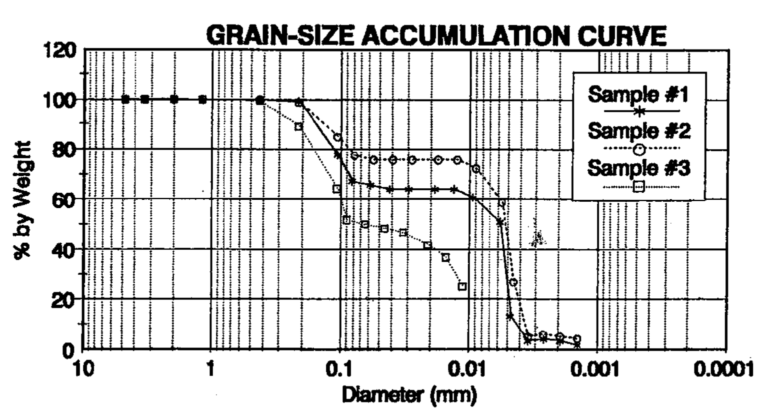

	Sample #1	Sample #2	Sample #3
Particle Density (g/cm^3)	——	——	——
Optimum Water Content (%,g/g)	38.8	——	——
Maximum Bulk Density (g/cm^3)	1.23	——	——
Saturated Hydraulic Conductivity (cm/s)	1.70E-07	3.30E-07	4.50E-07

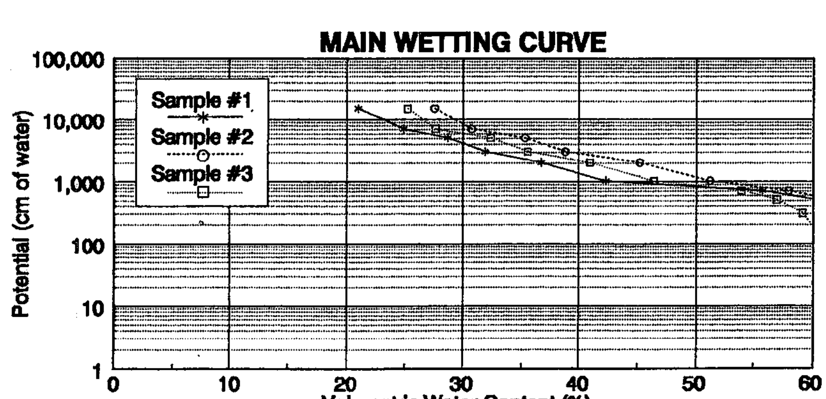

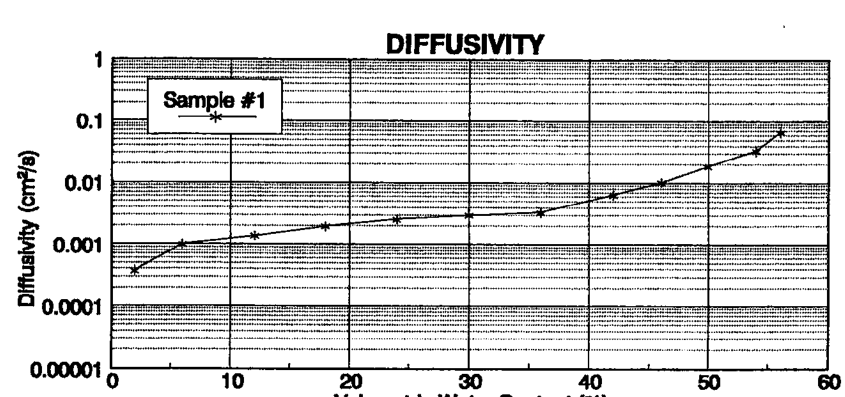

* Testing by Daniel B. Stephens and Associates, Inc., Albuquerque, NM.

SHAWNEE
SPENT-BED MATERIAL*

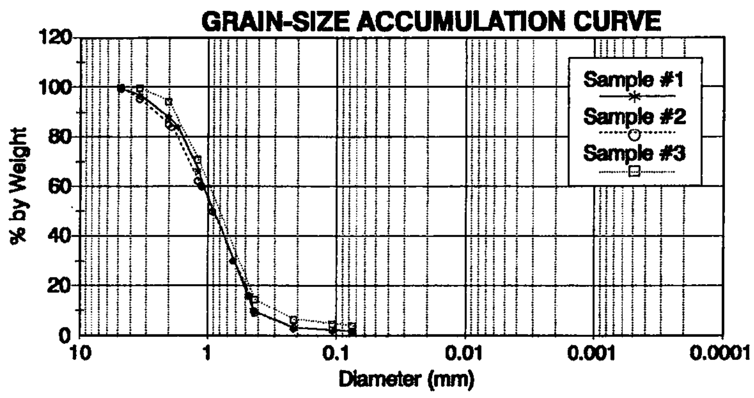

	Sample #1	Sample #2	Sample #3
Particle Density (g/cm^3)	———	———	———
Optimum Water Content (%,g/g)	21.3	———	———
Maximum Bulk Density (g/cm^3)	1.48	———	———
Saturated Hydraulic Conductivity (cm/s)	1.30E-03	1.50E-03	9.60E-04

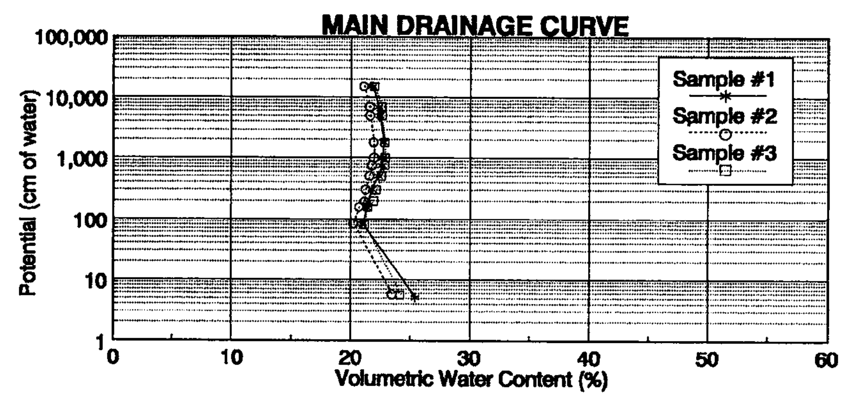

* Testing by Daniel B. Stephens and Associates, Inc., Albuquerque, NM.

HIGH-CHLORIDE FGD WASTE*

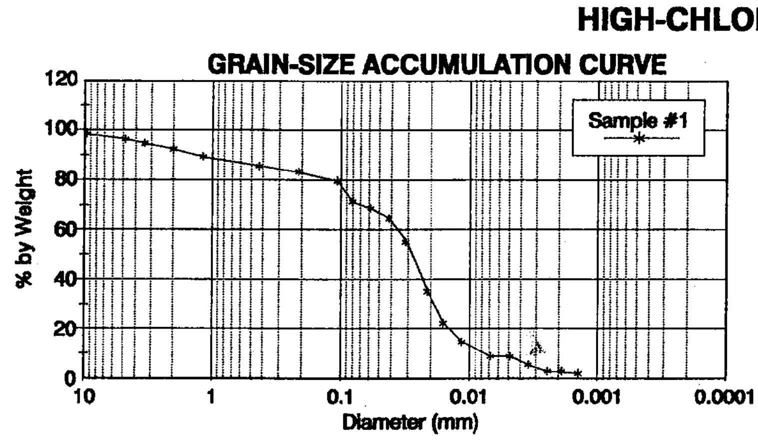

	Sample #1	Sample #2	Sample #3
Particle Density (g/cm^3)	2.58	———	———
Optimum Water Content (%,g/g)	46.7	———	———
Maximum Bulk Density (g/cm^3)	1.07	———	———
Saturated Hydraulic Conductivity (cm/s)	2.90E-05	7.30E-05	———

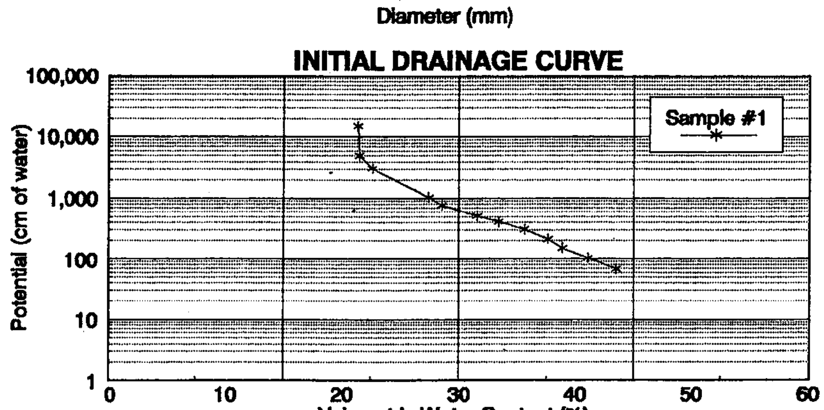

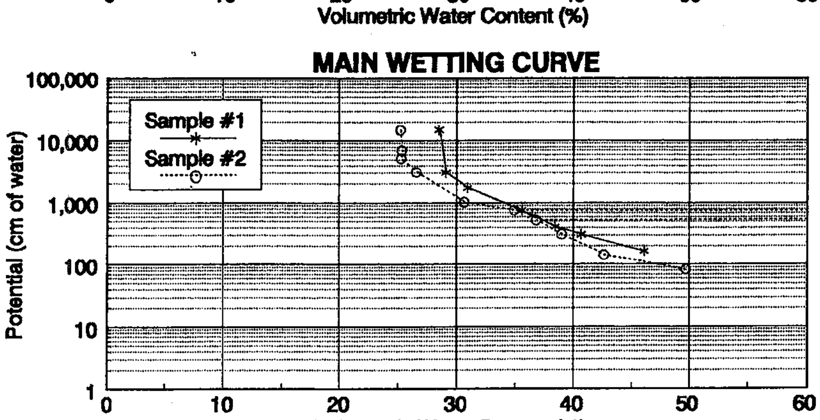

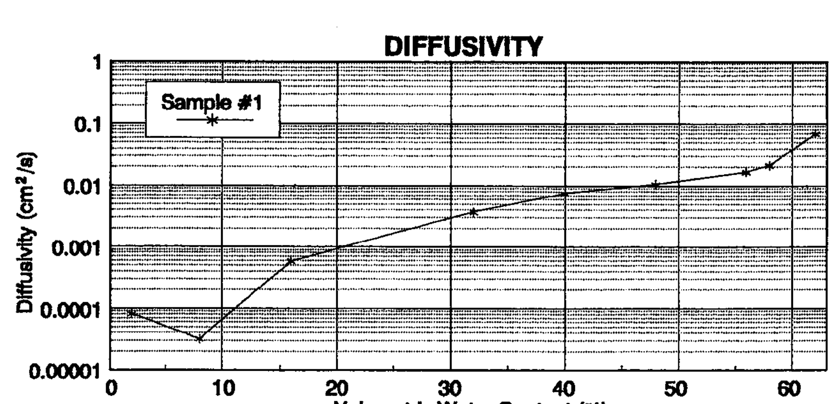

* Testing by Daniel B. Stephens and Associates, Inc., Albuquerque, NM.

APPENDIX B

Summary of Key Parameters for Coal Combustion By-Products

PHYSICAL PROPERTIES

	P_D (g/cm^3)	d_{10} (mm)	d_{50} (mm)	d_{90} (mm)	C_u	K_{sat} (cm/s)	θ_s (% vol)
Soil Type							
Silt Mont Cenis	----	0.0100	0.1500	1.30	25	1.45×10^{-5}	44
Rideau Clay Loam	----	0.0030	0.0095	0.30	~6	2.66×10^{-3}	42
Caribou Silt Loam	----	0.0055	0.0120	1.00	2.91	1.66×10^{-4}	44
Sand	----	----	0.3500	1.50	----	1.44×10^{-2}	31
Fly Ash							
Bull Run	2.11	0.0057	0.019	0.15	4.40	5.80×10^{-5}	42
Colbert	2.34	0.0048	0.019	0.08	5.17	1.18×10^{-4}	47
Kingston	2.41	0.0027	0.009	0.07	3.90	2.07×10^{-5}	47
Shawnee	2.23	0.0038	0.017	0.10	5.57	4.33×10^{-5}	51
Johnsonville	2.42	0.0045	0.034	0.70	14.00	1.33×10^{-5}	42
John Sevier	2.35	0.0038	0.027	0.13	10.00	1.51×10^{-4}	44
Non-Fly Ash							
AFBC Fly Ash	2.72	0.0054	0.024	0.13	4.80	3.17×10^{-7}	70
AFBC Char	2.51	0.0073	0.127	0.40	23.07	6.73×10^{-5}	60
AFBC SBM	2.52	0.3900	0.870	2.50	2.77	1.25×10^{-3}	24
FGD High Chloride	2.42	0.0075	0.029	1.50	5.00	5.10×10^{-5}	59

NOTATION:

P_D - Particle Density
d_x - Diameter for which x% of the Particles are Finer
C_u - Uniformity Coefficient, d_{60}/d_{10}
K_{sat} - Hydraulic Conductivity at Saturation
θ_s - Porosity

MUALEM COEFFICIENTS *

	Main Drainage Curve			Main Wetting Curve		
	N	α (cm^{-1})	θ_r (% vol)	N	α (cm^{-1})	θ_r (% vol)
Fly Ash						
Bull Run	2.93	0.0017	0.06	3.11	0.0025	0.07
Colbert	1.84	0.0026	0.12	2.56	0.0034	0.03
Kingston	-----	-----	-----	2.68	0.0030	0.104
Shawnee	2.18	0.0014	0.02	1.93	0.0039	0.02
Johnsonville	1.53	0.0028	0.00 +	2.59	0.0027	0.06
John Sevier	2.13	0.0033	0.042	2.53	0.0012	0.06
Non-Fly Ash						
AFBC Fly Ash	-----	-----	-----	1.80	0.0019	0.25
AFBC Char	-----	-----	-----	1.68	0.0080	0.21
AFBC SBM	1.65	0.0040	0.20	-----	-----	-----
FGD High Chloride	-----	-----	-----	1.77	0.0119	0.29

NOTATION:

N - Coefficient for Mualem's Diffusivity Model
α - Coefficient for Mualem's Diffusivity Model
θ_r - Residual Moisture Content
* - Mualem Coefficients Calculated with SOHYP(Van Genutchen, 1978).
\+ - Two Parameter Mualem Model

APPENDIX C

Unsaturated Flow Parameters From van Genuchten's (1978) Diffusivity Model Using Imbibition Data From Mualem and Dagen (1976)

UNSATURATED FLOW PARAMETERS FROM van GENUTCHEN'S (1978) DIFFUSIVITY MODEL USING IMBIBITION DATA FROM MUALEM'S AND DAGAN (1976) FROM STEPHENS ET AL, (1984)

Soil Type	Catalog Number	α cm^{-1}	N	θ_r
Silt "Columbia"	2001	0.016	1.77	0.14
Silt Mont Cenis (limon Silteaux)	2002	0.014	1.32	0.00
Silt of Nave-Yaar	2003	0.072	2.20	0.40
Rideau clay loam	3101	0.069	2.06	0.29
Yolo light clay	3102	0.027	1.60	0.18
Caribou silt loam	3301	0.047	1.70	0.30
Grenville silt loam	3302	0.031	1.29	0.03
Ida silt loam (>15 cm)	3305	0.040	1.27	0.00
Ida silt loam (0-15 cm)	3306	0.090	1.18	0.00
Touched silt loam	3308	0.027	3.54	0.10
Silt Loam G. E. 3	3310	0.004	2.06	0.13
Gilat loam	3402	0.017	2.30	0.08
Guelph loam	3407	0.074	1.78	0.22
Rubicon sandy loam	3501	0.052	1.86	0.14
Loamy Sand-Hamra Sharon	4004	0.019	5.15	0.20
Plainfield sand (210-250 μ)	4101	0.045	4.00	0.01
Plainfield sand (177-210 μ)	4102	0.039	4.04	0.01
Plainfield sand (149-177 μ)	4103	0.032	4.08	0.01
Plainfield sand (125-149 μ)	4104	0.025	5.83	0.03
Plainfield sand (104-125 μ)	4105	0.022	4.44	0.01
Sand	4106	0.094	2.04	0.00
Sand	4107	0.060	2.64	0.04
Del Norte fine sand	4108	0.016	4.36	0.05
Oakley sand	4112	0.095	2.01	0.03
G. E. 3 sand	4115	0.036	4.49	0.04
Crab Creek sand	4117	0.119	2.45	0.00
Sinai sand	4122	0.024	5.31	0.03
Sand (50-500 μ)	4124	0.019	4.67	0.07
Gravelly sand G. E. 9	4135	0.015	2.84	0.08
Fine sand G. E. 2	4136	0.007	3.89	0.06
Plainfield sand (0-25 cm)	4146	0.034	3.85	0.11
Plainfield sand (25-60 cm)	4147	0.032	4.19	0.07
Aggregated glass bead	5003	0.040	6.47	0.10
Monodispersed glass bead	5004	0.036	7.62	0.04

N - Mualem's Coefficient
α - Mualem's Coefficient
θ_r - Residual Moisture Content